DEVELOPMENT OF NOVEL FUNCTIONALIZED MEMBRANES FOR ANTIFOULING PERFORMANCES IN WATER OR WASTEWATER TREATMENT

ZHU XIAOYING

A THESIS SUBMITTED
FOR THE DEGREE OF DOCTOR OF PHILOSOPHY

DEPARMENT OF CIVIL AND ENVIORNMENTAL ENGINEERING
NATIONAL UNIVERSITY OF SINGAPORE

2011

DECLARATION

I hereby declare that this thesis is my original work and it has been written by me in its entirety. I have duly acknowledged all the sources of information which have been used in the thesis.

This thesis has also not been submitted for any degree in any university previously.

Zhu Xiaoying
17 July 2012

Acknowledgements

First and foremost, I would like to express my appreciation and gratitude to my supervisor, Prof. Bai Renbi, for offering me a chance to carry out my research work in his laboratory. His extraordinary scientific vision and creativity and his skill as a teacher are largely responsible for the success of this thesis. His constant guidance and invaluable advice have kept me on the right track of my research work. Through the constant discussion sessions I have with him, it has not only deepened my knowledge of membrane technologies but at the same time given me the inspiration to extend my views of research.

I would also like to thank my colleagues: Dr. Zhao Yonghong, Dr. He Yi, Dr. Wee Kin Ho, Dr. Liu Changkun, Dr. Han Wei, Ms. Han Hui, Ms. Zhang Linzi and Ms. Tu Wenting, who have provided me with help and suggestions in my research work. In addition, I would appreciate the assistance from all the lab and professional officers in Department of Civil and Environmental Engineering.

Last but not least, I would like to thank my family and friends for their support and encouragement.

Table of Contents

Summary

Water filtration processes using polymeric membranes have become an increasingly important subject of research in recent years. Due to the advantages of high separation efficiency, no chemical addition requirement and small system footprint, membrane filtration provides a choice for efficient water and wastewater treatments. The more widespread applications of the membrane separation technology have, however, suffered from the problem that polymeric membranes are often subject to severe and irreversible fouling by pervasive microbes and organics in the feeds. This study focused on developing methods to minimize irreversible fouling by changing the strong interactions between the membrane surface and the foulants such as microbe adhesion, biofilm formation (caused by microbes' fast reproduction) and organic adsorption into weak interactions such as physical deposition. The weak interactions can be effortlessly broken, and thus, the irreversible membrane fouling becomes reversible that can be easily removed.

Membrane biofouling is very difficult to be dealt with because of microbes' reproductivity. One strategy of membrane biofouling prevention is to inhibit the growth and reproduction of microbes on the membrane surface. The approach is to immobilize biocides on the membrane surface to kill the microbes attached. In the first part of this study (Chapter 3), ionic silver was immobilized onto cross-linked chitosan membrane (CS) to investigate the anti-biofouling performances of the membrane. The ionic silver immobilized membrane (denoted as CS_Ag^+) was also treated with ascorbic acid to reduce the silver ions on the CS_Ag^+ membrane

to obtain the membrane with reduced metallic silver (denoted as the CS_Ag^0). The valance states of the immobilized silver on CS_Ag^+ and CS_Ag^0 and the interaction between silver and chitosan were verified by X-ray photoelectron spectroscopy (XPS). The stability of the immobilized silver on the two types of membranes was evaluated through leaching test. It was found that silver was effectively immobilized onto the membranes through surface complexation and the immobilized silver on CS_Ag^0 was more stable than on the CS_Ag^+ membrane. Antibacterial and anti-biofouling experiments for the CS_Ag^+ and CS_Ag^0 membranes were conducted with two typical types of bacteria, *E. coli* and *Pseudomonas sp*. From the disk diffusion tests, it was found that the CS_Ag^+ membrane showed stronger antibacterial effect than the CS_Ag^0 membrane. In the longer term anti-biofouling experiments, however, both the CS_Ag^+ and the CS_Ag^0 membranes exhibited good anti-biofouling performance initially, but the CS_Ag^0 membrane displayed a more stable performance than the CS_Ag^+ membrane afterwards. The results of this stage indicate that immobilization of silver onto membrane surface can be an effective method to improve membrane anti-biofouling property. It is also one of the first efforts to evaluate the relative anti-biofouling performance of immobilized ionic or reduced silver on membrane surface.

The stability of the immobilized silver is of major interest in the second part of the study, because the results of the first part of the study indicated that the desired long term anti-biofouling performance was related to the stably immobilized silver. In the second part of this study (Chapter 4), a common

commercial polypropylene (PP) membrane that is chemically inert was selected and a method was developed to immobilize silver onto the PP membrane surface for improved anti-biofouling performance. The commercial PP membrane was first grafted with thiol groups, and then silver ions were immobilized onto the PP membrane surface through coordinating with the thiol groups. The immobilized silver was found to be very stable, with only about 1.1 % of the immobilized silver being leached out during a leaching test. The modified membrane (PPS-Ag) was verified the successful grafting of the thiol groups and the coordination of silver ions on the membrane surface through ATR-FTIR and XPS analyses. The membrane surface properties were also characterized by SEM, AFM and water contact angle measurements. The PPS-Ag membrane was found to have a smoother and more hydrophilic surface than the PP membrane. Both Gram-negative bacteria, *Escherichia coli* (*E. coli*), and Gram-positive bacteria, *Staphylococcus aureus* (*S. aureus*), were used to evaluate the PPS-Ag membrane's antibacterial and anti-biofouling performances. From the disk diffusion experiments, the PPS-Ag membrane exhibited the capability of effectively inhibiting the growth of both the Gram-negative and Gram-positive bacteria tested. The membrane anti-biofouling performance was assessed with the mixed *E. coli* and *S. aureus* suspension immersion and filtration tests. The PPS-Ag membrane showed a stable and significantly enhanced anti-biofouling performance as compared with the PP membrane. The results of this part of study demonstrated that the PP membrane's biofouling problem can be sufficiently overcome through immobilizing silver onto the membrane surface.

Organic fouling is another type of irreversible membrane fouling. The main reason of organic fouling is the adsorption of various organic substances by the membranes. In the third part of this study (Chapter 5), a functional additive polymer with hydrophilicity and oleophobicity was synthesized and blend with PVDF to produce novel membranes that were capable of resisting membrane organic fouling. The additive polymer was synthesized through graft copolymerization of tBMA from P(VDF-co-CTFE) *via* ATRP. The grafted PtBMA chains were subsequently hydrolyzed to PMAA that were then esterified with a surfactant containing an oleophobic perfluorinated hydrocarbon end and a hydrophilic PEG chain. The synthesis procedures and reactions were verified with the ATR-FTIR and NMR analyses. The surface morphology of the blend membranes with the additive polymer was examined with SEM images. It was found that the membrane surface morphology could be adjusted through changing the portion of the additive polymer in PVDF and the polymer concentration of the casting solution. The higher portion of the additive polymer or the lower concentration of casting solution made the produced membranes with more porous surfaces. The additive polymer introduced hydrophilicity and oleophobicity to the prepared membranes. They achieved rejections of at least 99.8 % of oil in the filtration of a 500 $mg \cdot L^{-1}$ oil/water emulsion. The membrane containing 30 wt% of the additive polymer showed effective inhibition of oil adsorption or oil fouling. Moreover, on the premise of providing enough oleophobicity, the membrane surface with smaller pores would more effectively reject emulsified oil droplets. The results of this part of study demonstrated that

the synthesized additive polymer endued the prepared membranes with excellent antifouling performance, especially for oils.

In the fourth part of this study (Chapter 6), the novel membrane with two different wettabilities was evaluated for its resistances against organic and biological fouling in a wider prospect. The membranes in flat sheet configuration were produced from PVDF as the base matrix polymer blended with the additive polymer that was synthesized in the third stage of this study with both hydrophilic and oleophobic segments. It was found that the additive polymer significantly increased the membrane's surface porosity and suppressed the undesired macrovoid formation in the cross section. The mechanical properties of the novel membranes showed slightly lower tensile stresses but had much lower tensile strains as compared to the control PVDF membrane. The prepared novel membranes had high water affinity but low oil affinity. Experimental results showed that the novel membrane provided high water flux and showed non-organic fouling performance during the filtration of protein solution, humic acid solution and oil/water emulsion, exhibited as slow flux decay and high flux recovery after membrane cleaning. The biofouling tests, including bacteria suspension immersion and filtration with the prepared membranes, showed that the novel membranes effectively prevented bacteria adhesion on the membrane and the flux decay during filtration can be fully recovered after a membrane cleaning with water. This stage of study demonstrated that the developed novel membrane with two different wettabilities can provide good antifouling

performances for both organic and biological foulants, and thus, has a great potential for water treatment applications.

In the last part of the study (Chapter 7), a novel hollow fiber membrane with both hydrophilic and oleophobic surface properties was prepared and tested for its oil/water separation performance. The hollow fiber membrane was prepared from the popular conventional membrane material of PVDF as the base material and the synthesized copolymer with hydrophilic and oleophobic segments as the additive (denoted as AP) described in details in the third part of this study. It was found that the developed hollow fiber membrane not only showed good mechanical strength, but also had a surface that exhibited both high hydrophilicity as well as oleophobicity simultaneously. The hollow fiber membrane was packed into membrane modules that can be operated under either the dead-end or cross-flow filtration mode and tested for the treatment of artificial oily wastewater samples prepared from hexadecane or crude oil emulsions and real oily wastewater samples collected from a palm oil mill in Malaysia. The experimental results indicated that, as compared to the control PVDF membrane, the developed novel hollow fiber membrane exhibited excellent performances, with much higher pure water flux, less flux decay during oily wastewater filtration, significantly higher or almost complete flux recovery by a simple physical cleaning method (i.e., DI water flushing or backwashing) after a filtration run, having similar or usually higher oil removal efficiency than the control membrane. Since the hollow fiber membrane can be easily scaled up to the full module for practical use, there

is a great prospect for the developed novel hollow fiber membrane to be used as an effective method for oily wastewater treatment.

List of Tables

List of Figures and Schemes

Nomenclature

AFM	Atomic Force Microscopy
AP	Additive Polymer
ATR-FTIR	Attenuated Total Reflection Fourier Transform Infrared
ATRP	Atom Transfer Radical Polymerization
BE	Binding Energy
BSA	Bovine Serum Albumin
CA	Contact Angle
CLSM	Confocal Laser Scanning Microscope
CS	Chitosan Membrane
CS_Ag^{+}	Ionic silver immobilized CS membrane
CS_Ag^{0}	CS membrane with reduced metallic silver
DCC	N,N-dicyclohexylcarbodiimide
DI	Deionised
DMAP	4-(Dimethylamino)pyridine
DMF	N,N-Dimethylformamide
E. coli	*Escherichia coli*
ECH	Epichlorohydrin
EPA	Environmental Protection Agency
EPS	Extracellular Polysaccharide
FPEG	Perfluoroalkyl PEG surfactants
HA	Humic Acid
ICP-OES	Inductively Coupled Plasma-Optical Emission Spectrometer

LYZ	Lysozyme
MF	Microfiltration
MWCO	Molecular Weight Cut-Off
NF	Nanofiltration
NMP	N-Methylpyrrolidinone
NMR	Nuclear Magnetic Resonance
NOM	Natural Organic Matters
OD/ID	Outer Diameter/Inner Diameter
P(VDF-co-CTFE)	Poly(vinylidene fluoride-co-chlorotrifluoroethylene)
PAMAM	Polyamidoamine
PAN	Polyacrylonitrile
PBS	Phosphate Buffer Saline
PEG	Polyethylene Glycol
PI	Propidium Iodide
PMAA	Poly(methacrylic acid)
PMDETA	1,1,4,7,7-Pentamethyldiethylenetriamine
PP	Polypropylene
PPS-Ag	Silver immobilized PP membrane
PtBMA	Poly(tert-butyl methacrylate)
PVA	Polyvinyl alcohol
PVDF	Polyvinylidene Fluoride
PVDF-g-POEM	Amphiphilic graft copolymers consisting of a PVDF

	backbone and poly(oxyethylene methacrylate) (POEM) side chains
RFD	Relative Flux Decay
RFR	Relative Flux Recovery
RO	Reverse Osmosis
S. aureus	Staphylococcus aureus
SEM	Scanning Electron Microscope
SMCL	Secondary Maximum Contaminant Level
tBMA	tert-Butyl methacrylate
TFC	Thin Film Composite
TOC	Total Organic Carbon
TSA	p-Toluenesulfonic acid monohydrate
TSB	Tryptone Soya Broth
UF	Ultrafiltration
UV	Ultraviolet
XPS	X-ray Photoelectron Spectroscopy

Chapter 1 **Introduction**

1.1 Overview

Membrane technology has been gaining momentum for becoming separation technology of choice for many applications over the past few decades. Nowadays, membrane separation is widely incorporated into many water or wastewater treatment plants to comply with more stringent water supply or wastewater discharge regulations. The main advantages of membrane technology include high separation effectiveness, possibly free from chemical addition, simple system configuration and small footprint.

Many unit operations are employed in conventional water purification and recycling systems to effectively remove contaminants or undesired components, such as ions, charged or neutral molecules, macromolecules, virus and bacteria, fine and coarse particulates through a combination of physical and chemical processes. For instance, most bacteria, colloidal and suspended particles may be removed through flocculation, sedimentation and granular media filtration. Charged solutes such as ions may be removed by ion-exchange process and organic components are often sequestrated through adsorption with activated carbon. The treatment systems are unavoidably complex and occupy large areas of space. Nowadays a wide range of membrane-based separation processes are available to replace many of the conventional treatment processes. The operating principle of a membrane separation process is relatively simple: the membrane generally acts as a physical barrier that selectively allows water and/or other small

components to permeate through the membrane pores while rejecting components, such as suspended solids or other substances, with larger sizes that cannot pass through the membrane pores. Depending on the pore size of a membrane and the size of contaminants to be rejected, most membrane separation processes for water purification and recycling can be divided into the groups of microfiltration (MF), ultrafiltration (UF), nanofiltration (NF) and reverse osmosis (RO); as indicated in Figure 1.1. When the removal of larger particles such as sludge flocs and bacteria is intended, MF or UF membrane processes are used. Because of the porous structures of these membranes, the throughput or productivity of MF or UF processes is high and the operation pressure required is usually low or modest (less than 500 kPa). When much smaller substances such as ions and low-molecular weight organic molecules need to be removed from water, NF or RO processes are applied. In these cases, purification of contaminated water is essentially achieved by diffusion of water molecules through these non-porous membranes. The operating pressures required for NF and RO are much higher than those for MF and UF, and their permeate fluxes obtained are also much lower than those of MF and UF. Compared to conventional water treatment systems, the membrane-based separation systems are generally much simpler.

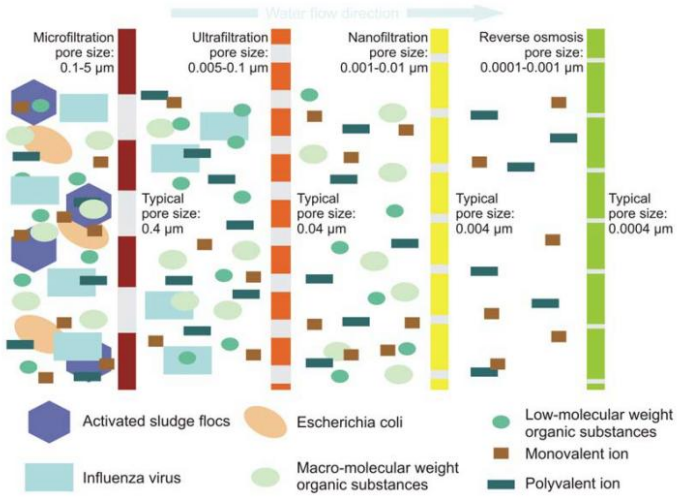

Figure 1.1 Schematics showing the separation of components in water by different types of membrane filtration systems.

Many advances made in material science and engineering in recent years have enabled more high performance materials to be fabricated into various types of membranes for applications in water purification and recycling.

Inorganic membranes for water purification are usually prepared from metallic oxides (alumina, titania and zirconia), and zeolite. The manufacturing cost of inorganic membranes is usually much higher than that of polymeric membranes. However, inorganic membranes may be preferred in separation processes that involve harsh and extreme operating conditions where polymeric membranes would degrade rapidly, i.e. high operating temperatures, radioactive/heavily contaminated feeds, and highly reactive environments (C.A.M et al., 1996).

Organic polymers have dominated the production of commercial membranes since the very beginning of the membrane industry. These polymers offer low-cost fabrication, ease of handling and improved performance in selectivity and permeability. Moreover, they can be easily derivatized physically or chemically to

provide the membranes with different structures and surface properties from a wide selection of synthetic and organic chemistries. In this study, the work is therefore focused on polymeric membranes.

Although membrane technology has its unique advantages, it also faces some challenges or problems. Especially, membrane fouling has been the major limiting factor that restricts a more widespread application of membrane technology. Membrane fouling is the process that results in a performance decrease of a membrane, caused by the deposition of suspended particles (mineral and biological) or adsorption of dissolved solutes on the external membrane surface, on or within the membrane pores (Koros 1996). Various types of foulants including inorganic (clays, flocs and mineral precipitates), organic (oils, proteins, humics) and biological (bacteria, fungi) ones can cause membrane fouling (Baker, 2004). According to the interaction strength between foulants and the membrane surface, membrane fouling may be divided into reversible and irreversible fouling (Choi et al., 2005). Inorganic fouling is usually considered as reversible fouling because it can be removed by a physical means, for example the shear force of cross-flow or backflushing. However, membrane fouling by some foulants in a membrane separation process may be considered as irreversible fouling that usually cannot be effectively removed by physical cleaning methods. Biological and organic foulants are often causing irreversible fouling.

Biological fouling or biofouling is due to the attachment and growth of microorganisms on a membrane and it is very difficult to be cleaned or recovered. Prevention of biofouling is rather challenging. Even if most of the microbes in the

feed are removed, the remaining ones still can grow and reproduce rapidly with the biodegradable substances in the feed as nutrients. Microorganisms are ubiquitous in almost any natural systems. A biofilm, soft and sticking, may be soon formed on a membrane surface, which significantly reduces the membrane's permeability, increases the operation pressure, and ultimately destroys the membrane's structure or material. Biofouling usually involves in three basic stages. Firstly, bacteria move or are brought to the membrane surfaces. Secondly, bacteria adhere and attach onto the membrane surfaces. Finally, the attached bacteria grow and multiply to form a biofilm that eventually completely foul the membrane. If a biofilm is formed, physical cleaning methods are often proven to be impossible to achieve the desired cleaning and recover the permeate flux of the membrane. Hence, to prevent membrane biofouling, a better solution could be to avoid the initial attachment of microbes onto the membrane surface. Many studies have shown that the increase of membrane surface hydrophilicity can effectively reduce or limit the adhesion of microbes. Another possible strategy to prevent biofouling can be the inhibition of microbe growth and reproduction on the membrane surface, if microbes do adhere onto it. This may be achieved by immobilizing biocides on the membrane surface to effectively kill the attached microbes. The dead microbes will become the same as mineral particles that usually cause only reversible membrane fouling and can be easily removed by physical cleaning methods.

Organic fouling is another typical type of irreversible fouling. Organic fouling is mainly caused by the adsorption or attachment of various organic substances on

the membrane surface or in the membrane pores. The attached organic substances, due to the strong chemical or physical interactions with the membrane, cannot be easily removed from the membrane by physical cleanings. Similar to biofouling, organic foulants can narrow and completely block the membrane pores, resulting in permanent lost of permeate flux. Most of the polymeric membranes commercially available in the market are hydrophobic and subject to a greater tendency of organic fouling caused by organic foulants. In general, it is commonly accepted that a more hydrophilic membrane surface provides better fouling resistance to organic foulants such as proteins and natural organic matters (NOM) in water or wastewater (Rana and Matsuura, 2010). Thus, the modification of membranes to increase their surface hydrophilicity can be one of the effective approaches to reduce organic fouling and biofouling as well.

Oils are a special group of organic substances that are highly hydrophobic or with low surface tensions. Due to the non-specific resistance effect, hydrophilic modification might reduce the possibility of oil droplets to contact the membrane surface. However, if the oil droplets are contacting with the hydrophilic surface due to the filtration convective flow, they would spread on the membrane surface or exhibit very small contact angle because the surface free energy of the hydrophilic surface is higher than the surface tensions of the oils (C.J, 1993; Stamm, 2008). This will lead to adhesion and then fouling of the membrane by oils. To effectively prevent the adhesion of oils, a membrane should be oleophobic meaning with surface energy lower than the surface tensions of oils. However, the low surface free energy membrane exhibited high hydrophobicity

that might boost other irreversible fouling caused by proteins, NOM and microbes (Rana and Matsuura, 2010). Thus, there is a great interest to develop new membranes that show both surface hydrophilicity and oleophobicity to examine their performance and potential in the prevention or reduction of membrane biological and organic fouling.

1.2 Research objective and scope of the study

The overall objective of the study is to develop membranes that could provide effective prevention or reduction of membrane biofouling and organic fouling. Various approaches that aim at controlling or altering the nature and strength of interactions between membrane surface and biological or organic foulants in water are attempted and examined.

In the prevention of membrane biofouling, two strategies will be used. One strategy is to inhibit the growth and reproduction of microbes on a membrane surface. Silver will be introduced onto membrane surfaces as a biocide. The other strategy is to avoid the attachment of microbes onto a membrane surface. A membrane surface exhibiting both hydrophilic and oleophobic surface properties will be prepared and tested with some typical microorganisms.

In the prevention of membrane organic fouling, the major attention will be placed on the prevention of organic matter adsorption on a membrane surface. Again, membrane surfaces with both hydeophilicity and oleophobicity will be prepared and tested with a broad spectrum of organic substances including protein, NOM and oils.

The special scope of this study includes the followings:

In Chapter 3, the anti-biofouling performances of chitosan membranes immobilized with silver in different oxidation states will be investigated first. Ionic silver will be immobilized onto the surface of chitosan membrane through chelating or surface complexing reactions. The immobilized silver ions on the membrane surface will be also reduced to metallic silver to obtain another type of membrane. The stability, antibacterial effect and anti-biofouling performance of the two types of membranes with ionic silver or reduced metallic silver will be evaluated.

In Chapter 4, the focus will be placed on achieving strong binding of silver ions on polypropylene (PP) membranes and examining their longer time anti-biofouling performance. PP membranes represent a common type of commercial membranes that do not have any active functional groups on the surface and therefore are impossible to immobilize silver ions directly. A method will thus be developed to graft the thiol groups onto the PP membrane surface because the thiol functional groups are known to bind silver ions strongly. The prepared membrane surface properties and the stability of the immobilized silver ions will be evaluated. Moreover, the antibacterial and anti-biofouling performances of the prepared membranes will be also examined.

In Chapter 5, an additive polymer will be synthesized by graft copolymerization of tert-butyl methacrylate (tBMA) from poly(vinylidene fluoride-co-chlorotrifluoroethylene) (P(VDF-co-CTFE)) *via* ATRP. Subsequently, the poly(tert-butyl methacrylate) (PtBMA) side chain of the graft copolymer (P(VDF-co-CTFE)-g-PtBMA) will be hydrolyzed to give poly(methacrylic acid)

(PMAA) side chain. Steglich esterification will be then used to react the perfluoroalkyl PEG surfactant (FPEG) onto the P(VDF-co-CTFE)-g-PMAA to produce the additive polymer. The synthesis processes will be verified with FTIR and NMR spectra. Flat membranes will be prepared by blending polyvinylidene fluoride (PVDF) with the additive polymer in different ratios. The hydrophilicity and oleophobicity of the prepared membranes will be investigated. The antifouling performances of the prepared membranes for oil will be evaluated through filtration of oil/water emulsion.

In Chapter 6, the novel flat membranes with both surface hydrophilicity and oleophobicity will be prepared from PVDF and the additive polymer at different casting solution concentrations. The performance of the membranes in resistances to biological and organic fouling will be more comprehensively evaluated through the use of different foulants including protein, NOM, bacteria and oil.

In Chapter 7, novel hollow fiber membranes will be spun from the mixture of PVDF and the additive polymer. Hollow fibers will be packed into a membrane module. A cross-flow membrane filtration system will be set up to simulate the real application environment for the fabricated membranes. The properties of the hollow fiber membranes will be characterized, and the separation efficiency and antifouling performance of the developed hollow fiber membranes will be examined with various oily water samples, including hexadecane/water emulsion, crude oil emulsion and real palm oil mill wastewater.

This study should provide more solutions and greater insights that can contribute to the effective prevention or reduction of biological and organic fouling of polymeric membranes in water or wastewater treatment applications.

Chapter 2 **Literature review**

2.1 Membrane cleaning methods

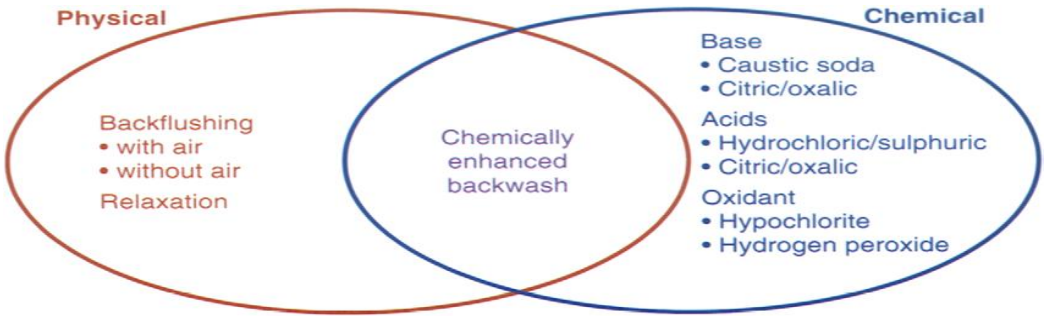

Figure 2.1 Membrane cleaning methods (Judd et al., 2006).

Membrane fouling is the major obstacle for the effective application of membrane technology. When membrane fouling occurs to a certain extent, cleaning the fouled membrane is the first thought coming into our minds. Membrane cleaning is often applied when a significant decrease in permeate flux is observed or when the transmembrane pressure has to be raised significantly to maintain the designed permeate flux (Li and Elimelech, 2004).

Membrane fouling is caused by the physical and chemical interactions between foulants and the membrane surface (Childress and Elimelech, 2000; Hong and Elimelech, 1997). In order to break these built up interactions, various physical and chemical cleaning methods are normally used; as indicated in Figure 2.1. However, physical cleanings such as back flushing are often only limited to the removal of physical deposits from the membrane surface and can require a tremendous operating pressure.

For chemical cleaning methods, different categories of cleaning agents are commonly used: alkalines, acids, surface-active agents, enzymes and disinfectants (Tragardh, 1989). These compounds are also mixed to achieve a better cleaning effect. Chemical cleaning of fouled membranes is realized through chemical reactions between the chemical agents and the foulants. A cleaning agent cleans the membrane by removing the foulants, changing the morphology of the foulants, or altering the surface chemistry of the fouling layer (Weis et al., 2003). A high effectiveness of chemical cleaning is difficult to achieve. Besides the fouling condition, it also depends on various factors, including temperature, pH, concentration of the cleaning chemicals, contact time with the cleaning solution, and operating conditions, such as cross-flow velocity and pressure (Bohner and Bradley Jr, 1992; Daufin et al., 1991). Moreover, the cleaning agents used in chemical treatments are often very aggressive and they can cause permanent damages to the membrane's surface selective layer (Kochkodan et al., 2008).

Both physical and chemical membrane cleaning methods can be expensive and they often work more effectively in reducing the effect of reversible membrane fouling than that of irreversible membrane fouling.

2.2 Membrane biofouling and prevention strategies

The irreversibly fouled membranes are difficult to be effectively cleaned. Hence, membrane fouling prevention strategies are applied to limit the formation of irreversible fouling.

Membrane biofouling is the undesirable attachment and reproduction of microbes on a membrane surface to form biofilms that result in reduced

performance, including severe flux decline, high energy consumption, and frequent membrane cleaning or shortened membrane life, which directly leads to large increases in maintenance and operating costs of the membrane systems (Miura et al., 2007). Thus, it is a major performance limiting factor in membrane filtration processes. Furthermore, biofouling is intrinsically more complicated than other membrane fouling phenomena because microorganisms can grow, multiply and relocate. Hence, even 99.9% removal of microorganisms from a feed stream still cannot impede the eventual formation of a biofilm (Flemming et al., 1997). Therefore, the effective control of membrane biofouling is one of the issues of particular concerns in modern membrane and membrane process development.

2.2.1 Feed water preliminary treatments

Preliminary treatment of feed water is an approach to prevent membrane biofouling. It usually reduces the number of bacteria or the amount of nutrients before the filtration of the feed water (Baker and Dudley, 1998). It had been suggested that feed water pretreatment to prevent cell deposition and subsequent growth would be a more effective method to deal with biofouling than subsequent membrane chemical cleaning (Speth et al., 1998).

The most direct pretreatment is to eliminate microbes in feed water. Biocides such as chlorine, ozone, and UV have been used to control microbial growth correlated to the biological fouling of membranes. It is a normal practice to chlorinate the feed water to kill microbes and it is necessary to dechlorinate with sodium bisulfate prior to the water entering the membrane section (Al-Ahmad et

al., 2000). Ozone was also used to disinfect feed water before membrane filtrations (Lee et al., 2005; Van der Hoek et al., 2000). UV treatment is gaining its popularity now since it does not produce any by-products during disinfection (Kim et al., 2009). Some other biocides were also added into feed water to test their anti biofouling performances. For example, molecularly capped silver nanoparticles were used as a pretreatment strategy for controlling biofilm development in aqueous suspensions using the model organism *Pseudomonas aeruginosa* (Dror-Ehre et al., 2010). On the other hand, UF was used as a pretreatment to remove most microorganisms from the feed to RO to prevent biofouling of RO membrane (Gwon et al., 2003). In this case, the less expensive UF membrane was sacrificed and subject to sever biofouling.

Attempts were also made to remove nutrients from feed to control membrane biofouling. For example, a chemical coagulation of phosphate in wastewater effluents was used as a pretreatment to remove nutrients for RO process in order to reduce biofouling (Katz and Dosoretz, 2008). Filter absorber (often packed with activated carbons) was used to remove biodegradable organic matters that were considered to be the nutrients of microbes in feed to minimize the biological and organic fouling of the membrane process (Kwon et al., 2005; Wend et al., 2003).

In order to achieve both disinfection and organic substance removal, combined pretreatment schemes, including ozonation, biological activated carbon filtration and slow sand filtration, was used to treat RO feed water (Van der Hoek et al., 2000).

Even pretreatments such as chlorinate might reduce the potential of membrane biofouling, the membranes still could be subject to biofouling because of the reproductivity of the remaining microbes in feed.

2.2.2 Surface modifications

Bacterial adhesion is one of the most important processes in the formation of biofilm that causes serious membrane biofouling. Bacterial adhesion is influenced by the properties of bacteria, membrane surface and feed water. The feed water can be pretreated as mentioned before. However, in practice, it is also desired that membrane surface can be modified to reduce bacterial adhesion, and then ultimately prevent biofouling of the membrane surface.

Various membrane surface properties, including roughness, surface charge and hydrophobicity, have been related to membrane biofouling (Gerhart et al., 1992; Pasmore et al., 2001). The correlations of each of the membrane surface properties with membrane biofouling mechanisms are different.

Surface roughness of a membrane may affect bacterial attachment in two main aspects. Rough surface can disrupt the fluid flow and create areas of low shear rate. Thus, the shear force at the membrane surface that might remove the attached bacteria is significantly reduced (Pasmore et al., 2001). In addition, high roughness of a membrane will produce more surface area that provides more sites available for cells to attach (Geesey et al., 1996). Therefore, surface roughness is expected to positively contribute to bacterial attachment and biofilm formation (Knoell et al., 1999; Park et al., 2005). Researchers have attempted to reduce membrane surface roughness to limit membrane biofouling. The surface

roughness of PVDF MF membrane was reduced through grafting with poly(ethylene glycol) methacrylate *via* surface-activated ozone treatment and thermally induced graft copolymerization. The modified PVDF MF membranes exhibited enhanced antifouling properties (Chang et al., 2008b). However, it was found that that surface roughness will only delay the onset of the biofilm but could not prevent the biofilm formation completely (Bos et al., 1999).

Bacteria attachment was also associated with membrane charge (Knoell et al., 1999; Liu et al., 2010; Pasmore et al., 2001). As most of the bacteria surfaces are negatively charged in water, positively charged membrane surfaces will attract them and kill them as well (Cheng et al., 2008). Researchers had produced positively charged surfaces to control biofilm formation. In an effort to reduce biofouling, a positively charged polymer was grafted onto a membrane surface to inhibit bacterial growth (Malaisamy et al., 2010). Positively charged polymer brushes were coated onto materials to prevent growth of adhered bacteria, and the results showed a large reduction in adhesion of a great variety of microorganisms (Grundke et al., 2006).

On the contrary, negatively charged membrane surface can repulse negatively charged bacteria in aqueous solutions, and then reduce biofouling (Norberg et al., 2007). Zhao and his co-workers grafted two oppositely charged monomers onto a PP membrane to achieve balancedly charged or more negatively charged surface to effectively prevent bacteria adhesion (Zhao et al. 2010).

Even membrane surface charge plays a significant role in the prevention of bacterial adhesion; the prevention effect would not last for a long time. It was

reported that on the negatively charged surfaces, despite a slower initial adhesion, surface growth of the adhered bacteria was exponential for both Gram-positive and Gram-negative strains (Gottenbos et al., 2001).

Hydrophilicity was another factor reported to be closely connected with bacterial adhesion behavior on membrane surfaces. Researchers showed that cells can attach to both hydrophobic and hydrophilic surfaces (Brinck et al., 2000). It was reported that the adhesion of microorganisms to more hydrophobic surfaces is greater and stronger than to hydrophilic surfaces (Kochkodan et al., 2008; Morra and Cassinelli, 1997). Hydrophilic surfaces were found to be much less likely to be fouled by *P. aeruginosa*, a common bacteria found in natural water, than hydrophobic surfaces (Pasmore et al., 2001). Consequently, there have been many attempts to mitigate biofouling through hydrophilic modification of membrane surfaces. Poly(ether sulfone) UF membranes were modified by photolysis with ultraviolet light and then graft polymerization of hydrophilic monomers onto the membrane surface to create more hydrophilic and thus lower fouling membrane surfaces (Pieracci et al., 1999). PVDF MF membranes were grafted with hydrophilic poly(ethylene glycol) methacrylate *via* surface-activated ozone treatment and thermally induced graft copolymerization (Chang et al., 2008b). Expanded poly(tetrafluoroethylene) membranes were also grafted with poly(ethylene glycol) methacrylate macromonomer *via* surface-activated plasma treatment and thermally induced graft copolymerization to increase the hydrophilicity and resist to fouling of the membranes (Chang et al., 2008a). Polyamide RO membranes were also modified by in situ cross-linking of amine-

functional polyamidoamine (PAMAM) dendrimers and PAMAM-polyethylene glycol multi-arm stars with difunctional PEG crosslinkers, resulting in more hydrophilic membranes with the potential for increased resistance to fouling by hydrophobic foulants (Sarkar et al.). Membranes have been prepared by incorporating in-situ hydrophilic surface modifying macromolecules into the thin-film-composite membranes, and the obtained membrane surfaces became significantly more hydrophilic to resist biofouling (Rana et al., 2011). Luo and his co-workers have attempted to modify poly (ether sulfone) UF membrane with self-assembly TiO_2 nanopartices to improve its hydrophilicity and they found that the prepared membrane showed good antifouling performance (Luo et al., 2005).

An adequate control of the three major properties mentioned above in membrane surface modification may play some important roles in inhibiting the initiation of biofilm formation and thus preventing or reducing membrane biofouling. To further ensure the effect, additional measures such as antimicrobial function, membrane cleaning, and reduction of soluble organic nutrients in the feed can be useful to increase the ability of membranes to resist biofilm formation.

2.2.3 Biocides immobilization

Biocides have been immobilized onto membrane surfaces to provide them with antibacterial function for the prevention of biofouling. This is different from adding disinfectants into the feed as a pretreatment. This approach is to introduce, on membrane, antibiotic slow-releasing materials that are able to mediate direct killing of microbes upon contact (Golomb and Shpigelman, 1991). Neodymium (III) and Zn (II) complex has been used to kill *E. coli* (Li et al., 2009). Zinc oxide

nanoparticles were found to have antibacterial activity against *E. coli* as well (Liu et al., 2009). However, many of such biocides used are also harmful for human beings.

Silver is an effective antibacterial metal that has been known by human being for a very long time (Ghandour et al., 1988). Despite the fact that silver possesses antibacterial efficacy equal to or greater than other heavy metals, silver has been known to have almost no toxic effects on mammals (Yimin Qin, 2007). Currently, the secondary maximum contaminant levels (SMCLs) set by U.S. Environmental Protection Agency (EPA) for silver is 0.1 $mg \cdot L^{-1}$ in water supply (United States. Environmental Protection Agency., 1984). This is established only as a guideline to assist the public water systems in managing their drinking water for aesthetic considerations, such as taste, color and odor. Contaminants are usually not considered to present a risk to human health at the SMCLs. In addition, very low concentrations of silver ions ($<0.001 mg \cdot L^{-1}$) have been reported to be effective in the antibacterial performance (Ghandour et al., 1988; Giangiordano and Klein, 1994).

Some researchers have examined silvers' effect on membrane anti-biofouling performance. Lee et al. immobilized silver nanoparticles onto the surface of the polyamide NF membrane to prevent biofouling (Lee et al., 2007). Silver nanoparticles were also coated onto a commercial polyamide RO membrane for mitigating biofouling in seawater desalination (Yang et al., 2009). Chitosan, a biopolymer, has been well know to show excellent heavy metal-binding capacities, such as chelating with silver ions (Ma et al., 2008). The antibacterial properties of

the chitosan-nylon-6 blended membranes by loading silver ions were shown to be effective to both Gram-negative and Gram-positive bacteria. Fu and his coworkers fabricated chitosan/heparin antibacterial multilayer films and found that the antibacterial effect could be significantly enhanced by the incorporation of silver nanoparticles into the multilayer films (Fu et al., 2006).

The immobilization of silver on membranes was usually achieved by chelating with the amino groups on membranes or blending silver nanoparticles with the membrane materials during membrane preparation. The stability of immobilized silver was often a concern. Chen et al (Chen et al., 2005) reported the fabrication of thiourea chitosan–Ag^{+} complex which showed a wide spectrum of antimicrobial activities. In addition, the thiol group was reported to provide stronger interaction with silver ions (Shea and Maccrehan, 1988). Thus, it is greatly possible that the strong coordination between silver ions and thiol groups can be used as a method to enhance the stability of immobilized silver on a membrane surface.

2.3 Membrane organic fouling and prevention strategies

Membrane organic fouling is another type of irreversible fouling. Successful application of membrane technology, also often requires efficient control of membrane organic fouling. Organic fouling, often associated with the adsorption or accumulation of organic substances on the membrane surface or within the membrane pore structure, decreases membrane performance and ultimately shortens membrane's life. A wide spectrum of organic matters in process waters were found to contribute to membrane fouling (Kaiya et al., 1994).

Dissolved natural organic matters (NOM) are considered to be a major source of organic matters for fouling in membrane filtration of natural waters (Kaiya et al., 1994). Several studies have shown that the extent of NOM fouling is greatly influenced by the hydrophobicity of the membrane and NOM. Static adsorption experiments by Jucker and Clark demonstrated that humic macromolecules adsorbed more significantly onto hydrophobic membranes (Jucker and Clark, 1994). Other studies also investigated the effect of NOM properties on NOM fouling of NF membranes. NOM was fractionated into hydrophilic and hydrophobic components. Fouling tests revealed that the hydrophobic fraction of NOM was mostly responsible for permeate flux decline, whereas the hydrophilic fraction caused much less fouling (Nilson and DiGiano, 1996).

Proteins are also considered to be important organic foulants during membrane filtrations. Protein–membrane and protein–protein interactions are the main factors determining the membrane organic fouling caused by proteins. The protein–protein interactions influenced by solution chemistry of the feed, including pH, ionic strength, and ionic composition, affect the structure of the cake layer formed on the membrane surface (Huisman et al., 2000). On the other hand, the protein–membrane interactions influenced by the membrane surface properties affect irreversible adsorption onto the membrane surface and within the membrane pores (Kang et al., 2007). Proteins usually show more significant adsorption on a hydrophobic surface than a hydrophilic one (Krishnan et al., 2008). As one of the main components of microbes, proteins have also been used

as probes of biofouling to evaluate membranes' anti-biofouling performances (Hyun et al., 2006; Wang et al., 2006b; Zhao et al., 2010).

Oils are another group of organic foulants causing membrane organic fouling. In oil industry such as oil and natural gas drilling, petroleum refining and processing, large quantities of oily wastewater is generated. In addition, ocean oil spill accident produces another source of oily wastewater that is often directly harmful to the ocean environment and human health. The oily wastewater is not only a scientific and industrial problem, but also an environmental and health concern. Oily wastewater is very difficult to be efficiently treated. The conventional methods treating oily water usually cannot meet today's effluent standards for discharge or reuse because of the remaining stable emulsified oil that is difficult to be removed (Cheryan and Rajagopalan, 1998). However, the UF membrane was shown the promising results for achieving required discharge specifications for the treatment of oil industry wastewater by effectively removing emulsified oil (Bilstad and Espedal, 1996; Cheryan and NetLibrary Inc., 1998; Elmaleh and Ghaffor, 1996b; Santos and Wiesner, 1997; Teodosiu et al., 1999). The permeate of the UF treatment is usually clean enough for discharge; and the concentrated oil phase (typically 3-5wt%) can be recovered or incinerated (Cheryan and NetLibrary Inc., 1998). Unfortunately, the prospect of UF treatment has been greatly limited due to the severe oily fouling of the conventional membranes (Bilstad and Espedal, 1996; Santos and Wiesner, 1997).

2.3.1 Hydrophilic modification

Studies have been conducted to inhibit or control membrane organic fouling. In general, hydrophilic modification has been the main strategy to inhibit or reduce membrane organic fouling. Thus, there have been significant amounts of studies for organic fouling control by membrane hydrophilic modification.

Membrane surface modification for increased hydrophilicity can be carried out in several ways. The various physical or chemical membrane surface modification processes can be classified into the following groups: (1) adsorption of hydrophilic components to the membrane surface; (2) coating of hydrophilic components to the membrane surface; (3) surface chemical reaction that introduces different hydrophilic functional groups to the membrane surface; (4) surface graft copolymerization of hydrophilic monomers or polymers onto the membrane surface and (5) incorporation of hydrophilic polymers or nanoparticles with matrix polymer to produce hydrophilic membrane surface (Rana and Matsuura, 2010).

Surface adsorption and coating are popular methods to enhance membrane surface hydrophilicity with little or nil chemical reactions. For example, PS membranes were adsorbed with various polymers and surfactants to increase their hydrophilicity for resisting protein fouling (Brink and Romijn, 1990; Fane et al., 1985; Kim et al., 1988). Hydrophilization has also been achieved by coating the membrane surface with more hydrophilic compounds. It has been reported that stable performance over time has been attributed to a hydrophilic poly(vinyl alcohol) (PVA) coating on the surfaces of conventional hydrophobic RO or NF membranes, (Tang et al., 2009) and UF membrane (Wang et al., 2006a). However,

the surface layer prepared through this approach is physically bound to the membrane surface and therefore could easily leach away or be detached, and the functions eventually diminish after extended usage of the membranes.

To overcome the low stability of physically coated layers, another effective method to enhance membrane surface hydrophilicity is to use chemicals such as strong acids/bases, or high energy irradiation sources such as plasma and UV to permanently alter the surface properties of the membranes. Through optimizing the modification chemistry, hydrophilic functional groups can be produced on the membrane surfaces to boost their hydrophilicity. For example, poly(vinyl butyral) UF membrane was treated with hydrochloric acid to resist BSA fouling (Ma et al., 2007). PAN UF membrane was reacted with organic bases (ethanolamine, triethylamine) and inorganic bases (NaOH, KOH) to prevent BSA fouling (Lohokare et al., 2006). PS membranes were treated with CO_2 plasma, (Gancarz et al., 1999) N_2 plasma (Gancarz et al., 2000) and O_2 plasma (Kim et al., 2002) to inhibit protein fouling. NOM fouling of PES and sulfonated PS membranes were reported to be significantly reduced after UV treatment of the membranes (Kilduff et al., 2000).

Surface grafting covalently attaches functional monomers onto the membrane surface *via* either free radical-, photochemical-, radiation-, redox- or plasma-induced grafting. A variety of functional monomers are available for preparing multifunctional membranes. To improve membrane hydrophilicity, hydrophilic functional monomers can be grafted onto the membrane surfaces. For example, a layer of polymer brushes is formed by gas plasma surface activation followed by

free radical graft polymerization using methacrylic acid or acrylamide monomers onto the surface of conventional PA TFC membranes to effectively reduce the adhesion of foulants (the protein BSA and alginic acid) (Lin et al.). Hydrophilic monomers were also grafted onto PES UF membranes *via* UV induced graft polymerization to render the membrane surfaces more hydrophilic and less prone to biofouling (Pieracci et al., 1999).

Incorporation of hydrophilic polymers or nanoparticles with membrane matrix polymer is another method for membrane hydrophilic modification. For example, UF membranes was prepared through blending of Pluronic F127 with poly(ether sulfone), resulting in remarkable reduction of the irreversible fouling of BSA (Wang et al., 2005b; Wang et al., 2006c). Titanium dioxide (TiO_2)-entrapped Poly(phthalazine ether sulfone ketone) UF membranes were prepared by dispersing uniformly nanosized TiO_2 particles in the casting solutions, and the obtained membrane exhibited significant improvement in the antifouling properties for BSA (Li et al., 2007).

It is clear that membrane surface hydrophilic modification will improve membrane's resistance to organic foulants such as proteins and NOM. However, oils are different from other organic foulants because of their very low surface tensions. Membrane surface is hydrophilic because its high surface free energy that provides good affinity with water which also has high surface tension (72.8 $mN \cdot m^{-1}$, 20 °C) (Speight and Lange, 2005). However, oils such as decane (23.83 $mN \cdot m^{-1}$, 20 °C) and hexadecane (27.47 $mN \cdot m^{-1}$, 20 °C) have much lower surface tensions than water (Speight and Lange, 2005). When oils are in contact with

surfaces that have higher surface free energy, the contact angles will be low, according to Young's equation (Stamm, 2008). In other words, a hydrophilic surface is not simply equal to an oleophobic surface.

2.3.2 Oleophobic modification

Some attempts have been made to increase the oleophobicity of a membrane surface to prevent organic fouling caused by oily foulants, especially during the filtration of oil/water emulsions. The oleophobic surfaces providing resistances to oils should usually have lower surface free energies than oils.

Hamza et al. proposed a modification of polyethersulfone UF membrane utilizing low surface free energy (oleophobic) macromolecules to reduce the fouling of the membrane for the treatment of oil/water emulsion (Hamza et al., 1997). Fluoropolymer with low surface free energy was coated onto the membranes *via* initiated chemical vapor deposition (Gupta and Gleason, 2009).

There were researches focused on the preparation of polymers with oleophobic surfaces though not on membranes. For example, to improve oil and water repellency, fluorine-containing block copolymers, which were composed of methyl methacrylate, glycidyl methacrylate, and 1H, 1H, 2H, 2H-heptadecafluorodecyl acrylate, were blended with an epoxy resin (Kasemura et al., 1993). Functionalized perfluoropolyethers with water- and oil-repellent wetting properties have been reported (Gan et al., 2002). Polyimides, which are high-thermal resistant heteroaromatic polymers, were synthesized, and fluor oligomers were added to these polymers to obtain hydrophobic–oleophobic properties (Uyanik et al., 2006).

Although surfaces with low surface energies can prevent the adhesion of oils, they exhibit poor affinity with water or are highly hydrophobic. Hydrophobic surfaces are easily subject to fouling by many other biological and organic foulants as reviewed earlier. In addition, hydrophobic membrane can result in high water resistance and low permeate water flux.

2.3.3 Hydrophilic and oleophobic modification

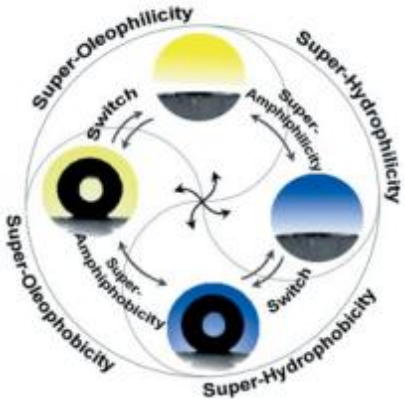

Figure 2.2 Schematics showing the major superwetting/antiwetting surfaces and their relations (Feng and Jiang, 2006).

Membrane surfaces with single wetting property inevitably have some drawbacks when the membranes are dealing with different biological and organic foulants. However, as shown in Figure 2.2, a surface can be made to simultaneously obtain two different wetting properties. This shows a prospect in membrane surface modification to optimize the performance of membranes for effective prevention of fouling by various organic components. It can be expected that membrane surfaces with different wetting properties including hydrophilicity and oleophobicity will be more effective to improve the membrane's antifouling performance.

Researchers have attempted to covalently attach perfluorinated end-capped polyethylene glycol surfactants whose perfluorinated end is oleophobic and the PEG chain is hydrophilic onto fritted glass membranes as a means to improve the separation performance of the membrane for oil/water emulsion (Howarter and Youngblood, 2009). However, glass membranes are more expensive and difficult to prepare than polymeric membranes.

Some researchers synthesized hydrophilic and oleophobic polymers (Perrier et al., 2003). Monomers were copolymerized with a water–oil discriminate fluorosurfactant to create hydrophilic–oleophobic coatings that rendered the surfaces with hydrophilicity and oleophobicity (Howarter et al., 2011). A surface-active polymer was obtained by grafting fluorinated molecules with hydrophilic and oleophobic blocks to a block copolymer precursor, as shown in Figure 2.3 (Krishnan et al., 2006).

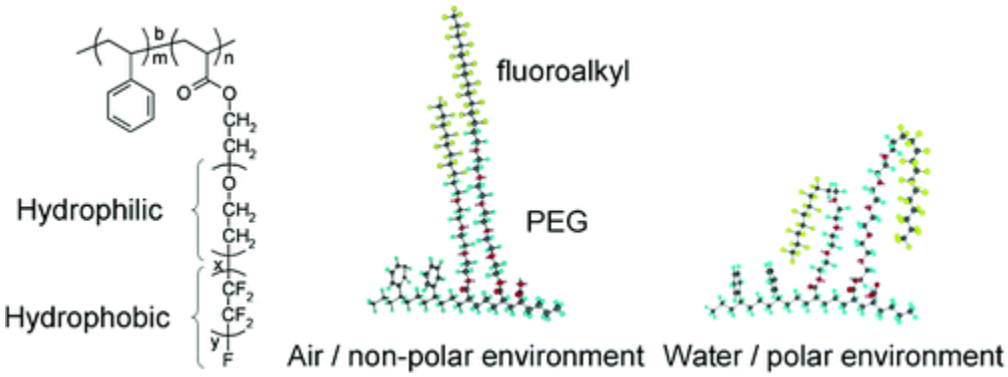

Figure 2.3 Proposed mechanism for surface reconstruction of the ethoxylated fluoroalkyl side chains upon immersion of the surface in water (Krishnan et al., 2006).

Researches focusing on the development of polymeric membrane surface with two different wettabilities are very limited. One group constructed ternary amphiphilic block copolymers consisting hydrophilic block (polyethylene oxide),

and nonpolar hydrophobic fluorine-containing blocks (oleophobic) as additive to prepare modified PVDF antifouling membranes (Chen et al., 2011b). However, the prepared membranes' water contact angles were still all above 80°, indicating hydrophobic membrane surfaces. It was also reported that hydrophilic and oleophobic monomers were grafted onto cellulose acetate (CA) rigid backbone, and then, the modified CA was used to prepare antifouling membranes (Chen et al., 2011a). However, gradually grafting two types of monomers onto the same active site made this approach more complicated, time consuming and difficult to control.

Chapter 3 **Membranes immobilized with ionic or reduced silver and their anti-biofouling performances**

Summary

Silver was immobilized onto the surface of a chitosan membrane to examine the anti-biofouling performance of the membrane surface. The chitosan base membrane (denoted as CS) was first immobilized with ionic silver (denoted as CS_Ag^+) and then the CS_Ag^+ membrane surface was chemically treated to obtain the membrane surface with reduced or metallic silver (denoted as the CS_Ag^0). The oxidation states of the immobilized silver on CS_Ag^+ and CS_Ag^0 and the interaction between silver and CS were investigated with X-ray photoelectron spectroscopy (XPS). The stability of the immobilized silver on the two types of membrane surfaces was evaluated through a leaching test. It was found that silver was effectively immobilized onto CS through surface complexation and the immobilized silver on CS_Ag^0 was at a reduced or lower oxidation state and was more stable than that on CS_Ag^+. Antibacterial and anti-biofouling experiments for CS, CS_Ag^+ and CS_Ag^0 were conducted with two types of typical bacteria, i.e., *E. coli* and *Pseudomonas sp.*. From the disk diffusion tests (24 h), it was found that, as compared to CS, both CS_Ag^+ and CS_Ag^0 showed significantly improved antibacterial performance, even though the CS_Ag^+ membrane surface seemed to exhibit slightly stronger antibacterial effect than the CS_Ag^0 membrane surface. In the longer time immersed experiments for anti-biofouling performance (up to 10 d), both CS_Ag^+ and

CS_Ag^0 showed much less biofouling than CS and they behaved almost equally good in their anti-biofouling behavior initially (24 h), but the CS_Ag^0 membrane surface gradually exhibited more stable and eventually better anti-biofouling performance than the CS_Ag^+ membrane surface afterwards. The results in this study demonstrated that the immobilization of silver onto membrane surfaces can be an effective method to improve a membrane's anti-biofouling property. The study was also the first of its kind that evaluated the relative anti-biofouling performance by immobilized silver in ionic and reduced states on a membrane surface.

3.1 Introduction

Membrane biofouling usually refers to the undesirable accumulation of microorganisms on a membrane surface. Membrane biofouling is one of the most common and serious problems in many membrane separation applications such as membrane bioreactor and reverse osmosis desalination (Baker and Dudley, 1998; Flemming et al., 1997; Miura et al., 2007). Membrane biofouling causes a number of problems including the increase in the operational pressure and the decline in the permeate quantity and quality of the membrane systems. More seriously, biofouling often makes the membrane become non-regenerable and thus more frequent replacement of the membrane is incurred, which significantly contributes to the application cost (Baker and Dudley, 1998).

Membrane biofouling is initiated by microbes that attach and grow on the surface of the membranes in use (Flemming et al., 1997; Vrouwenvelder and van der Kooij, 2001). Since most conventional membranes are prone to bacteria

attachment and growth (Baker and Dudley, 1998; Flemming et al., 1997), the common strategy in preventing membrane biofouling is often to add biocides or antibacterial agents, such as chlorine, into the feed stream of the membrane process. However, even though 99.99% of bacteria are killed in the feed, this approach may not be effective to eliminate membrane biofouling because the remaining bacteria can still migrate and multiply rapidly.

Besides chlorine, silver has been another type of biocide or antibacterial agent widely used or studied in many other application fields, in spite of the fact that the study of silver for the purpose of membrane anti-biofouling has been very limited. Lee et al. reported the immobilization of silver nanoparticles onto the surface of polyamide nanofiltration membrane for anti-biofouling performance. The silver nanocomposite membrane was shown to effectively prevent biofouling, and preserve the nanofiltration membrane performance (Lee et al., 2007).

Silver as an effective antibacterial metal has been known by mankind for hundreds of years (Ghandour et al., 1988). Although silver possesses antibacterial efficacy equal to or greater than other heavy metals, silver has almost had no known toxic effects on mammals, including human beings. Currently, the Secondary Maximum Contaminant Levels (SMCLs) set by the U.S. environmental protection agency (EPA) for silver in drinking water is 0.1 $mg \cdot L^{-1}$ (United States. Environmental Protection Agency., 1984). This level is established only as a guideline to assist the public water systems in managing their drinking water for aesthetic considerations, such as taste, color and odor. Contaminants are not usually considered to present a risk to human health at the

SMCLs. However, very low concentrations of silver ions (<0.001mg·L^{-1}), have been reported to be effective in killing bacteria (Ghandour et al., 1988; Giangiordano and Klein, 1994).

The antibacterial mechanism of silver ions has been related to their interaction with the thiol (-SH) group of cysteine that normally exists in the cell membrane of a bacterium (Liau et al., 1997; Matsumura et al., 2003). Silver ions can react with cysteine by replacing the hydrogen atom of the thiol group to form a S–Ag complex, thus hindering the normal enzymatic function of the affected protease (Kim et al., 2008). This kind of denaturing of the enzyme is lethal for living bacteria. Moreover, as reported by various researchers, not only silver ions (Chen et al., 2005; Feng et al., 2000; Ma et al., 2008), but also reduced metallic silver can be used for disinfection purpose (Lok et al., 2006; Sanpui et al., 2008). When metallic silver is exposed to aqueous environments, some ionic silver species would be produced and released. Therefore, the antibacterial mechanism of metallic silver has been considered to be the same as that of silver ions (Fu et al., 2006; Lok et al., 2006). The good antibacterial efficacy of silver and its non-toxicity to human beings has therefore made silver a desired candidate as the biocide for membrane anti-bifouling performance in water or wastewater treatment. An effective strategy to achieve this could be the immobilization of silver directly onto the surfaces of the membranes to be used.

Chitosan, a biopolymer produced from the deacetylation of chitin that is one of the most abundant natural polymers on the earth, has widely been studied in recent years. Owing to the high content of active amino groups, chitosan can

easily chelate with transitional metals, and therefore is extensively explored for the application of removing toxic heavy metal ions in water or wastewater. For example, chitosan was made into hydrogel beads to adsorb lead (Jin and Bai, 2002), copper (Li and Bai, 2005; Ngah et al., 2002) and mercury (Li and Bai, 2005). Furthermore, chitosan has been used directly or blended with cellulose acetate to prepare adsorptive hollow fiber membranes for the removal of heavy metal ions (Liu and Bai, 2005; Liu and Bai, 2006; Vincent and Guibal, 2001). The ability of chitosan to chelate transitional metal ions provides a good prospect for the immobilization of silver ions onto chitosan-based membranes to obtain the membrane anti-biofouling property. In the literature, there have been reports on the preparation of chitosan-Ag nanoparticle composite for the inactivation of *E. coli* (Sanpui et al., 2008) and the preparation of thiourea chitosan flakes coordinated with ionic silver for antimicrobial activity of bacteria and molds (Chen et al., 2005).

In this chapter, the anti-biofouling performances of chitosan membranes immobilized with silver in different oxidation states were investigated. Ionic silver was firstly immobilized onto the surface of chitosan membrane through chelating or surface complexing reactions. The immobilized silver ions on the membrane surface were also reduced to metallic silver to obtain another type of membrane. The stability, antibacterial effect and anti-biofouling performance of the two types of membranes with ionic silver or reduced metallic silver were evaluated.

3.2 Materials and methods

3.2.1 Materials

Chitosan flakes (85% deacetylated), silver nitrate, ascorbic acid, glutaraldehyde, hexadecane, chloroform, ethylacetate and epichlorohydrin (ECH) were purchased from Sigma-Aldrich. Silver standard solution (1000 $mg \cdot L^{-1}$) and acetic acid were supplied by Merck. Phosphate Buffer Saline (PBS, 10x) was supplied by 1^{st} BASE, diluted by 10 times and sterilized before use. LIVE/DEAD Bacterial Viability Kit L-13152 (BacLight) was purchased from Invitrogen, including two nucleic acid-binding stains: SYTO 9 and propidium iodide (PI) in solid forms. One pipet of SYTO 9 (yellow-orange solids) and one pipet of PI (red solids) were dissolved together into 5 mL 0.85 % NaCl solution to obtain a BacLight stock solution. All chemicals used in the study were of the reagent grade. Deionized (DI) water was used to prepare all solutions as needed in the study.

3.2.2 Preparation of silver immobilized membranes

Chitosan base membrane was prepared by the general method available in the literature (Liu et al., 2010). In this study, 3g chitosan flakes was first dissolved in 200 mL acetic acid solution (1.5% w/v) in a 500 mL beaker stirred at 200 rpm and 70 °C on a magnetic hot-plate stirrer. The heating and stirring continued until the solution volume in the beaker was reduced, due to evaporation, to a volume of 150 mL to obtain a 2% (w/v) chitosan solution. The solution was subsequently spread and cast onto a glass plate to form a membrane film with a thickness of around 1 mm. The membrane film was solidified in a 4% (w/v) NaOH solution for 5 h and subsequently washed with DI water. The prepared membrane film was

then cut into discs with a diameter of 47 mm or 19 mm and stored in DI water for further use.

To increase the strength and chemical stability, the prepared chitosan membrane was cross-linked in an ECH solution that was prepared by adding ECH into 0.067 M NaOH solution to obtain an ECH concentration of 0.10 M. The cross-linking reaction was conducted by placing five pieces of the chitosan membranes with a diameter of 47 mm or thirty pieces of the chitosan membranes with a diameter of 19 mm into 200 mL of the prepared ECH solution in a beaker. The contents in the beaker were shaken at 160 rpm and 45 °C for 2 h in a water bath shaker. After cross-linking, the chitosan membrane, denoted as CS, was washed with DI water.

Then, a CS membrane was placed into 10 mL 0.05 M $AgNO_3$ solution in a beaker to immobilize silver ions onto the surface of the membrane under room temperature (23-25°C). The process continued for 24 h with shaking at 160 rpm on a shaker. The concentrations of silver ions in the solution before and after the immobilization process were analyzed with an inductively coupled plasma-optical emission spectrometer (ICP-OES, Perkin-Elmer Optima 3000DV) to determine the amount of immobilized silver. The membrane obtained from this process, denoted as CS_Ag^+, was washed with DI water, dried in air at room temperature and then stored in a dessicator for further use.

The immobilized silver ions on the CS_Ag^+ membrane surface were also reduced to obtain silver at a lower oxidation state. A CS_Ag^+ membrane was immersed into a 0.01 M ascorbic acid solution for 1 min and then removed from

the solution. This process was expected to reduce the silver ions on the surface of CS_Ag^{+} into metallic silver. The membrane obtained from this process is denoted as CS_Ag^{0}. Finally, the CS_Ag^{0} membrane was washed with DI water, dried in air at room temperature and then stored in a dessicator for further use.

The valence state of the immobilized silver on the CS_Ag^{+} or CS_Ag^{0} membranes was examined by X-ray photoelectron spectroscopy which characterizes the biding energies of Ag 3d and N 1s. The X-ray photoelectron spectra of prepared membrane samples were obtained with a VGESCALAB MKII spectrometer using an Al Kα X-ray source (1486.6 eV photons).

3.2.3 Silver leaching test

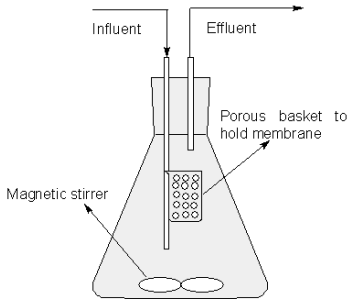

Figure 3.1 Schematic diagram of the dynamic leaching system.

The stability of the immobilized silver on the CS_Ag^{+} and CS_Ag^{0} membranes was evaluated with a dynamic leaching system as shown in Figure 3.1. A piece of a newly prepared CS_Ag^{+} or CS_Ag^{0} membrane was put into this system, and the process continued for a sufficiently long time until no further leaching of silver was detected in the solution. The feed was DI water at a flow rate of 2.7 mL·min^{-1}. In the first 3 h, the effluent samples were collected at every 30 min and the interval was increased to 1 h after 3 h of the test. Silver concentrations in the effluent samples were analyzed by the ICP-OES.

3.2.4 Bacteria used in the experiments

Escherichia coli (*E. coli*) and *Pseudomonas sp.* bacteria were used as test organisms in the experiments for the membrane antibacterial and anti-biofouling performances. The selection of these bacteria was based on the consideration that *E. coli* is the most commonly found bacteria in water and waste water and *Pseudomonas sp.* is reported to often promote or accelerate membrane biofouling (Lebleu et al., 2009). *E. coli* strain 15597 was obtained from the Environmental Molecular Biotechnology Laboratory at the National University of Singapore. *E. coli* was first cultured in Tryptone Soya Broth (TSB) solution (30 $g \cdot L^{-1}$), and then grown on Agar No.3 containing TSB (TSB and Agar No.3 were purchased from OXOID) (Feng et al., 2000). *Pseudomonas sp.* strain NCIMB 2021 was obtained from the National Collection of Marine Bacteria (Sussex, UK). It was cultured in Marine Broth 2216 solution (37.4 $g \cdot L^{-1}$) (Difco) and grown on Marine Agar 2216 (55.1 $g \cdot L^{-1}$) (Difco) (Yuan and Pehkonen, 2007).

3.2.5 Antibacterial tests

The disk diffusion method was used to evaluate the antibacterial property of the silver immobilized membrane surfaces. Bacteria in the stationary growth phase was separated from the nutrient solution through centrifugation at 3000 rpm for 10 min and washed with 30 mL PBS for 3 times. The cleaned stationary phase bacteria were subsequently suspended in 30 mL PBS and gradually diluted into a concentration at about 10^5 $CFU \cdot mL^{-1}$ with NaCl solution (0.9 wt%). Diluted suspensions (0.1 mL) of *E. coli* or *Pseudomonas sp.* were transferred and spread onto each of the TSB and Marine Agar plates respectively. A piece of the CS,

CS_Ag^{+} or CS_Ag^{0} membrane was first immersed into the PBS solution for 1 h and then placed onto the surface of a agar plate with spread bacteria. The agar plates with bacteria and membrane samples were all subsequently incubated for 24 h at 37 °C for *E. coli* and 28 °C for *Pseudomonas sp.* respectively. After the incubation, the surface area below and the zone around the membrane sample in a plate were examined for bacteria colonies with a digital camera.

3.2.6 Anti-biofouling tests

The anti-biofouling tests focused on the performance of the CS_Ag^{+} or CS_Ag^{0} membrane surface in the prevention of bacteria adhesion and reproduction on the membrane surface. Thus, a solution with a much higher bacteria concentration ($\sim 10^{9}$ CFU·mL^{-1}) that would not be significantly changed by the existence of the silver immobilized membrane sample in it was used and the concentration was maintained during all the anti-biofouling experiments. The CS, CS_Ag^{+} and CS_Ag^{0} membranes were immersed into the suspension of *E. coli* or *Pseudomonas sp.*, respectively, at the stationary growth phase.

For the shorter time test, the membrane samples were removed from the bacteria suspensions after 24 h of immersion. The membranes were then rinsed 3 times with 0.85% (w/v) NaCl solution, followed by staining for 15 min in dark condition in 10 mL of the 0.85 % (w/v) NaCl solution that had 100 µL of the BacLight stock solution added. The staining solution contained the two nucleic acid-binding stains: SYTO 9 and PI. SYTO 9 can penetrate all bacterial cell membranes while PI only penetrates cells with damaged cell membranes. After staining, the samples were washed with 0.85 % (w/v) NaCl solution again and

subsequently observed with a Nikon A1 Confocal System. The viable cells stained by SYTO 9 would be excited by a laser at 488 nm and appear as green fluorescence. In contrast, the unviable cells stained by both SYTO 9 and PI would be excited by a laser at 561 nm and produce red fluorescence. Thus, the distribution and viability of bacteria attached on the membrane surface can be characterized from the images obtained by the confocal laser scanning microscope.

The membrane surfaces in the anti-biofouling tests were also observed with a scanning electron microscope (SEM, JEOL JSM-5600LV). The membrane samples after the immersion in the bacteria suspensions were washed with PBS, and then the bacteria on the membrane surfaces were fixed in a 3 vol. % glutaraldehyde PBS solution for 5 h at 4 °C. After the fixation, the membranes were rinsed with PBS to remove any remaining glutaraldehyde on the surfaces. Step dehydrations were subsequently performed with 25, 50, 75 and 100 % ethanol, for 10 min for each of the membrane samples respectively to reduce their water contents. Finally, the membrane samples were dried in air and stored in a desiccator. The dried membrane samples were then coated with platinum through a vacuum electric sputter coater (JEOL JFC-1300) and scanned for the SEM images following the standard operation procedures.

In the longer time tests, the membranes were immersed in the stationary phase bacteria suspensions for up to 10 d. During the test period, the membranes were transferred to freshly prepared stationary phase bacteria suspensions in every 48 h to maintain the desired bacteria concentration. Small pieces of the membrane samples were initially taken every day from the immersed membranes, and then at

a 2 d interval after 4 d of the test. The collected membrane samples were fixed and dried with the same method as described above, and then scanned for the SEM images. The SEM images were analyzed with the ImageJ program (available as a public domain Java image processing program provided by NIH Image). The attached and grown bacteria clusters had different gray scale, as compared with the membrane surface, and the threshold between them was thus identified. Subsequently, the total area covered by the bacteria clusters was calculated, and then divided by the total area of the membrane sample to give the information on percentage coverage of bacteria on each of the membrane surfaces.

3.3 Results and discussion

3.3.1 Amounts and valence states of silver immobilized on the membranes

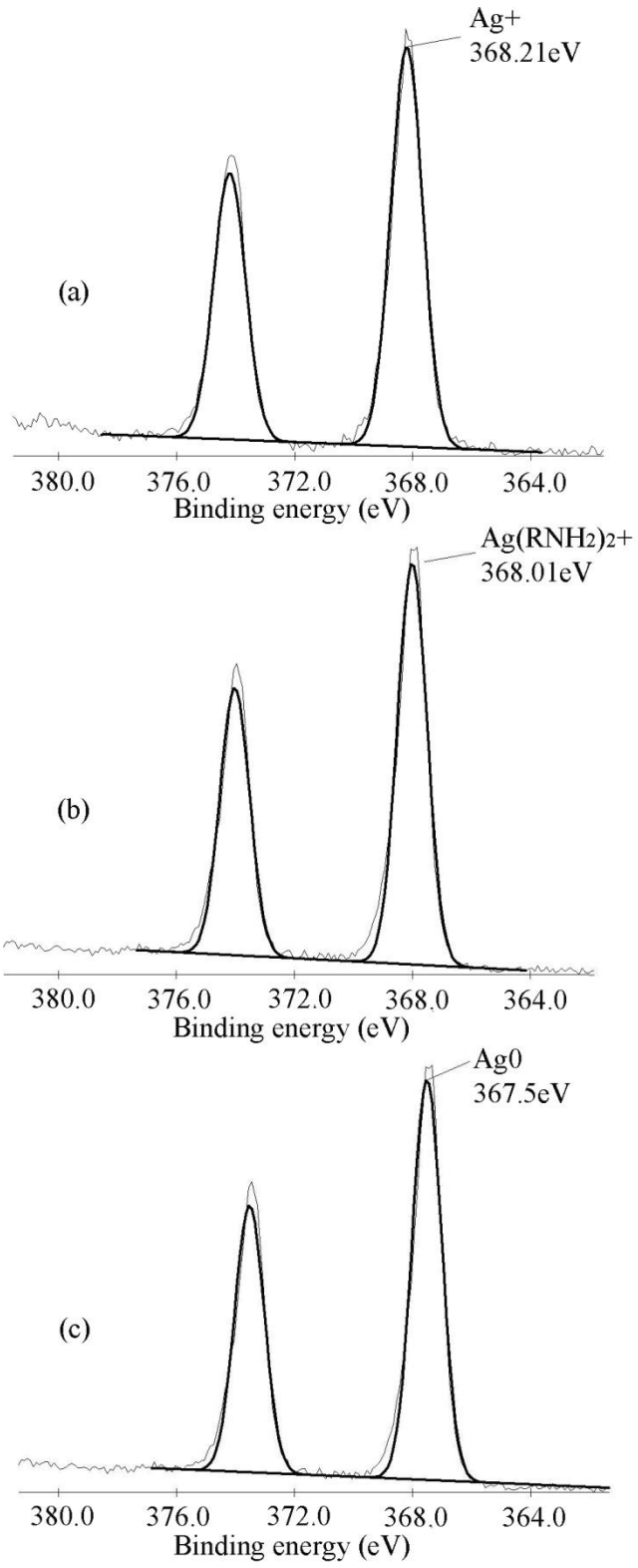

Figure 3.2 XPS spectra for Ag (3d) from (a) $AgNO_3$, (b) CS_Ag^+ and (c) CS_Ag^0.

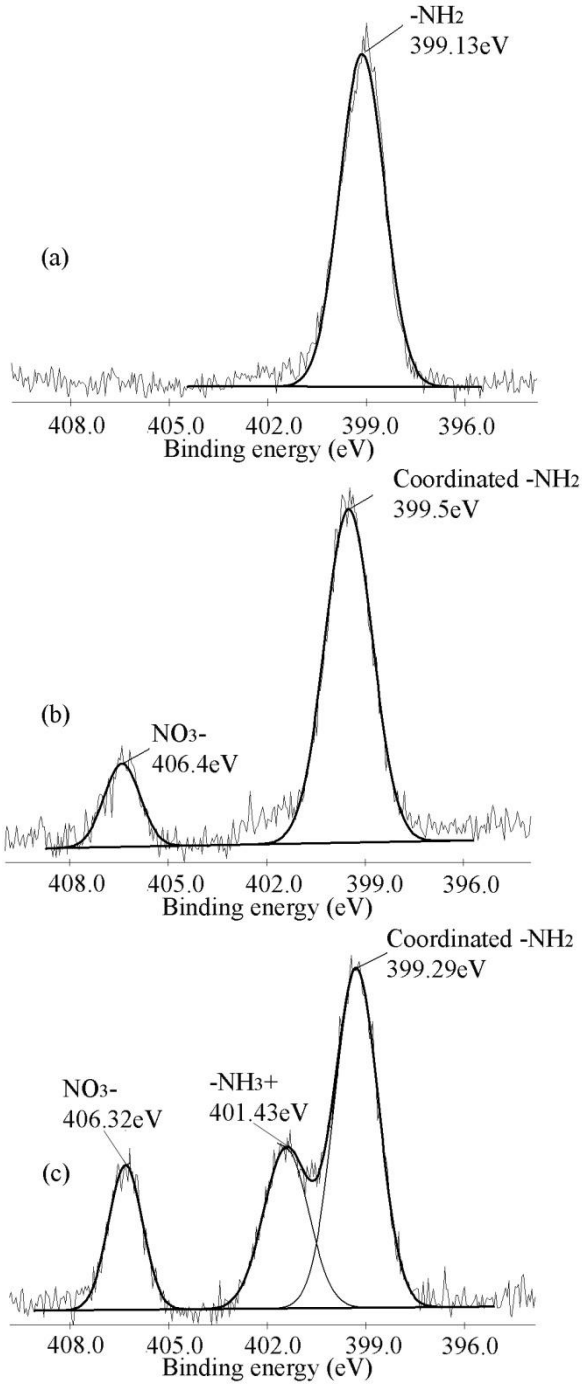

Figure 3.3 XPS spectra for N (1s) from (a) CS, (b) CS_ Ag^{+} and (c) CS_ Ag^{0}.

The amount of silver immobilized on the CS_Ag^{+} membrane from the early described process was found to reach 447.82 $mg \cdot g^{-1}$, and the amount of silver on

the CS_Ag^0 membrane was essentially the same without noticeable change by the reduction process. XPS analysis was used to examine the binding energies of the silver species on the surfaces of the CS_Ag+ and CS_Ag^0 membranes. As shown in Figure 3.2, the XPS spectra of silver atom from the emission of 3*d* orbital did not give rise to a single photoemission peak, but a closely spaced doublet that is caused by the spin-orbit splitting of *d*-orbitals. Furthermore, the interval between the double peaks is fixed. Thus, in this study, only the binding energy (BE) of the right peak was discussed. The valance states of silver on the membrane surfaces were of particular interest. The BE of the electron from ionic silver of silver nitrate was detected as 368.21 eV; see Figure 3.2 (a). The BE for the silver immobilized on the CS_Ag^+ membrane was found to be slightly shifted to a lower value of 368.01 eV [see Figure 3.2 (b)], indicating the silver existed in a slightly less oxidized state. The reason may be attributed to that the amino groups on chitosan coordinated with the silver ions and formed complexes. In this process, the nitrogen atom in the amino group contributed one electron pair to silver atom's vacant orbital forming a coordinate bond. As a result, the electron density of the silver atom on the CS_Ag+ membrane would be increased, causing the decrease of the BE value. For the CS_Ag^0 membrane, the BE of the silver atom was further shifted to 367.5 eV; see Figure 3.2 (c). This more noticeable decrease in the BE of the silver atom on the CS_Ag^0 membrane can be contributed to the reduction reaction with ascorbic acid, which caused significant increase in the electron density of the silver atom. As a general conclusion, coordinating reaction can be inferred to have occurred between the chitosan membrane and the

immobilized silver ions. In addition, silver on CS_Ag^0 appeared to be greatly reduced as verified by its much lower BE value. The reduction also seemed quite obvious in the experiment because the brown color of the CS_Ag^+ membrane was visually found to change the color into gray for the CS_Ag^0 membrane.

To further support the interaction mechanism between the immobilized silver and the chitosan membrane surface, the XPS spectra of the nitrogen atoms on the CS, CS_ Ag^+ and CS_ Ag^0 membranes were obtained; as shown in Figure 3.3. Only one peak at 399.13 eV BE was observed for the CS membrane in Figure 3.3 (a). It means that all nitrogen atoms on the CS membrane sample existed in one valence state. However, after the immobilization of silver, the nitrogen atoms on the CS_Ag+ membrane showed two BE peaks. As shown in Figure 3.3(b), a peak at a higher BE of 399.5 eV appeared. This peak indicates that some nitrogen atom existed at a more oxidized state after silver immobilization. During the immobilization process, nitrogen atoms in the amino groups of chitosan chelated with silver ions, which gave rise to the decrease of the electron density of the nitrogen atom, and thus the increased BE. The other peak at 406.4 eV in Figure 3.3(b) can be attributed to the adsorbed nitrate ions (Li and Bai, 2005), because the silver immobilizing process took place in the silver nitrate solution, and an electrical neutrality needs to be maintained on the membrane surface, (between immobilized silver ions and adsorbed nitrate ions). In Figure 3.3(c), three peaks are observed for the CS_Ag^0 membrane. The peak with the highest BE (406.32 eV) was again attributed to the nitrogen in the adsorbed nitrate ions. The peak with a BE of 401.43eV can be assigned to the -NH^{3+} groups (Moulder and

Chastain, 1992). Since the reducer (ascorbic acid) was used, some amino groups ($-NH_2$) on the chitosan membrane were protonized into $-NH^{3+}$. The major peak with the lowest BE (399.29 eV) was also attributed to the amino groups. There was a small but noticeable decrease in the BE as compared with that of the $-NH_2$ on the CS_Ag^+ (399.5 eV). Hence, the silver on the CS_Ag^0 membrane were, to a large extent, reduced, which can decrease the attraction of the silver atoms to the electrons of the nitrogen atoms, thus lowering the BE of nitrogen on the CS_Ag^0 membrane surface observed from the XPS analysis.

In summary, the XPS results indicate that the silver ions were immobilized onto the CS_Ag^+ membrane by chelating with the amino groups of chitosan, and the silver on the CS_Ag^0 membrane were in a less oxidized state and probably reduced into metallic silver.

3.3.2 Stability of immobilized silver on the membranes

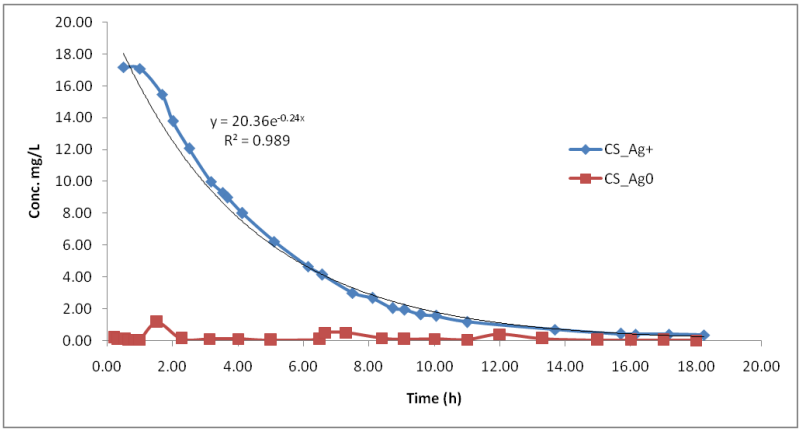

Figure 3.4 Leaching test results for silver immobilized on the CS_ Ag^+ and CS_ Ag^0 membranes (the figure shows the silver concentration in the leaching solution versus leaching time).

It is of interest to know the stability difference for the ionic and reduced silver immobilized on the membranes. In the leaching tests, two pieces of CS_ Ag^{+} and CS_ Ag^{0} membranes, each immobilized with approximately 51 mg silver on the surface for CS_ Ag^{+} and 47.4 mg for CS_ Ag^{0} were examined, respectively.

The results from the leaching tests for the CS_ Ag^{+} and CS_ Ag^{0} membranes are presented in Figure 3.4. It is observed that the silver ions on the CS_ Ag^{+} membrane were leached out and the concentration in the leaching solution decreased rapidly with time until about 18h, after which leaching was no longer detected. The total amount of leached silver from the CS_ Ag^{+} membrane was found to be about 13.75 mg. In comparison with the initially immobilized amount (51 mg), about 27% of the immobilized silver ions were leached out from the CS_ Ag^{+} membrane. The reason may be attributed to that some silver ions were possibly only physically adsorbed on the surface or some others were only weakly chelated with the amino groups, thus being leached out in the experiment. Nevertheless, about 73% of the immobilized silver on the CS_Ag^{+} membrane surface still appeared to be stable. In contrast to the CS_Ag^{+} membrane, only a very small amount of silver (< 1%) was leached out from the CS_ Ag^{0} membrane; see Figure 3.4. Silver concentration in the leaching solution was below 0.1 $mg \cdot L^{-1}$ in the beginning and soon became non-noticeable. The results indicate that the reduced silver on the CS_ Ag^{0} membrane was much more stable than the ionic silver on the CS_ Ag^{+} membrane. The reason may be that the reduced silver was more difficult to be dissolved or ion-exchanged into the solution.

3.3.3 Antibacterial effects of silver immobilized membranes

Two types of bacteria were tested in the experiments. *E. coli* was selected because it is the most common bacteria in the environment including water and waste water. Although *E.coli* may not be the most efficient bacteria for membrane biofouling, the bacteria have commonly been used by other researchers to evaluate a material's antibacterial property (Feng et al., 2000; Lok et al., 2006). Another type of bacterium was *Pseudomonas sp.* that is separated from the marine microbes. The bacteria are not only present in various environments, but also identified as one of the most possible bacteria promoting biofouling, due to the extracellular polysaccharide (EPS) secreted (Pang et al., 2005). Pseudomonas species have often been used to examine the biofouling formation process (Al-Tahhan et al., 2000; Lee et al., 2007). In addition, sea water desalination is one of the major fields using membrane technology, such as RO, and the study in membrane biofouling with these marine microbes is of great practical interest.

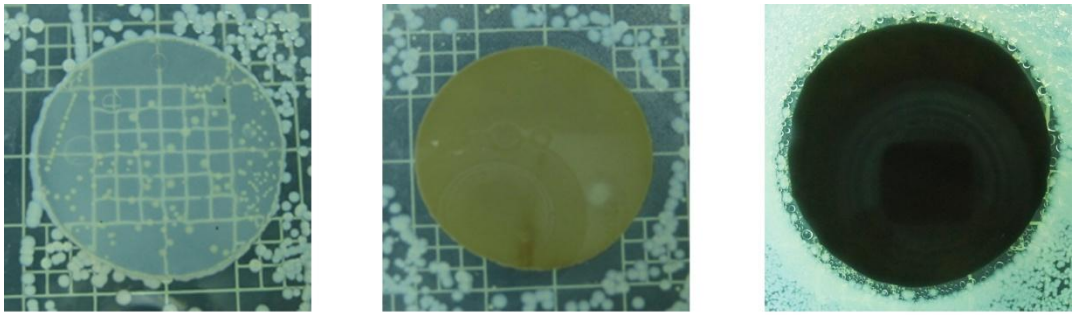

(a) (b) (c)

Figure 3.5 Disks diffusion tests for *E. coli* on the membranes of (a) CS, (b) CS_Ag^{+} and (c) CS_ Ag^{0}.

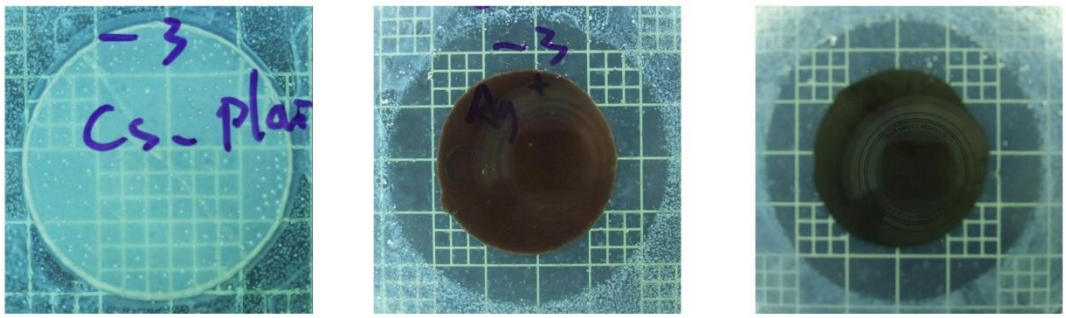

(a) (b) (c)

Figure 3.6 Disks diffusion tests for *pseudomonas sp.* on the membranes of (a) CS, (b) CS_Ag^+ and (c) CS_ Ag^0.

From the disk diffusion test, the typical results for *E. coli* growth on the different types of membranes are shown in Figure 3.5. *E. coli* was found to grow below and above the CS membrane as well as in the surrounding zone; see Figure 3.5(a). This indicates that the CS membrane did not show good inhibition for the growth of *E. coli*. However, *E. coli* colonies were not found above and below the CS_Ag^+ and CS_ Ag^0 membranes from the results in Figure 3.5(b) and (c). Moreover, both the CS_Ag^+ and CS_ Ag^0 membranes showed an inhibition zone surrounding the membrane. The inhibition zone of the CS_Ag^+ membrane was wider than that of the CS_Ag^0 membrane. Some of the silver may diffuse from the membrane surface into the nearby area of the membrane, thus killed the bacteria in the nearby region. Silver on the CS_ Ag^+ membrane appeared to be easier to diffuse into the nearby zone than that on CS_ Ag^0, resulting in a wider inhibition zone. Both CS_Ag^+ and CS_ Ag^0 appeared to have good antibacterial performance for controlling the growth of *E. coli* in the experiments.

Similar results for *Pseudomonas sp.* were also obtained as shown in Figure 3.6. Again, the CS membrane did not show inhibition in the growth of *Pseudomonas sp.* Both the CS_Ag^{+} and CS_ Ag^{0} membranes however effectively inhibited the growth of *pseudomonas sp.* and therefore no bacteria colonies were observed above and below the CS_Ag^{+} and CS_ Ag^{0} membranes. The inhibition zones around the membrane samples in Figure 3.6(b) and (c) were also observed.

It is clear that the CS membrane could not inhibit the growth of both *E. coli* and *Pseudomonas sp.*, but both the CS_Ag^{+} and CS_ Ag^{0} membranes showed the effectiveness in controlling the growth of the two types of bacteria examined.

3.3.4 Anti-biofouling performances of the CS_Ag^{+} and CS_ Ag^{0} membranes

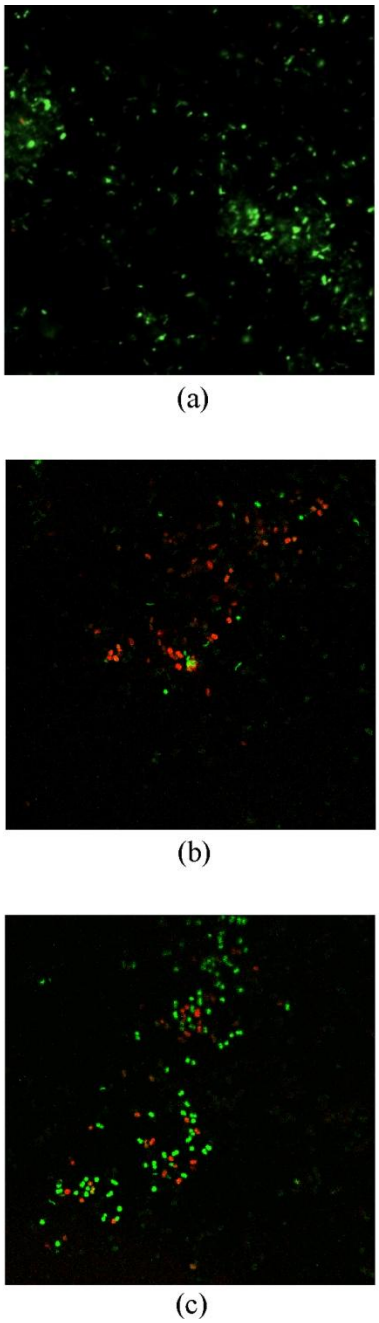

Figure 3.7 CLSM images of *E. coli* on the membranes of (a) CS, (b) CS_Ag^{+} and (c) CS_ Ag^{0}.

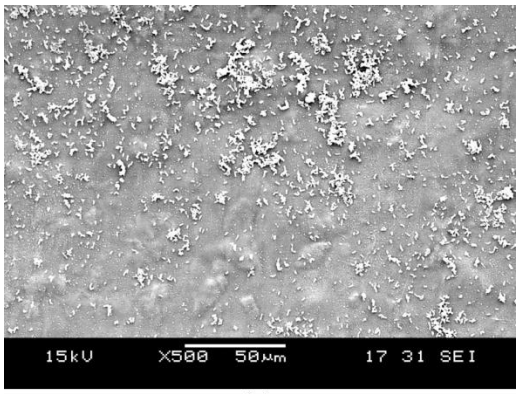

(a)

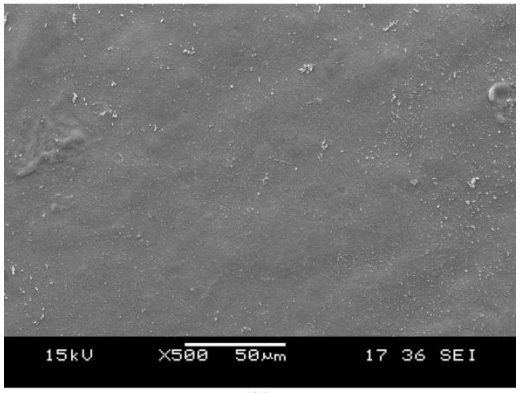

(b)

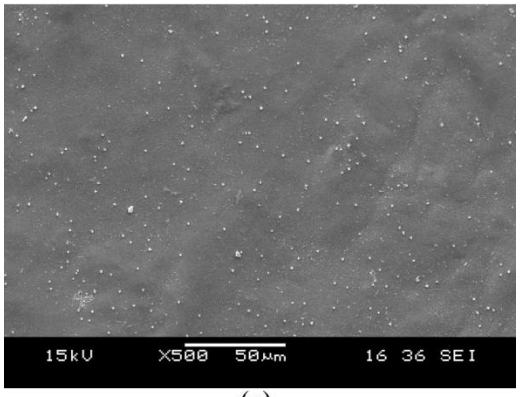

(c)

Figure 3.8 SEM images of *E. coli* on the membranes of (a) CS, (b) CS_Ag^{+} and (c) CS_ Ag^{0} .

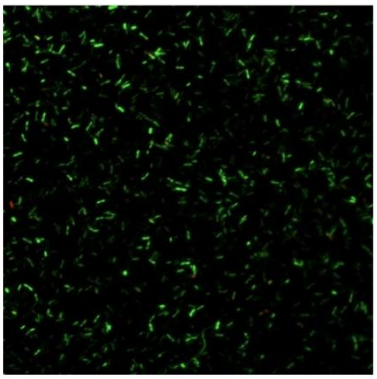

(a)

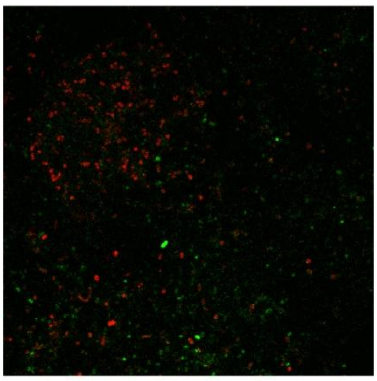

(b)

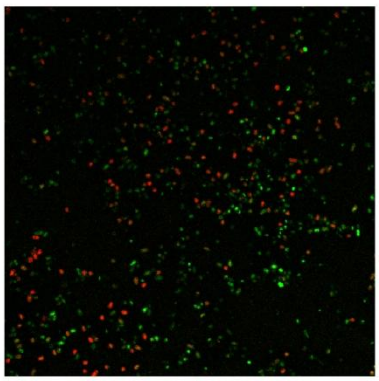

(c)

Figure 3.9 CLSM images of *Pseudomonas sp* on the membranes of (a) CS, (b) CS_Ag^{+} and (c) CS_ Ag^{0}.

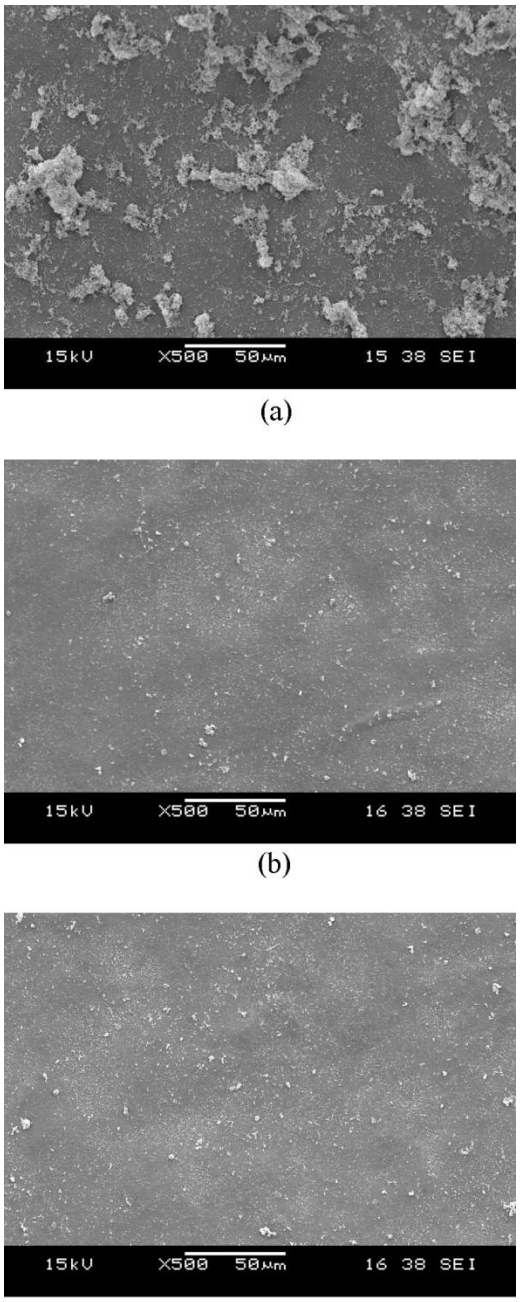

Figure 3.10 SEM images of *Pseudomonas sp.* on the membranes of (a) CS, (b) CS_Ag^{+} and (c) CS_ Ag^{0}.

The anti-biofouling performances of the prepared membranes were investigated first with high concentration bacteria suspensions (~10^{9} CFU·mL^{-1}). The membrane samples were immersed in the bacteria suspensions for 24 h to allow the possible formation of biofilms on the membrane surfaces. Then, the

membrane samples were stained and observed by CLSM. The samples, after fixation and dry, were also observed by SEM.

The CLSM and SEM results for membranes tested with *E. coli* are shown in Figure 3.7 and Figure 3.8 respectively. As observed in Figure 3.7 (a), the cells on the CS membrane sample were viable and appeared green. Accordingly, the SEM image in Figure 3.8 (a) clearly shows that bacteria colonies or clusters formatted on the membrane surface. Hence, the CS membrane was prone to biofouling by *E. coli*.

The results for the CS_Ag^{+} and CS_ Ag^{0} membranes appeared to be very different from that of the CS membrane; see Figure 3.7(b) and (c). Fewer cells were observed on the membrane surfaces and many of them appeared to be red, i.e., unviable cells. The SEM images in Figure 3.8(b) and (c) showed that the CS_Ag^{+} and CS_Ag^{0} membrane surfaces were relatively clean and free of bacteria growth.

Similarly, the CLSM and SEM images for the membrane samples tested with *Pseudomonas sp.* are shown in Figure 3.9 and Figure 3.10. Figure 3.9(a) and Figure 3.10(a) indicate that the bacteria could grow on the CS membrane surface without inhibition. However, the CS_Ag^{+} and CS_ Ag^{0} membranes appeared to be very good at preventing the formation of biofilms, and only red spots, indicating unviable bacteria, were observed on the membrane surfaces; see Figure 3.9(b) and Figure 3.9(c). Correspondingly, only discrete cells were found on the membrane surfaces from the SEM images in Figure 3.10(b) and Figure 3.10(c). The results indicate that bacteria could not develop biofilms on the surfaces of the

CS_Ag^+ and CS_ Ag^0 membranes. In summary, both the CS_Ag^+ and CS_Ag^0 membranes prevented the formation of biofilms, and showed good anti-biofouling performances in the shorter period (24h) test.

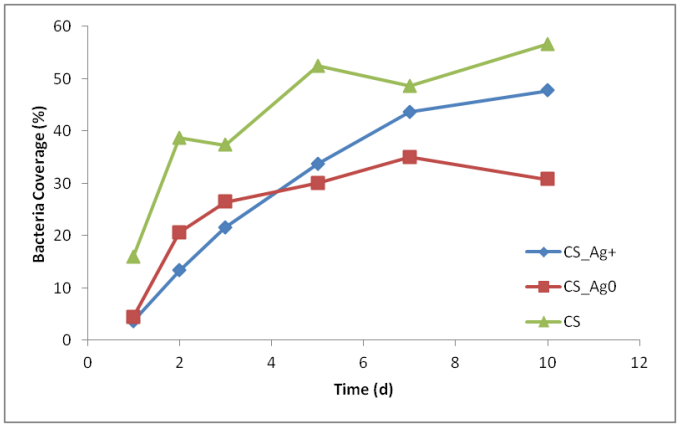

Figure 3.11 The coverage of ***E. coli*** on the membrane surfaces at different immersion times during the 10d anti-biofouling test.

The membrane samples were further tested in a stationary phase *E. coli* suspension for up to 10d. During the experimental period, the bacteria concentration was maintained. The results are shown in Figure 3.11. As can be observed, after 1d immersion, the CS membrane already had a significantly higher bacteria coverage than the CS_Ag^0 and CS_Ag^+ membranes, although the results for the CS_Ag^0 and CS_Ag^+ membranes were similar. The bacterial coverage on the CS and CS_Ag^+ membranes in general showed gradual increase during the 10d expermients. The coverage on the CS_Ag^0 membrane proceeded more slowly and became considerably lower than those on the CS and CS_Ag^+ membranes at the end of the test (i.e., 10d). As a general conclusion, the CS membrane did not show anti-biofouling performance, in comparison with the silver immobilized membranes. However, the decrease in the performance of CS_Ag^+ membrane, as compared to that of CS_Ag^0 membrane, in the longer

period of test may be attributed to the lower stability of the silver ions on the CS_Ag^+ membrane. In terms of longer operation performance, the CS_Ag^0 membrane appears to be more stable and better than the CS_Ag^+ membrane.

3.4 Conclusion

Membrane surfaces immobilized with ionic or reduced silver showed effective antibacterial and anti-biofouling performance. XPS spectra indicated that silver immobilized on the CS_Ag^+ membrane was in a more oxidized state than silver on the CS_Ag^0 membrane. XPS spectra also indicated that silver immobilized on the CS_Ag^+ membrane surface involved in the coordination with the amino groups (nitrogen atoms) of chitosan. The leaching test showed that the reduced silver on the CS_Ag^0 membrane was more stable than ionic silver on the CS_Ag^+ membrane. From the disk diffusion experiment, both *E. coli* and *pseudomonas sp.* were found to be unable to grow on the CS_Ag^+ or the CS_Ag^0 membranes. In the longer time anti-biofouling experiments, *E. coli* or *pseudomonas sp.* was found to attach or grow on the CS membrane as viable cells. In contrast, only discrete bacteria, most of them being unviable cells, were observed on the CS_Ag^0 and CS_Ag^+ membranes, with the CS_Ag^0 membrane having more stable and better overall anti-biofouling performance than the CS_Ag^+ membrane. Thus, the immobilization of silver on a membrane surface can be an effective way to control bacterial growth on the membrane and hence contribute to improved or enhanced anti-biofouling performance for the prepared membranes.

Chapter 4 **Immobilization of silver on polypropylene membrane for anti-biofouling performance**

Summary

In this chapter, a method was developed to immobilize silver onto polypropylene (PP) membrane surface for improved anti-biofouling performance. A commercial PP membrane was first grafted with the thiol functional groups, and then silver ions were immobilized onto the PP membrane surface through coordinating with the thiol groups. The immobilized silver was found to be very stable, with only about 1.1 % of the immobilized silver being leached out during a leaching test. The surface of the modified membrane (PPS-Ag) was examined with ATR-FTIR and XPS analysis techniques and was verified the successful grafting of the thiol groups and the coordination of silver ions on the membrane surface. The membrane surface properties were also characterized by SEM, AFM and water contact angle measurements. The PPS-Ag membrane was found to have a smoother and more hydrophilic surface than the PP membrane. Both Gram-negative bacteria, Escherichia coli (*E. coli*), and Gram-positive bacteria, Staphylococcus aureus (*S. aureus*), were used to evaluate the PPS-Ag membrane's antibacterial and anti-biofouling performances. From the disk diffusion experiments, the PPS-Ag membrane exhibited the capability of effectively inhibiting the growth of both the Gram-negative and Gram-positive bacteria tested. The membrane anti-biofouling performance was assessed with the mixed *E. coli* and *S. aureus* suspension immersion and filtration tests. The PPS-

Ag membrane showed a stable and significantly enhanced anti-biofouling performance as compared with the PP membrane. The results in this chapter demonstrated that PP membrane's biofouling problem can be sufficiently overcome through immobilizing silver onto the membrane surface.

4.1 Introduction

Membrane separation technology is becoming a more commonly used separation method in water and wastewater treatments. However, membrane fouling, especially biofouling, remains one of the main problems that hinder the wider applications of the membrane separation technology. Membrane fouling causes the decline of membrane flux either temporarily or permanently. The reversible membrane fouling is temporary and can be removed by applying physical methods such as back wash. In contrast, the permanent membrane fouling is usually irreversible, and thus, a lot of efforts have been attempted to prevent its happening (Rana and Matsuura, 2010). Membrane biofouling is considered to be often a permanent one and is very difficult to handle because the attached microbes on the membrane surface will reproduce very fast. Even initially only are a few microbes attached onto the membrane surface, they could eventually foul the entire membrane in a short period of time. Membrane separation is a surface process and the surface of a membrane plays a vital role. Hence, there have been numerous studies aiming at reducing membrane biofouling, through surface functionalization. It has been reported that membrane surface properties played important roles in the behavior of initial bacterial adhesion and biofilm development (Myint et al.). Thus, some researchers

attempted to modify the membrane surface properties to minimize adhesion, particularly to mitigate biofouling through the hydrophilic modification (Krishnan et al., 2006; Luo et al., 2005; Pieracci et al., 1999). Others also tried to decrease membrane surface's roughness to reduce biofouling (Knoell et al., 1999). In addition, negatively charged membrane surface is considered to be an effective method to reduce biofouling because it can repulse bacteria with negatively charged in aqueous solutions. For example, Zhao and his co-workers grafted two oppositely charged monomers onto a PP membrane to achieve negatively charged surface to prevent bacteria adhesion (Zhao et al., 2010). On the other hand, some developments have been made to endow a membrane with antibacterial property that prevents biofouling. One of the examples has been to introduce, on a membrane, the antibiotic and slow-releasing materials that are able to mediate direct killing of microbes upon contact (Golomb and Shpigelman, 1991). Neodymium (III) and Zinc (II) complexes were also examined to kill *E. coli* (Li et al., 2009). Zinc oxide nanoparticles have been found to have antibacterial activity against *E. coli* as well (Liu et al., 2009). However, many of such approaches only provided a temporary effect for antibacterial performance and some of the species used may be harmful to human beings.

Silver is an effective antibacterial metal that has been known by human being for a very long time (Ghandour et al., 1988). Despite the fact that silver possess as antibacterial efficacy equal to or greater than other heavy metals, silver has been known to have almost no toxic effects on mammals (Yimin Qin, 2007). Some researchers have immobilized silver nanoparticles onto the surfaces of

nanofiltration membranes to prevent biofouling (Lee et al., 2007; Zodrow et al., 2009). In addition, Chen et al reported the preparation of thiourea chitosan–Ag^{+} complex which exhibited a broad-spectrum of antimicrobial activities (Chen et al., 2005). More recently, Liu et al. also reported the immobilization of silver ions on chitosan/cellulose acetate blend membrane surface for anti-biofouling performance (Liu et al., 2010). Nevertheless, most of those reported immobilization methods had a common problem that the immobilized silver was not very stable and may not be able to provide a long term effective anti-biofouling performance for the membranes. In order to achieve long term anti-biofouling performance, Zhu and his coworkers attempted to reduce the oxidation state of the coordinated silver ions on the membrane surface (Zhu et al., 2010). However, the reduction process is possible to change the membrane's pore structure because the reduced silver is usually in particle form that is much bigger than the coordinated silver ions.

Commercially available PP membranes are widely used in water and wastewater treatments because of their high void volume, well-controlled porosity, good thermal and chemical stability as well as low cost (Kim and Lloyd, 1991; Yu et al., 2008). However, PP membranes are highly hydrophobic and are easily subject to membrane biofouling due to microbial attachment and growth during membrane filtration; and thus, many researchers have tried to render PP membranes more hydrophilicity to reduce the biofouling (Kou et al., 2003; Ma et al., 2000; Yang et al., 2005). Nevertheless, PP membranes are relatively inactive

and a method to introduce silver as biocide onto the PP membrane surface to prevent membrane biofouling has not been reported so far.

In this chapter, a focus was placed on achieving strong binding of silver ions on PP membranes for desired long term anti-biofouling performance. Since PP itself does not have any active functional groups to immobilize silver ions through coordination, a method was developed to graft the thiol groups onto the PP membrane surface. The PP membrane with the thiol functional groups was then used to bind silver ions. The prepared membrane surface properties and the stability of the immobilized silver ions were evaluated; the antibacterial and anti-biofouling performances of the prepared membrane were also examined.

4.2 Materials and methods

4.2.1 Materials

PP membrane (AN0604700) was purchased from Whatman, with an average pore size of 0.6 μm. Bromine, thiourea, potassium hydroxide and silver nitrate were of reagent grade and supplied by Sigma-Aldrich. Silver standard solution (1000 $mg \cdot L^{-1}$) was obtained from Merck. 10X Phosphate Buffer Saline (PBS) from 1st BASE was diluted by 10 times and sterilized before using in this study. LIVE/DEAD Bacterial Viability Kit L-13152 (BacLight) was obtained from Invitrogen, including two nucleic acid-binding stains: SYTO 9 and propidium iodide (PI) in solid forms. One pipet of SYTO 9 (yellow-orange solids) and another pipet of PI (red solids) were dissolved and mixed into 5 mL 0.85 % NaCl solution to obtain a 5 mL BacLight stock solution. Deionized (DI) water (18 MΩ)

purified with a Milli-Q system from Millipore was used to prepare all solutions as needed in the study.

4.2.2 Immobilization of silver on PP membrane

A piece of PP membrane was weighted, and then put into a glass bottle with 30 mL saturated bromine water solution (32 $g \cdot L^{-1}$). Subsequently, the bottle was sealed and radiated under a xenon lamp (Newport 150w). In order to provide an equal amount of bromide, both sides of the membrane were exposed to the xenon lamp for 45 min. The irradiated membrane was rinsed with ethanol. Then, the membrane was transferred into a boiling thiourea ethanol solution (3 M). After 10 min, the treated membrane was taken out and rinsed with ethanol again. Subsequently, the membrane was moved into a boiling potassium hydroxide ethanol solution (7 M) for 1 h. The membrane was then taken out and cleaned with DI water. Subsequently, the membrane was immersed in a 1 M sulfuric acid solution for 1 h to acidify the grafted thiol groups, and then, remained acid on the membrane was cleaned by DI water. These processes allowed thiol groups to be grafted onto the membrane surface. The grafted percentage was estimated from the membrane dry weights before and after the treatment. To immobilize silver ions on the membrane, it was immersed in a 0.1 M silver nitrate solution for 24 h at ambient temperature. Finally, the membrane was rinsed with DI water and dried at 60°C for 5 h. The amount of immobilized silver was calculated from the membrane dry weights after silver immobilization and that before silver immobilization. 10 pieces of the membrane immobilized with silver were examined, and the

average was reported as the representative amount of silver immobilized on the membrane. The obtained membrane will be denoted as PPS-Ag hereafter in this chapter.

4.2.3 Characterization of the prepared membrane

4.2.3.1 Analysis of surface chemical compositions

The surface chemical compositions of the prepared membranes were characterized by X-ray photoelectron spectroscopy (XPS) and Attenuated Total Reflection Fourier Transform Infrared (ATR-FTIR). The membrane samples were dried at 60°C for 5 h, and then, used in the analyses without further pretreatments. The XPS analyses were carried out on an AXIS HIS spectrometer (Kratos Analytical Ltd., UK) with an Al KR X-ray source (1486.71 eV of photons). The X-ray source was run at 250 W with an electron take-off angle of 45° relative to the sample surface. The pressure in the analysis chamber was maintained at about 5×10^{-7} Pa during the analysis. ATR-FTIR spectra were collected through a FTIR spectrometer (Varian 660-IR) with an ATR component supplied by Perkin Elmer.

4.2.3.2 Analysis of silver stability on the membrane surface

The stability of the immobilized silver on the prepared PP membrane was evaluated with a dynamic leaching system. The experiment procedures were similar with those in Section 3.2.3. The silver concentrations of the effluent solutions versus time were plotted, and then, a curve was regressed. The total leached amount of silver was calculated from the integral of the curve equation.

4.2.3.3 Observation of surface morphology and roughness of the membranes

The surface morphologies of the PP and PPS-Ag membranes were observed with a scanning electron microscope (SEM, JEOL JSM-5600LV). The membrane samples were dried at 60 °C for 24 h. The samples were cooled to room temperature, and then, coated with platinum with a vacuum electric sputter coater (JEOL JFC-1300).

The surface roughness of the PP and PPS-Ag membranes were examined by atomic force microscopy (AFM). The membrane samples were dried at 60 °C for 24 h. After cooling to room temperature, they were analyzed with a model NS3A NanoScope 111a multimode scanning probe microscope (Digital Instruments, Santa Barbara, CA). Imaging was carried out in a tapping mode using a silicon nitride probe (Veeco, Santa Barbara, CA). Obtained images were then processed with the Nanoscope software, and membrane surface roughness was quantified by the software as well.

4.2.3.4 Measurement of water contact angle

The water contact angles of the membranes were measured with a contact angle goniometer (250-F1) from Ramé-Hart Instrument Co.. The membrane samples were dried at 60 °C for 24 h, and then, put on the horizontal platform of the instrument. A 10 μL droplet of DI water was dropped onto the membrane surface. The droplet image was magnified and analyzed by the instrument to obtain the water contact angle value. Each sample was measured for 15 times at different locations of the membrane, and the reported result was the average value of these measurements.

4.2.3.5 Measurement of membrane pure water flux

The pure water flux of the membranes was investigated using a dead-end filtration system consisting of a nitrogen gas cylinder, a pressure controller (Alicat Scientific PCD, USA), a clear reservoir, and an Advantec stirred cell (effective filtration area 11.8 cm^2, Advantec UHP-43, Japan) coupled with a magnetic stirrer. The transmembrane pressure was precisely controlled *via* the pressure controller with an accuracy of ±0.5%. Permeate weight was measured by an electronic balance (Precisa XT-220-A, Switzerland) that was serially linked to a computer for automated data collection at desired time intervals. In the study, the transmembrane pressure was set at 0.05 MPa and the data collection was made at every 10 s. The membrane pure water flux was taken to be the one at the stabilized state.

4.2.4 Bacteria assay

4.2.4.1 Antibacterial test

Escherichia coli (*E. coli*) and *Staphylococcus aureus* (*S. aureus*) were used in the experiments for bacteria assay. In order to verify the immobilized silver to have a broad-spectrum of antibiotic effect, *E. coli* as a typical Gram-negative bacterium and *S. aureus* as a typical Gram-positive bacterium were examined. Moreover, the two types of bacteria are commonly found in water and wastewater.

E. coli strain 15597 and *S. aureus* ATCC 6538 were obtained from the Environmental Molecular Biotechnology Laboratory at the National University of Singapore. *E. coli* and *S. aureus* were cultured in a Tryptone Soya Broth (TSB) solution (30 $g \cdot L^{-1}$), and then grew on Agar No.3 containing TSB (TSB and Agar No.3 were purchased from OXOID) (Feng et al., 2000; Yao et al., 2008).

The disk diffusion method was used to evaluate the antibacterial properties of the silver immobilized membrane. The experimental procedures were similar to those in Section 3.2.5. *E. coli* and *S. aureus* were used in this chapter.

4.2.5 Anti-biofouling tests

4.2.5.1 Bacteria suspension immersion test

Anti-biofouling tests focused on the capability and performance of the PPS-Ag membrane in preventing bacteria adhesion and reproduction on the membrane surface. Thus, a high bacteria concentration (~10^9 CFU·mL^{-1}) suspension was used in the tests.

The PP and PPS-Ag membranes were immersed in the suspension of mixed stationary phase *E. coli* and *S. aureus* for a time up to 12 d. During the test period, the membranes were transferred to a newly prepared stationary phase bacteria suspensions in every 48 h to maintain the viable bacteria concentration. Small pieces of membrane samples were taken from the immersed membranes in 1 d, 2 d, 4 d, 6 d and 12 d. The collected membrane samples with bacteria on the surfaces were fixed in 3 vol. % glutaraldehyde PBS solutions for 5 h at 4 °C. After the fixation, these membrane samples were rinsed with PBS to remove remaining glutaraldehyde and dried at 60 °C for 24 h. The dried membrane samples were then scanned for SEM images.

The viability of the bacteria on the membrane surfaces were observed with confocal laser scanning microscope (CLSM). The membrane samples were removed from the bacteria suspensions after 4 d and 6 d of immersion. The membranes were then rinsed with 0.85% (w/v) NaCl solution for 3 times,

followed by staining in 10 mL 0.85 % (w/v) NaCl solution that had 100 μL BacLight mixed stock solution in it for 15 min in dark. The CLSM observation procedures were the same as those in Section 3.2.6.

4.2.5.2 Bacteria suspension filtration test

The anti-biofouling performance of the prepared membrane was further evaluated by the mixed bacteria suspension filtration test. In order to observe the permeate flux of the membrane in the filtration of mixed bacteria suspension, and calculate the membrane flux recovery, the experiment was separated into 3 parts, including 1 h pure water filtration, followed by 24 h mixed bacteria suspension filtration, and then, after a membrane cleaning procedure, another 1 h pure water filtration. The mixed bacteria suspension was prepared by mixing stationary phase *E. coli* and *S. aureus* and diluting the mixture to give a suspension of about ~10^7 CFU·L^{-1}. The filtration system was the same with the one used to measure the membrane pure water flux. The pressure was also set at 0.05 MPa.

The pure water flux of the membrane in the first hour was denoted as J_{w0}. After 24 h filtration with the mixed bacteria suspension, the membrane was rinsed with DI water and shaken in a beaker with 50 mL DI water for 30 min at 200 rpm. Then pure water flux of the cleaned membrane in the last hour of filtration was denoted as J_{w1}. The relative flux recovery (RFR), indicating the extent of the possible reversible fouling, was calculated by RFR = $(J_{W1}/J_{W0}) \times 100\%$ for PP and PP-Ag, respectively.

4.3 Results and discussion

4.3.1 Characteristics of membranes

4.3.1.1 Grafting degree of thiol group and immobilization amount of silver on PP membrane

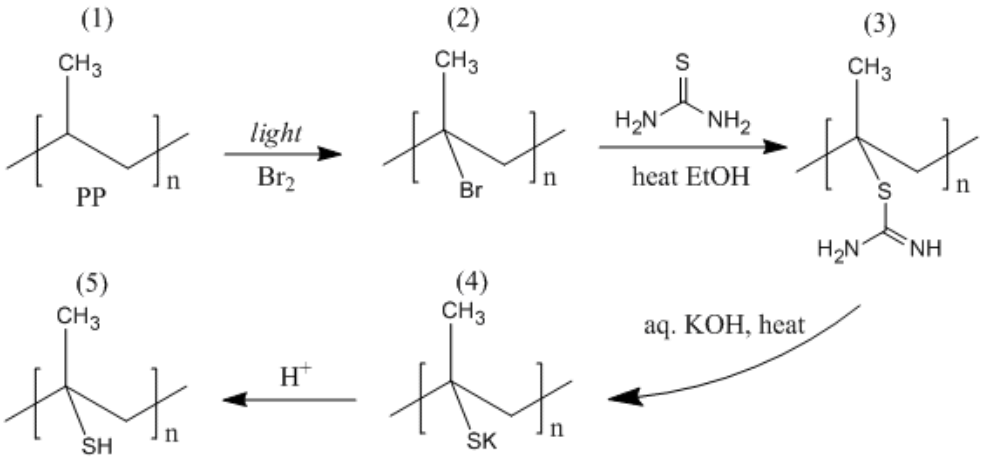

Scheme 4.1 Reaction steps for the grafting of thiol groups on PP membrane.

The thiol groups cannot be directly grafted onto PP membrane due to PP lacking of reactive sites. Thus, a radical halogenations reaction was carried out for PP first. PP, as a hydrocarbon, can be easily reacted with bromine under gentle reaction conditions (Podgorsek et al., 2006; Shaw et al., 1997). The reaction is a radical substitution and, can be launched under the radiation of a light such as sunlight. In this study, a xenon lamp that simulates the solar radiation was used. In the radical substitution, bromine radicals tended to be highly selective, and preferred to react with the tertiary alkyls rather than the other alkyls of PP, as shown in Scheme 4.1 at step 2, because less energy was needed to overcome the bond dissociation energy (McMurry, 2004). After the halogenations, the generated alkyl halides were converted to the thiol groups desired. To do this, an ethanol solution containing thiourea was heated and reacted with the halogenoalkanes on the membrane surface, as shown in Scheme 4.1 at step 3. Subsequently, potassium hydroxide was used to remove

the amino groups with the thiol groups being preserved, as shown in Scheme 4.1 at step 4. The acidification, as shown in Scheme 4.1 at step 5, was the last step of the thiol groups grafting. After the reactions, the grafted thiol groups took 15 wt% of the PP membrane.

The modified membrane with the thiol groups was then immersed into a 0.1M silver nitrate solution for 24h. For the immobilization of silver, it was found that about 22 mg silver ions were chelated with the thiol groups on per gram of membrane, producing the PPS-Ag membrane desired for this study.

4.3.1.2 Surface compositions

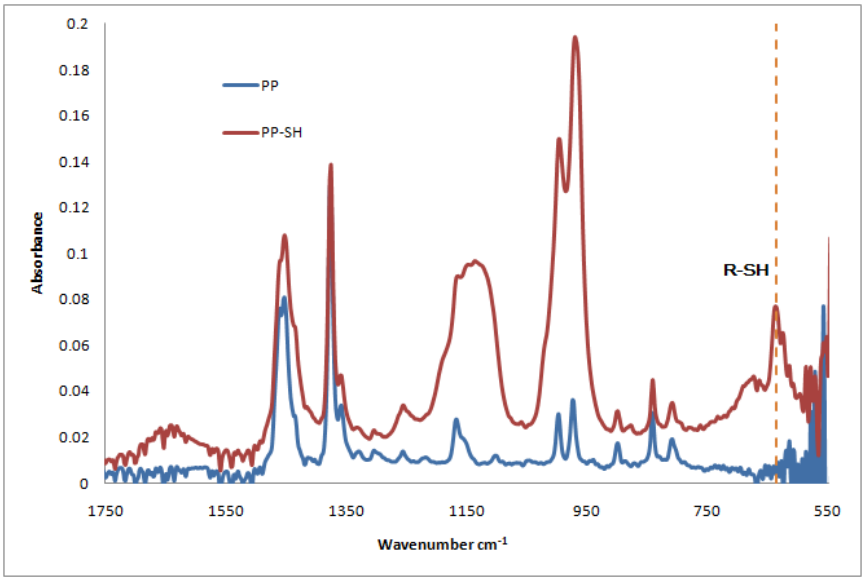

Figure 4.1 ATR-FTIR spectra of the PP membrane and the modified PP-SH membrane.

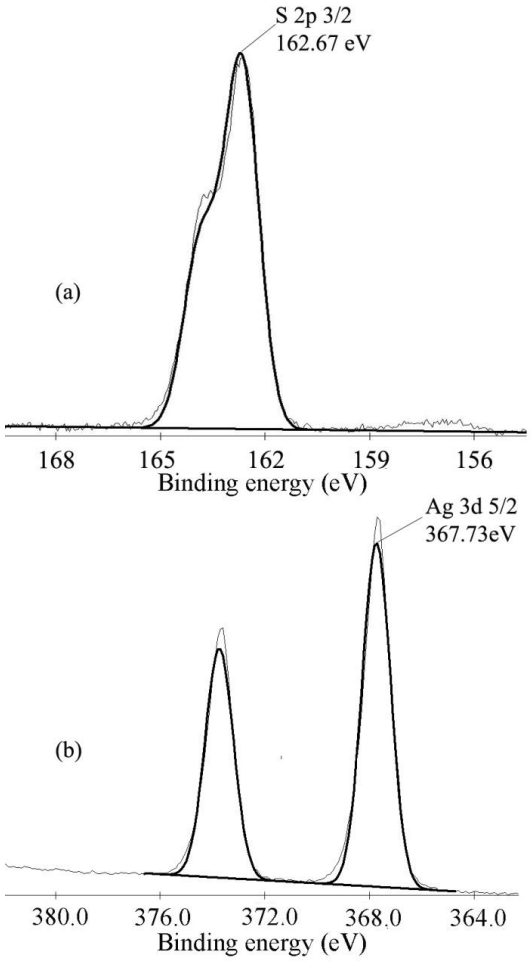

Figure 4.2 XPS spectra for (a) S (2p) and (b) Ag (3d) of the PPS-Ag membrane.

The membrane surfaces were characterized with ATR-FTIR and XPS to determine their characteristic chemical compositions and interactions. The ATR-FTIR spectra were used to identify the successful grafting of thiol groups onto the PP membrane. For convenience of discussion, the PP membrane grafted with thiol groups is denoted as PP-SH. As shown in Figure 4.1, a peak at 634.6 cm^{-1} which represents the thiol group C-S bond stretching vibration (Stuart, 2004) is observed for PP-SH, indicating that the thiol groups were successfully grafted onto the PP membrane and hence are present on the PP-SH membrane surface.

To further verify the coordination between the thiol groups and the silver ions, the XPS spectra of the PPS-Ag membrane was obtained. Typical S (2p 3/2) binding energy (BE) for unbound thiol groups are between 163 and 164 eV (Castner et al., 1996). After coordination with the silver ions on the modified membrane surface, the S (2p 3/2) BE shifted to 162.67 eV, as shown in Figure 4.2(a), which is very close to the previously reported BEs at around 162.4 eV for thiol bound to silver (Castner et al., 1996; Gutkin et al., 2009).

On the other hand, Zhu and his coworkers reported that the BE of ionic silver (3d 5/2) in silver nitrate was at 368.21 eV; but that of coordinated silver would slightly shift to a lower value (Zhu et al., 2010). As shown in Figure 4.2(b), the Ag (3d 5/2) peak at 367.73 eV indicated the presence of coordinated silver on the surface, confirming the immobilization of silver onto the PPS-Ag membrane.

4.3.1.3 Stability of the immobilized silver

The stability of the immobilized silver on the membrane surface is of great interest in the study as that may affect the long term anti-biofouling performance of the prepared membrane.

In the leaching experiment, a piece of the PPS-Ag membrane with 6.2 mg silver immobilized on it was used in the experiment. As shown in Figure 4.3, the effluent silver ion concentration dropped from initially about 0.33 $mg \cdot L^{-1}$ to non-detectable or 0 $mg \cdot L^{-1}$ in around 240 min. A mass balance calculation indicated that the amount of silver ions leached out was about 0.07 mg. In other words, only about 1.1 % of the immobilized silver ions were subject to leaching in the experiment. It has been reported that the silver ions coordinated with the amino

groups would achieve a 27 % leaching amount (Zhu et al., 2010). Thus, it appears that the thiol groups provided a much stronger interaction with the silver ions immobilized on the PPS-Ag membrane surface.

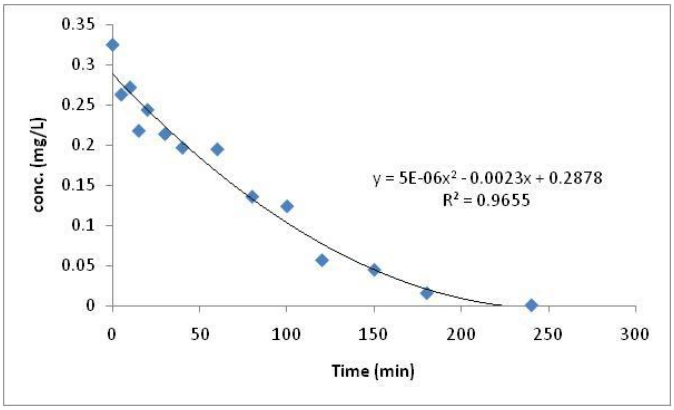

Figure 4.3 Silver leaching test of the PPS-Ag membrane.

The stronger interaction between the immobilized silver and the thiol groups is desired. A more stable anti-biofouling performance of the modified membrane was expected, due to the stably immobilized silver. The possible antibacterial mechanism of the modified membrane surface should be similar with that of the metallic silver. It has been reported that bulk metallic silver is antimicrobial, ascribed to its surface oxide layer and/or release of Ag (I) species (Fan and Bard, 2001; Russell et al., 1994). In this study, even the immobilized silver was firmly chelated with the thiol groups; there is a balance in the interface between the bulk silver and the aqueous environment. In the very limited interfacial area, silver was not very strongly bound to the bulk, due to the affects of the environment. Thus, when the bacteria contacted the membrane surface, they will snatch and then be killed by the silver in this area. However, the unstable immobilized silver leached into bulk feed or permeate was not the portion providing the anti-biofouling performance.

4.3.1.4 Surface morphology

The surface morphology of the original and the modified PP membranes was observed through SEM and AFM. Obvious differences were not observed from the SEM images of the PP and PPS-Ag membranes as shown in Figure 4.4 [(a) and (b)]. It seems that the thiol groups grafting and silver immobilization processes did not severely affect the membrane's original physical structures.

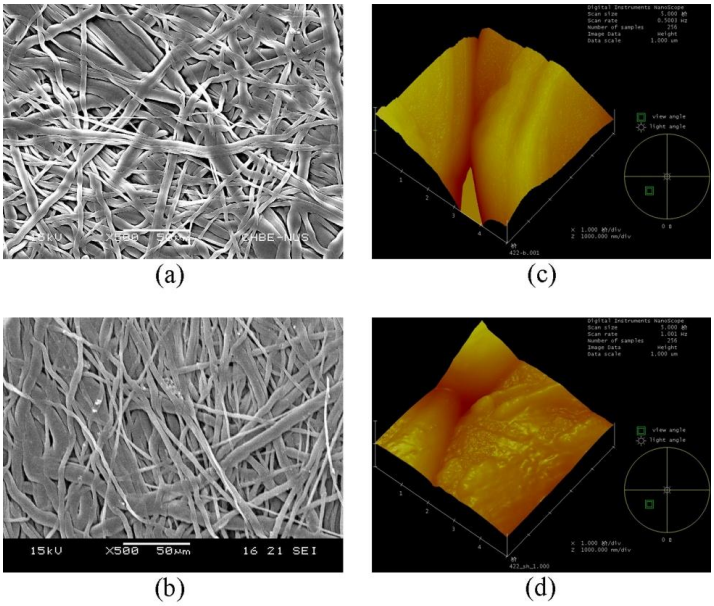

Figure 4.4 SEM and AFM images of the PP membrane [(a) and (c)], and the PPS-Ag membrane [(b) and (d)].

Table 4.1 Membrane surface characteristics determined by AFM

Membrane	Mean Roughness (nm)	Root Mean Squares (nm)	Maximum Height (nm)
PP	268	354	2235
PPS-Ag	74	103	995

The surface morphology of the PP and PPS-Ag membranes was also examined by AFM. As shown in Figure 4.4 [(c) and (d)], in comparison with the PP membrane surface, some tubercles were observed on the PPS-Ag membrane surface. The tubercles may be the sites grafted with the thiol groups, which were chelated with silver ions. Table 4.1 shows the roughness of the two membranes obtained from the AFM analysis. The PPS-Ag membrane had much lower values in terms of the mean roughness, root mean squares and the maximum height than the PP membrane. These data indicated that the PPS-Ag membrane had a smoother surface than the PP membrane. It may be speculated that the grafting of the thiol groups and the immobilization of silver ions probably reduced the surface roughness of the PPS-Ag membrane, attributed to the filling of the voids among the fibers of the PP membrane. It has been known that surface roughness, which can affect the affinity between foulants and membrane surfaces, is an important factor in the extent in bacterial adhesion (Knoell et al., 1999; Pasmore et al., 2001). Thus, the improved smoothness of the PPS-Ag membrane surface may be expected to have a positive effect on the anti-adhesion or anti-biofouling performance of the prepared membrane.

4.3.1.5 Surface hydrophobicity

Water contact angle measurements were usually used to characterize the membrane surface hydrophobicity. The surface water contact angles of the original and prepared membranes were measured and were 117.5° and 109.0° for the PP and PPS-Ag membranes, respectively. The PP membrane was highly hydrophobic and the prepared PPS-Ag membrane appeared to become slightly

more hydrophilic. The reason may be that both the grafted thiol groups and the immobilized silver ions on the membrane surface are hydrophilic. Often, bacterial adhesion is considered to be the critical first step in membrane biofouling. In general, most bacteria show hydrophobic properties and hence tend to attach to hydrophobic surface (Vanloosdrecht et al., 1987). Thus, the less extent of hydrophobicity of the PPS-Ag membrane surface may provide another positive contribution in the anti-adhesion and anti-biofouling performance of the prepared membrane.

4.3.1.6 Pure water flux

Higher permeate flux is always desired for a membrane filtration process. The purpose of preventing membrane biofouling is also to try to maintain a long term stable permeate flux for the used membrane. It is therefore of great interest to examine whether the membrane modification process for anti-biofouling performance sacrifice the permeate flux of the original membrane. The pure water fluxes of the original and the prepared membranes were measured with a dead end filtration system.

Under a pressure of 0.05 MPa at room temperature the PP membrane had a pure water flux of 0.129±0.015 $m \cdot h^{-1}$ (n=8, the number of runs), and that of the PPS-Ag membrane was 0.193±0.018 $m \cdot h^{-1}$ (n=8). The prepared PPS-Ag membrane even showed a higher pure water flux than the original PP membrane. The higher pure water flux of the PPS-Ag membrane may be caused by the increased hydrophilicity of the PPS-Ag membrane after the thiol groups grafting and silver immobilization.

4.3.2 Antibacterial effects of the silver immobilized membrane

Figure 4.5 [(a) and (b)] shows the antibacterial results for *E. coli* growth on the two different types of membrane surfaces from the disk diffusion test. It was observed that *E. coli* actually grew below and above the PP membrane as well as in the surrounding zone; see Figure 4.5(a). The result indicates that the original PP membrane did not provide any antibacterial effect for the Gram-negative bacteria such as *E. coli* that might easily grow on the PP membrane surface. In contrast, *E. coli* colonies were not observed above and below the PPS-Ag membrane, as shown in Figure 4.5(b). Moreover, the PPS-Ag membrane showed an inhibition zone surrounding the membrane sample, possibly due to some silver ions leached from the membrane. The results indicate that the PPS-Ag membrane appeared to have a good antibacterial effect for inhibiting the growth of Gram-negative bacteria such as *E. coli*.

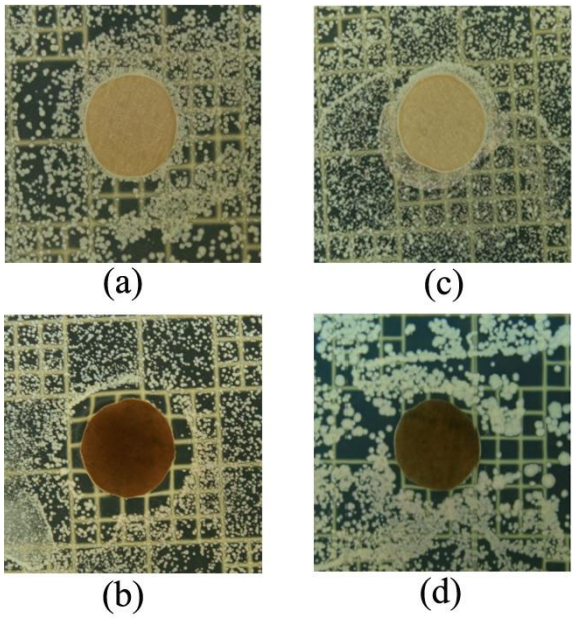

Figure 4.5 Disk diffusion tests for *E. coli* and *S. aureus* on the membranes of PP [(a) and (c)] PPS-Ag [(b) and (d)].

Figure 4.5 [(c) and (d)] presents the results for *S. aureus* from the disk diffusion test. Again, the PP membrane did not show inhibition in the growth of *S. aureus*, as shown in Figure 4.5(c). However, the PPS-Ag membrane effectively prevented the growth of *S. aureus* and therefore no bacteria colonies were observed above and below the PPS-Ag membrane. The inhibition zone around the membrane sample was also observed; see Figure 4.5(d).

In summary, the results from the disk diffusion experiments illustrated PP membrane was highly prone to bacterial growth on the surface, but the PPS-Ag membrane showed great effectiveness in controlling the growth of both the Gram-negative and Gram-positive bacteria tested. The good antibacterial effect of the PPS-Ag membrane is the major premise on which the anit-biofouling performance of the membrane is based.

4.3.3 Anti-biofouling performances of the PPS-Ag membrane

4.3.3.1 Bacteria suspension immersion results

The anti-biofouling performances of the PPS-Ag membrane were investigated by immersing the membrane samples in high concentration mixed bacteria suspensions (~10^9 CFU·mL^{-1}) containing both Gram-negative (*E. coli*) and Gram-positive (*S. aureus*) bacteria for a period of up to 12 d. The membrane samples were taken and observed with SEM and CLSM.

The SEM results for the PP and PPS-Ag membranes tested with the mixed bacteria suspensions are shown in Figure 4.6. The corresponding CLSM results for the PP and PPS-Ag membranes are present in Figure 4.7.

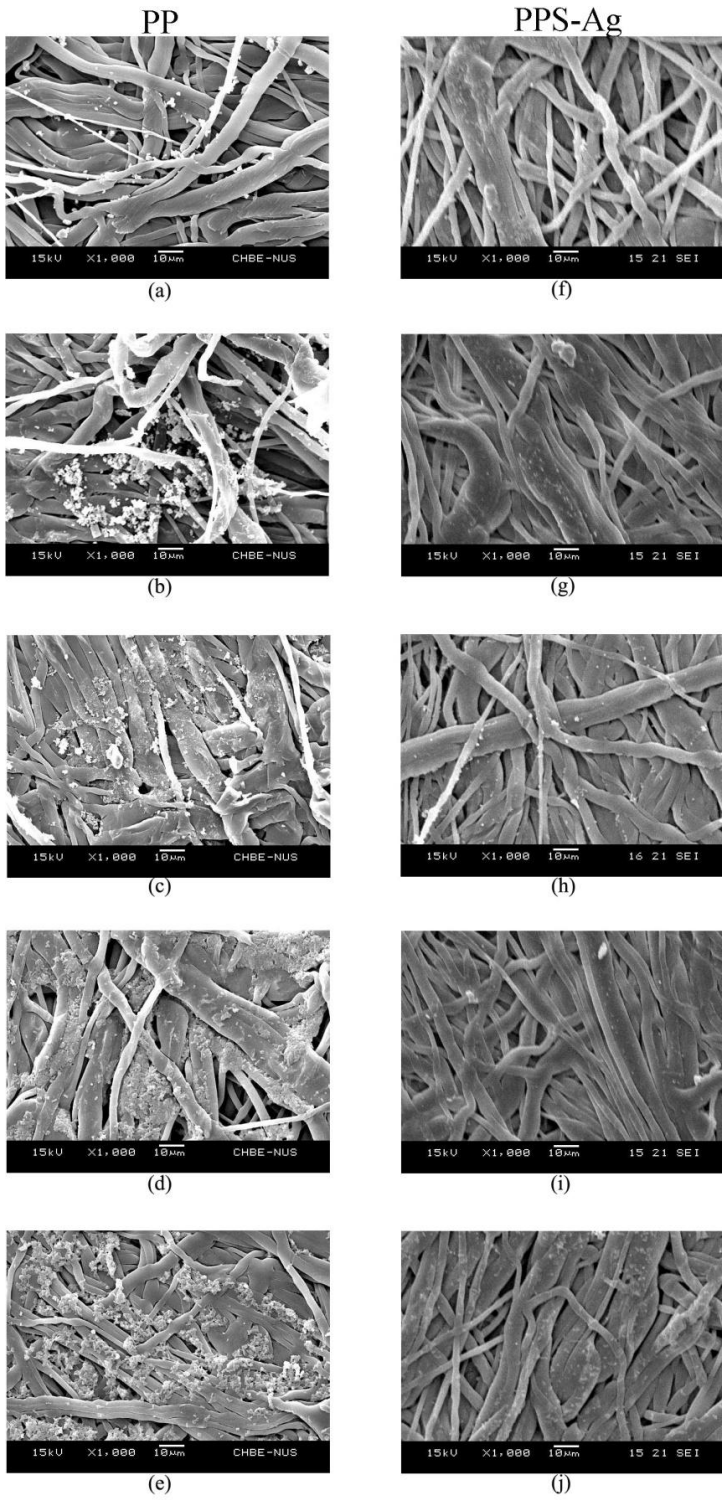

Figure 4.6 SEM images of bacteria on the PP and PPS-Ag membranes after 1d [(a) and (f)], 2d [(b) and (g)], 4d [(c) and (h)], 6d [(d) and (i)] and 12d [(e) and (j)] immersion in bacteria suspension.

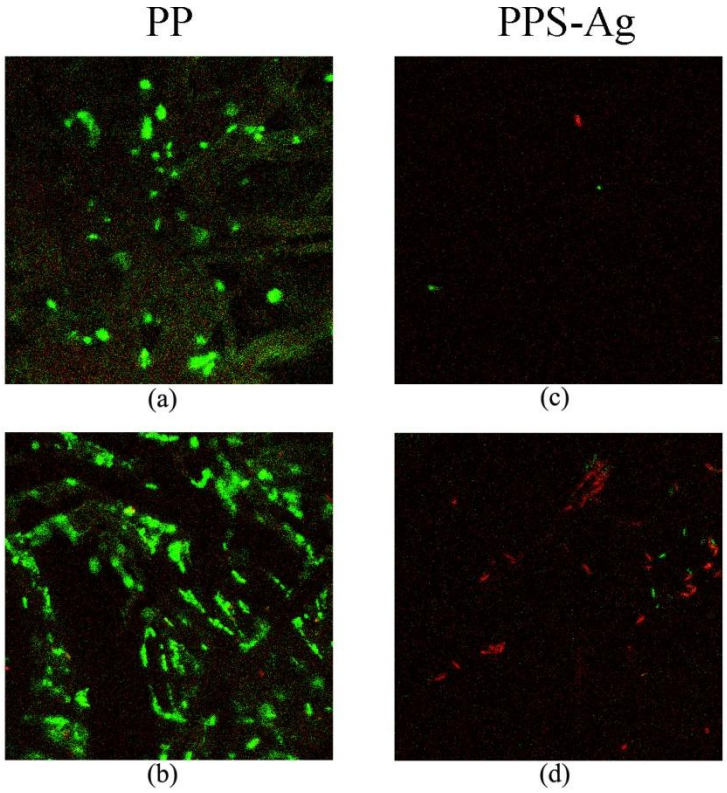

Figure 4.7 CLSM images of bacteria on the PP and PPS-Ag membranes after 4d [(a) and (c)] and 6d [(b) and (d)] immersions in bacteria suspension.

From Figure 4.6 (a), the PP membrane was found to have been attached bacteria after 1 d immersion. More colonies were observed on the PP membrane surface after 2 d immersion; see Figure 4.6 (b). Thick and uniform bacteria clusters were found to cover the membrane surface after 4 d immersion; see Figure 4.6 (c). The corresponding CLSM images in Figure 4.7 [(a) and (b)] proved that the cells on the PP membrane sample were viable (appeared green), and more viable bacteria were found with the increase of immersion time. Most area of the PP membrane was fully covered by bacteria after 6 d or longer immersion; the bacteria coverage on the PP membrane in general showed gradual increase during the 12 d period of the immersion experiments.

However, the SEM images in Figure 4.6 [(f) to (j)] showed that the PPS-Ag membrane surface was relatively clean and free of bacteria growth during the 12 d experiments. Correspondingly, the CLSM images in Figure 4.7 [(c) and (d)] show that only few and discrete bacteria on the PPS-Ag membrane surface and most of them were unviable bacteria appeared as red.

From the immersion experiments, it is clear that the PP membrane was strongly subjected to biofouling by the tested bacteria. The PPS-Ag membrane appeared to show good inhibition of biofilm formation on the membrane surface.

4.3.3.2 Bacteria suspension filtration

As shown in Figure 4.8, the fluxes in stage 1 show the initial pure water flux (J_{w0}) of the PP and PPS-Ag membranes. The PPS-Ag membrane had a higher J_{w0} than the PP membrane.

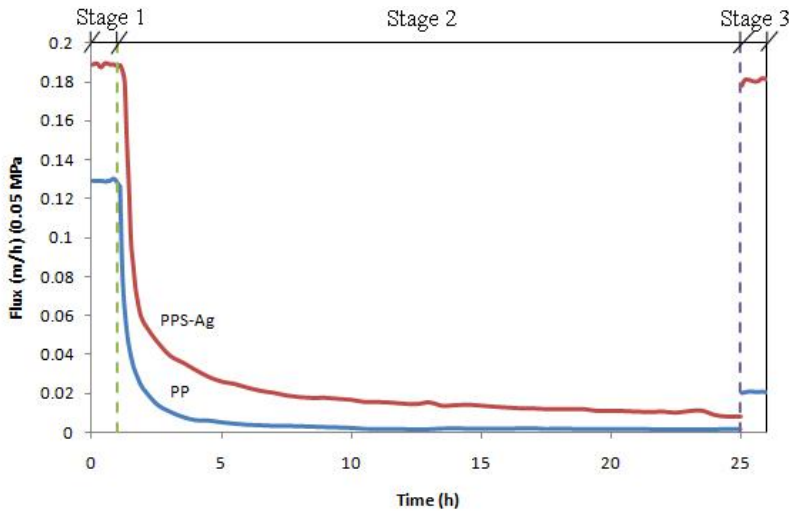

Figure 4.8 Permeate fluxes of PP and PPS-Ag membranes in the three stages of filtration experiments.

During the stage 2 for mixed bacteria separation filtration, the fluxes of both PP and PPS-Ag membranes decreased with the filtration time, although the flux decay was slightly slower for the PPS-Ag membrane than the PP membrane. This can be attributed to the accumulation of bacteria that formed cake on the membrane surfaces and the cake thickness may increase with time. The slower flux decrease indicated a surface more difficult to be fouled or a better anti-biofouling performance of the membrane.

After filtration of the mixed bacteria suspension, the membranes were cleaned and the fluxes with pure water were measured again (denoted as J_{w1} shown in stage 3 in Figure 4.8). Based on J_{W0} and J_{W1}, the relative flux recovery (RFR) was calculated. The RFR of the PPS-Ag and PP membranes were found to be 95.7% and 16.2%, respectively. The results suggest that the PPS-Ag membrane, even if it had fouling or biofouling, this was mainly of a reversible nature. Most of the flux decrease could be easily recovered by simple physical cleaning. While membrane biofouling is usually found to cause a permeate flux decrease that cannot be recovered by physical cleaning, the bacteria deposited on the PPS-Ag membrane surface during the filtration experiments were actually killed by the immobilized silver and the fouling as unviable particles could be easily removed by physical cleaning. In contrast, the permeate flux drop of the PP membrane could not be effectively recovered by the physical cleaning. The irreversible fouling of the PP membrane was considered to be due to the viable bacteria that attached and grew on the membrane and were difficult to be removed by the physical cleaning. Thus, the modified membrane in this chapter exhibited a good anti-biofouling

performance, attributed at least in part to the irreversible biofouling being changed to reversible physical fouling.

4.4 Conclusion

In this chapter, PP membrane was found to be highly subject to biofouling that was largely irreversible with the bacteria tested. In order to achieve anti-biofouling performance of PP membrane through surface modification, a method was developed to graft the thiol groups to PP membrane surface, and then silver ions were immobilized onto the membrane through coordinating with the thiol groups. The grafted thiol groups on the PP membrane were verified with ATR-FTIR analysis, and the coordination between the thiol groups and silver ions were confirmed from the XPS spectra. The immobilized silver was found to be stable in the leaching test, and only about 1.1 % of the immobilized silver was subject to leaching. SEM and AFM observations of the surface of the prepared membrane (PPS-Ag) showed smoother surface than that of the original PP membrane. Water contact angle measurement indicated that the PPS-Ag membrane surface became slightly more hydrophilic than the PP membrane. From the disk diffusion experiment, both *E. coli* and *S. aureus* were found to be able to grow on the PP membrane, but unable to grow on the PPS-Ag membrane. In the mixed bacteria suspension immersion test, *E. coli* or *S. aureus* was found to attach or grow on the PP membrane as viable cells, in contrast, only discrete bacteria, most being non-viable cells, were observed on the PPS-Ag membrane. Furthermore, in the mixed bacteria suspension filtration experiments, the PPS-Ag membrane showed higher permeate fluxes, slower flux decay and, particularly, greater relative flux recovery

(RFR) than the PP membrane, indicating that the fouling on the PPS-Ag membrane, if any, was mostly reversible, and the flux could be recovered by simple physical cleaning. Since the immobilization of silver on the PP membrane can be relatively easily carried out and the immobilized silver was stable, the modified membrane immobilized with silver that can provide an excellent anti-biofouling performance, has a great prospect for many practical applications of the membrane technology in water and wastewater treatment.

Chapter 5 **Development of both hydrophilic and olephobic membrane surface for antifouling performance**

Summary

A functional additive polymer with hydrophilicity and oleophobicity was synthesized and blend with PVDF to produce membranes that would be able to provide antifouling performance for both microorganisms and a wider spectrum of organic foulants including oils. The additive polymer was synthesized through graft copolymerization of tBMA from P(VDF-co-CTFE) *via* ATRP. The grafted PtBMA chains were subsequently hydrolyzed to PMAA which were further esterified with FPEG that contained an oleophobic perfluorinated hydrocarbon end and a hydrophilic PEG chain. The synthesis procedures were verified with ATR-FTIR and NMR analyses. It was found that the developed membrane surfaces showed two distinctively different wettabilities simultaneously, i.e., highly hydrophilic as well as highly oleophobic. The surface morphologies of the prepared membranes with the additive polymer were examined with SEM. The membrane surface morphology could be adjusted through the change of the additive polymer amount in the casting solution. A higher portion of the additive polymer or a lower concentration of polymer in the casting solution made the produced membranes have more porous surfaces. All prepared membranes retained at least 99.8 % of oil in the filtration of an oil/water emulsion sample (500 $mg \cdot L^{-1}$). Especially, the membrane containing 30 wt% of the additive

polymer could completely inhibit oil adsorption or prevent oil fouling. Hence, the synthesized additive polymer provides the great prospect to prepare membranes that are both hydrophilic and oleophobic, which may play an important role in improving a membrane's antifouling performances for biological and organic foulants.

5.1 Introduction

In Chapter 3 and Chapter 4, the strategy to prevent membrane biofouling has been through the inhibition of the growth and reproduction of microbes on the membrane surface by immobilizing biocides, such as silver, onto the membrane surface. This has provided ultimate protection for membranes in case microorganisms do attach to the surfaces of the membranes. However, another more desired strategy to prevent membrane biofouling can be the avoidance of the initial attachment of microbes onto the membrane surface from the beginning. It has been known that a hydrophilic surface can reduce the adhesion of cells (Krishnan et al., 2008). Many approaches have therefore been taken to mitigate biofouling through the hydrophilic modification of membrane surfaces (Krishnan et al., 2006; Luo et al., 2005; Pieracci et al., 1999).

Membrane organic fouling is another type of irreversible fouling. In general, it is also commonly accepted that a hydrophilic membrane surface can provide better resistance against organic foulants such as protein and natural organic matter (NOM) (Rana and Matsuura, 2010). Hence, hydrophilic polymers have been blended with base membrane materials to prepare hydrophilic membranes to enhance their antifouling performances for organic substances (Asatekin et al.,

2007; Zhao et al., 2007). It seems useful that constructing a hydrophilic surface for a membrane may provide non-specific resistance to both biological and organic foulants because of the formation of a compact hydration layer that can hinder their attachments (Chen et al., 2011b).

Oils, as a special group of organic substances, are highly hydrophobic because of their very low surface tensions. Hydrophilic surfaces might also reduce the possibility for oil droplets to directly contact the membrane surface, and thus, to some extent, mitigate oil fouling (Chakrabarty et al., 2008; Li et al., 2006a). However, if oil droplets are indeed in contact with the hydrophilic surface due to the reasons such as the convective filtration flow or displacement of water lager, they would easily spread on the membrane surface (exhibiting very small contact angles) because the surface free energy of the hydrophilic surface is much higher than the surface tensions of oils (C.J, 1993; Stamm, 2008). This will lead to adhesion and then fouling of the membrane by oils significantly, which is different to be cleaned. In the literature, there has been a report that used ultrafiltration membrane with low surface free energy for oil/water emulsion separation to facilitate membrane cleaning (Hamza et al., 1997). However, the membrane surfaces with low surface free energies were highly hydrophobic, which lead to low water permeability and other fouling caused by protein, NOM and microbes (Rana and Matsuura, 2010).

The normal polymeric additives used in membrane surface modification *via* blending and other incorporation methods usually provide only single surface wetting property, i.e., hydrophilic or hydrophobic. There is a dilemma to prepare

a membrane surface with high water permeability and high antifouling performance for a broad spectrum of organic and biological foulants, which ideally needs the membrane surface to be both hydrophilic and oleophobic – two distinctively different wettabilities.

In order to solve this dilemma, a copolymer with both hydrophilicity and oleophobicity was synthesized as a novel additive in this chapter. Antifouling membranes were then developed by blending the novel additive polymer with, a popular base membrane material, PVDF, to fabricate membranes with hydrophilic and oleophobic surfaces. The additive polymer was synthesized by firstly graft copolymerization of tBMA from P(VDF-co-CTFE) *via* ATRP. Secondly, the PtBMA side chains of the graft copolymer (P(VDF-co-CTFE)-g-PtBMA) was hydrolyzed to give PMAA side chains. Steglich esterification was then used to react FPEG with P(VDF-co-CTFE)-g-PMAA to produce the additive polymer. The prepared membranes with the additive polymer were characterized and their antifouling performances for oil were preliminarily evaluated in this chapter.

5.2 Materials and methods

5.2.1 Materials

Poly(vinylidene fluoride-co-chlorotrifluoroethylene) [P(VDF-co-CTFE), 31508] containing 5.68 wt% of chlorine, was provided by Solvay Solexis. Perfluoroalkyl surfactant (FPEG, Zonyl® FSN-100) was provided by DuPont. Tert-butyl methacryale (tBMA, 98%), CuCl (99.99%), 1,1,4,7,7-pentamethyldiethylenetriamine (PMDETA, 99%), p-toluenesulfonic acid monohydrate (TSA, 98.5%), N,N-dicyclohexylcarbodiimide (DCC, 99%), 4-

(Dimethylamino)pyridine (DMAP, 99%), anhydrous toluene (99.8%), hexadecane (99%), and polyvinylidene fluoride (PVDF, Mw ca. 550 000 $g \cdot mol^{-1}$) were purchased from Sigma-Aldrich and used without further purification. N,N-dimethylformamide (DMF, Tedia, HPLC grade), and N-methylpyrrolidinone (NMP, Teida, HPLC grade) were used as received without further purification. Deionized (DI) water (18 MΩ) purified with a Milli-Q system from Millipore was used to prepare all solutions as needed in the study.

5.2.2 Synthesis of graft copolymer P(VDF-co-CTFE)-g-PtBMA

4 g of P(VDF-co-CTFE) was dissolved in 30 mL NMP at 60 °C and mechanically stirred at 500 rpm in a air-tight flask purged with N_2. 512 mg of CuCl and 1.136 mL of PMDETA were subsequently added into the flask and completely mixed with the polymer solution. Then, 4.11 g of tBMA was added in the flask and the atom transfer radical polymerization (ATRP) started. The polymerization was allowed to process for 2 h at 60 °C under mechanical stirring (500 rpm). The product, i.e., (P(VDF-co-CTFE)-g-PtBMA), was precipitated in a 1:1 water : ethanol mixture, and then purified by twice redissolving it in NMP and precipitating it in 1:1 water : ethanol solutions. The product was finally recovered by filtration and then dried with a freeze drier (Labconco, FreezeZone Plus).

5.2.3 Hydrolysis of P(VDF-co-CTFE)-g-PtBMA

P(VDF-co-CTFE)-g-PtBMA (5 g) was swelled and mixed with anhydrous toluene (100 mL) in a 250 mL three neck flask with mechanical stirring at 500 rpm. 10 g of TSA was added into the three neck flask and completely dissolved by vigorous stirring. The hydrolysis reaction was processed for 7 h at 85 °C. After

7 h, the heterogeneous reaction mixture was poured into a beaker with 500 mL DI water. The product, P(VDF-co-CTFE)-g-PMAA, was collected by filtration and washed with DI water to remove remaining TSA. Subsequently, the product was freeze dried.

5.2.4 Esterification of P(VDF-co-CTFE)-g-PMAA with FPEG

The FPEG were reacted onto the P(VDF-co-CTFE)-g-PMAA through Steglish esterification. 2 g of the P(VDF-co-CTFE)-g-PMAA and 1 g of FPEG were completely dissolved and mixed in a capped bottle with 40 mL DMF at ambient temperature and magnetically stirred at 800 rpm. Subsequently, 0.24 g of DCC and 0.013 g of DMAP were added. The reaction was carried out for 48 h. The produced graft copolymer was precipitated in DI water, and further rinsed with DI water to remove unreacted FPEG. Finally, the produced additive polymer was freeze dried and stored in dessicator for further use.

5.2.5 Characterization of graft copolymers

The various intermediate and final products in the different synthesis steps were characterized through the analyses of attenuated total reflection fourier transform infrared (ATR-FTIR) and nuclear magnetic resonance (NMR) spectra. Samples were completely dried and the ATR-FTIR spectra were collected through a FTIR spectrometer (Varian 660-IR) with an ATR component supplied by Perkin Elmer. The 1H NMR spectra of 10 wt% polymer solutions in DMSO-d6 were measured at 300 K with a Bruker Avance DRX500 spectrometer at 500 MHz resonance frequency.

5.2.6 Membrane preparation

Table 5.1 Compositions of blend membrane casting solutions

Membrane type	Additive polymer : PVDF	Casting solution polymer concentration (wt%)
B	4:6	12
C	3:7	12
D	2:8	12
E	1:9	12
C16	3:7	16
C18	3:7	18
C20	3:7	20

The synthesized functional additive polymer and PVDF (Mw ca. 550 000 $g \cdot mol^{-1}$) as a matrix support polymer were mixed in different ratios, including 4: 6, 3: 7, 2: 8 and 1: 9, but in the same polymer concentration of 12 wt% for the B, C, D and E membranes, respectively. The C16, C18 and C20 membranes are prepared with the same ratio of 3 parts additive polymer vs. 7 parts PVDF, but higher concentrations of 16 wt%, 18 wt% and 20 wt%, respectively. The compositions of the prepared membranes in this chapter are given in Table 5.1.

The components of each of the casting solutions were dissolved in DMF as the solvent and the mixture was mechanically stirred at 300 rpm in a glass container placed in an oil bath at 80 °C for 5 hours to obtain a homogenous polymer casting solution. Then, any air bubbles entrapped in the casting solution were removed by centrifuging the casting solution at 9000 rpm for 20 minutes.

After that, the casting solution was spread onto a clean glass plate with an Elcometer 3600 Doctor Blade Film Applicator set to a film thickness of 250 µm. The cast glass plates were then immediately immersed in a DI water coagulation bath at 60 °C for 5 hours for phase inversion and surface segregation to take place. Finally, the membrane was moved from the water bath and dried in air at a room temperature of around 25 °C for 12 h, and then stored in desiccators for further use.

5.2.7 Characterization of membranes

5.2.7.1 Membrane morphology

The morphologies of the prepared membranes were observed with a scanning electron microscope (SEM, JEOL JSM-5600LV). The membrane samples were completely dried in an oven at 60 °C for 12 h before the observation. For the membrane cross section, the membrane samples were freeze-fractured in liquid nitrogen to produce regular cross sections. The membrane surfaces and cross sections were then coated with platinum through a vacuum electric sputter coater (JEOL JFC-1300) for 50 seconds with a current of 30 mA following the standard procedures. Subsequently, the surfaces and cross sections of the prepared membranes were scanned for the SEM images. Surface pore sizes of the prepared membranes were also measured from the surface SEM images by the software named Smile View (JEOL) supplied with the microscope. The thicknesses of the membrane samples were determined from their corresponding SEM images, and then their cross section areas were calculated.

5.2.7.2 Mechanical properties

The mechanical properties (tensile stress and tensile strain) of the prepared membranes were measured by an INSTRON advanced mechanical testing system 5542. The dry membrane samples were cut into pieces of 6 cm length and 1 cm width with the thickness measured to calculate the cross section area. A membrane piece was vertically clamped at both ends to the instrument with an initial gauge length of 5 cm. The dragging rate of the grip was set at 1 $cm \cdot min^{-1}$. At least 5 tests for each type of the membranes were made and the average was reported for the tensile stresses and tensile strains in this study.

5.2.7.3 Membrane surface wetting properties

The prepared membranes' surface wetting properties were evaluated through contact angle measurements with different testing liquids using a contact angle goniometer (250-F1) from Ramé-Hart Instrument Co. The water contact angles of the prepared membranes were obtained by the static captive bubble method. A membrane sample was immersed in the measuring cell filled with DI water and fixed at a horizontal position with the target membrane surface facing down in the cell. An air bubble (~10 μL) was injected from a microsyringe with a stainless steel needle onto the target membrane surface in the DI water. The air bubble image on the membrane surface was captured and analyzed by the instrument to give the water contact angle value. The surface wettability of the prepared membranes was also examined with the oil contact angle measurement through the static sessile drop method. Instead of using an air bubble, a 10 μL droplet of hexadecane (oil) was dropped onto the dry membrane surface. The droplet image was captured and analyzed by the instrument to obtain the oil contact angle value

of the tested membrane. At least 10 measurements for each membrane sample at different locations on the membrane surface were made, and the average value of the measurements was used as the representative contact angle of the tested membrane.

5.2.8 Membrane filtration and antifouling tests

The membrane filtration experiments were conducted with a dead-end filtration system which had been described in Section 4.2.3.5.

An oil/water emulsion (500 $mg \cdot L^{-1}$) was prepared by mixing 0.5 g of hexadecane in 1 L DI water with a homogenizer (Cole-Parmer, Labgen 700) stirred at 14,000 rpm for 20 min.

The filtration experiment consisted of three stages, in order to observe the permeate flux change of the membrane during the filtration of the oil/water emulsion, and investigate the membrane flux recovery. Initially, the prepared membrane was filtered with pure water until the flux became constant. This constant pure water flux was then recorded for 10 min and denoted as J_{W0}. Secondly, the membrane was filtered with the 500 $mg \cdot L^{-1}$ oil/water emulsion for 2 h. The change of permeate flux was recorded. After the 2 h filtration of oil/water emulsion, the membrane was rinsed with DI water and mechanically shaken at 200 rpm in a beaker with 50 mL DI water for 30 min. Finally, the cleaned membrane was filtered with pure water again until the flux became constant. The constant pure continued for another 10 min and was recorded and denoted as J_{w1}. The relative flux recovery (RFR) indicating the extent of the possible reversible fouling was calculated by $RFR = (J_{W1}/J_{W0}) \times 100\%$.

The transmembrane pressures were set at 0.014, 0.05, 0.1 and 0.1 MPa, respectively, for the membranes prepared from casting solutions with polymer concentrations of 12 wt%, 16 wt%, 18 wt% and 20 wt%.

Oil concentrations in the feed and permeate samples were measured with a handheld fluorometer (TD- 500D). The procedures are as the followings. 100 mL of water sample was moved into a 250 mL separating funnel and pH value was adjusted with 2 M HCl to 2. Subsequently, 10 mL of hexane was added, and the separating funnel was vigorous shaken for 5 min with frequent outgassing. Then, the separating funnel was settled on a stand for 5 min to achieve completely separating of the hexane layer with the water layer. 1 mL was taken from the hexane layer and transferred into a cell of the handheld fluorometer to detect the oil concentration.

5.3 Results and discussion

5.3.1 Reactions in preparing the hydrophilic and oleophobic copolymer as the additive based on P(VDF-co-CTFE)

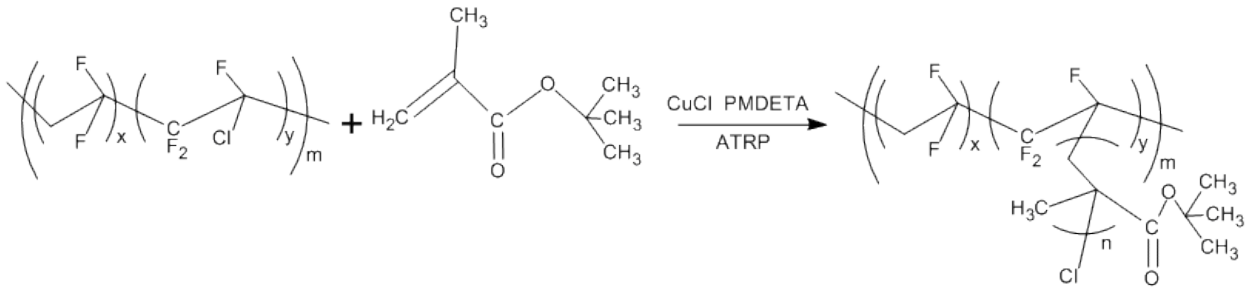

Scheme 5.1 Graft copolymerization from P(VDF-co-CTFE) with tBMA *via* ATRP.

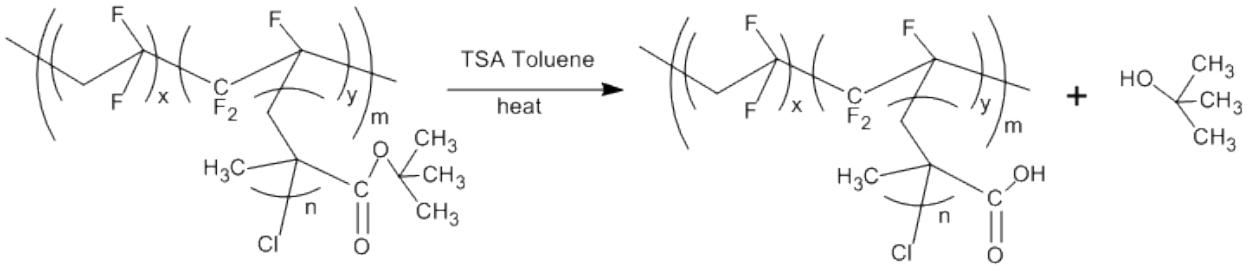

Scheme 5.2 Hydrolysis of P(VDF-co-CTFE)-g-PtBMA with TSA.

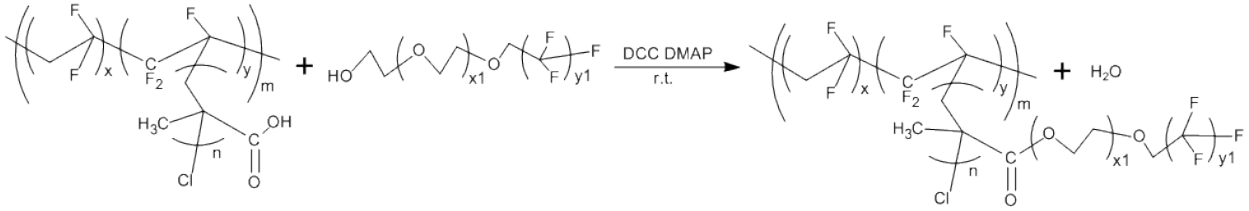

Scheme 5.3 Esterification of P(VDF-co-CTFE)-g-PMAA with FPEG.

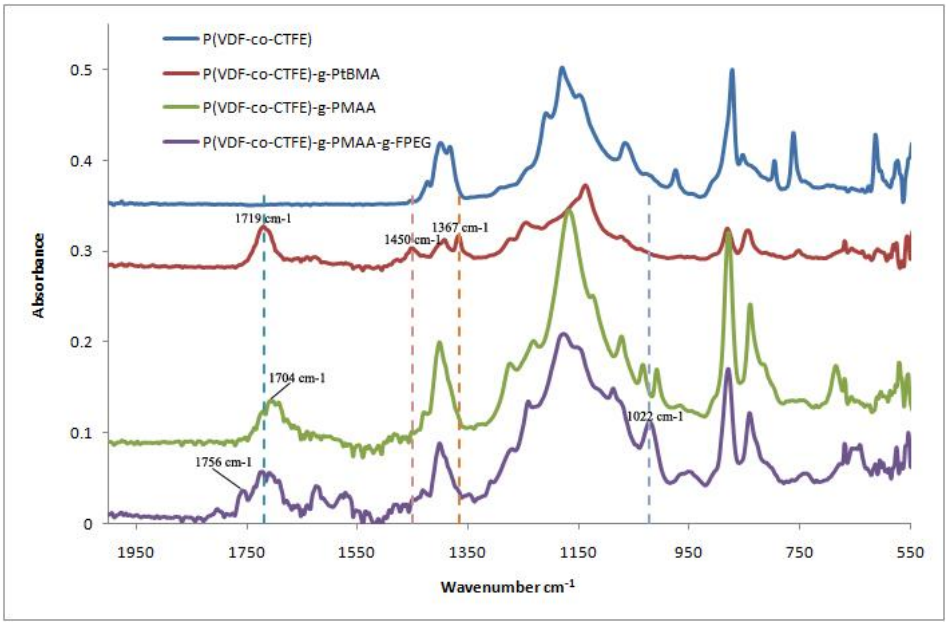

Figure 5.1 ATR-FTIR spectra of the intermediate and final produced copolymers.

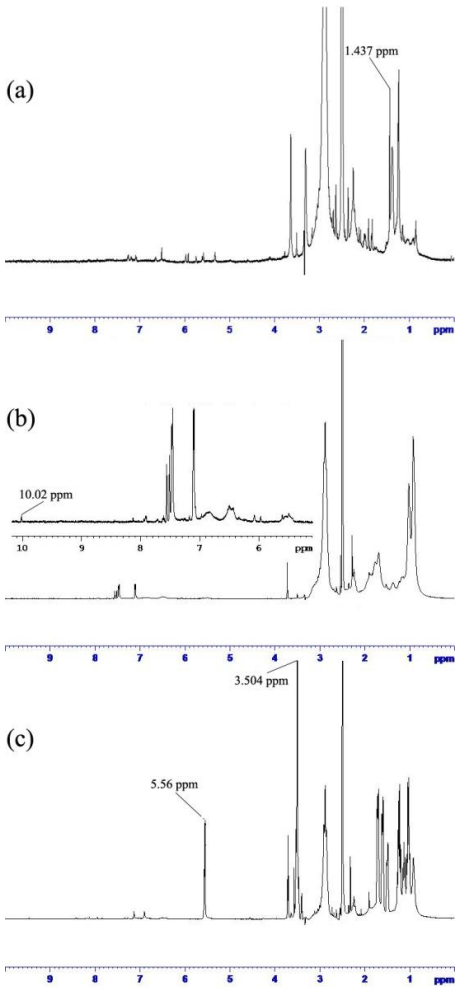

Figure 5.2 NMR spectra of (a) P(VDF-co-CTFE)-g-PtBMA, (b) P(VDF-co-CTFE)-g-PMAA and (c) P(VDF-co-CTFE)-g-PMAA-g-FPEG.

The hydrophilic and oleophobic additive polymer was synthesized through 3 steps. In the first step, tBMA was grafted from P(VDF-co-CTFE) *via* ATRP, see Scheme 5.1. After the polymerization, the produced P(VDF-co-CTFE)-g-PtBMA was identified with ATR-FTIR and NMR spectra. As shown in the spectrum of P(VDF-co-CTFE)-g-PtBMA of Figure 5.1, a peak at 1719 cm^{-1} is observed, which can be assigned to the ester carbonyl (Lei and Liao, 2001); and there are two peaks at 1367 cm^{-1} and 1450 cm^{-1} caused by the methyl C–H bending vibration (Stuart, 2004). Both the ester groups and the methyl groups belong to

tBMA because P(VDF-co-CTFE) does not have any of them. The NMR spectrum of P(VDF-co-CTFE)-g-PtBMA in Figure 5.2 (a) shows a peak at 1.437 ppm, indicating the appearance of the tert-butyl group (Pretsch et al., 2009). These spectra indicate the successful grafting of tBMA from P(VDF-co-CTFE) *via* ATRP. The conversion of tBMA up to 83.7 % in the graft copolymerization was achieved.

Secondly, P(VDF-co-CTFE)-g-PtBMA, the product of the first step, was hydrolyzed with TSA to produce P(VDF-co-CTFE)-g-PMAA; as the reaction shown in Scheme 5.2. By comparing the ATR-FTIR spectra after with that before the hydrolysis in Figure 5.1, the peaks at 1367 cm^{-1} and 1450 cm^{-1} attributed to tert- butyl group disappeared; and the peak at 1719 cm^{-1} shifted to 1704 cm^{-1} that could be assigned to the C=O stretching vibration of carboxylic acids (Stuart, 2004). In Figure 5.2 (b), the NMR spectrum indicates the disappearance of methyl protons on tert-butyl group at 1.437 ppm and the present of proton on carboxylic group at 10.02 ppm (Pretsch et al., 2009). These spectra data support the successful hydrolysis reaction given in Scheme 5.2, including the disappearance of the tert-butyl group and the appearance of the carboxylic group. The hydrolysis conversion was found to achieve 94 %, indicating that most of the grafted PtBMA were hydrolyzed into PMAA.

Thirdly, FPEG was grafted from P(VDF-co-CTFE)-g-PMAA *via* esterification; see the reaction in Scheme 5.3. As shown in the ATR-FTIR spectrum of P(VDF-co-CTFE)-g-PMAA-g-FPEG in Figure 5.1, a peak at 1756 cm^{-1} attributed to the aliphatic C=O stretching of ester groups appeared; and

another peak at 1022 cm^{-1}, assigned to the C–O–C stretching of ethers, was also observed (Stuart, 2004). The NMR spectrum in Figure 5.2(c) show a peak at 3.504 ppm, indicating the existence of the ether group, and a peak at 5.56 ppm, belonging to the proton of ethyl group connected with the perfluoroalkyl end of FPEG (Pretsch et al., 2009). The appearance of the ester group and the ether group (belonging to FPEG) in the produced polymer verified the successful esterification between P(VDF-co-CTFE)-g-PMAA and FPEG. After the esterificatin reaction, 80% of FPEG was found being grafted to P(VDF-co-CTFE)-g-PMAA.

5.3.2 Morphologies of the prepared membranes

The morphologies of the prepared membranes were observed with SEM. Membranes prepared with the same casting solution polymer concentration of 12 wt%, but different additive polymer ratios showed different surface morphologies; see Figure 5.3. With the decrease of additive polymer or increase of PVDF ratio, the membrane surface became less porous and denser [from B(1) to E(1) in Figure 5.3, left column]; and the sponge-like structure in the cross section was suppressed with and more macrovoids showed up [from B(2) to E(2) in Figure 5.3, right column].

The formation of macrovoids can be caused by the instantaneous liquid–liquid demixing during the coagulation (Smolders et al., 1992). The polymer solvent (DMF) in the casting solution has a good affinity with the nonsolvent water, and then, induce a rapid demixing, which resulted in thinner surface selective layers and more macrovoids in the cross section. However, the ternary diffusions among

components in the phase inversion system could be hindered with a higher portion of additive polymer such as that more than 20 wt%, resulting in a delayed precipitation in the membrane sub layer, caused less macrovoids formed in the cross section. The reason may be that the synthesized additive polymer was highly compatible with PVDF because they had similar main molecular chain structures and close molecular weights. The existence of strong interactions among the additive and base polymer in the casting solution can reduce the polymer precipitation rate during the phase inversion process, and thus produce less macrovoids in the membrane cross section structures (Shi et al., 2007).

B(1)

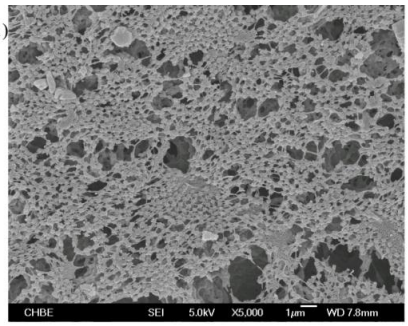

B(2)

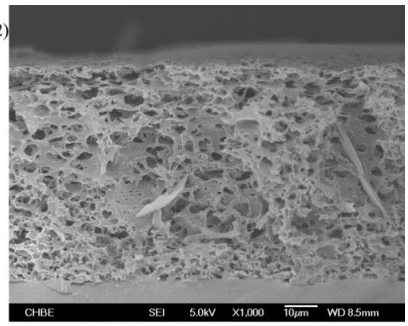

C(1)

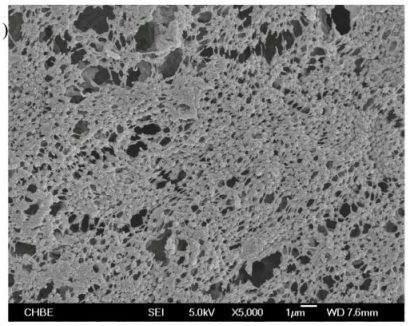

C(2)

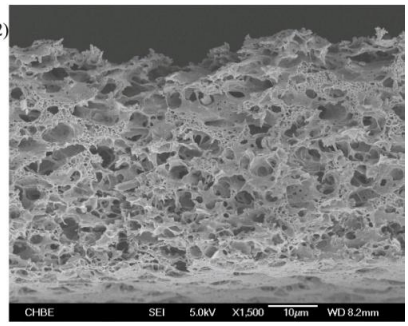

D(1)

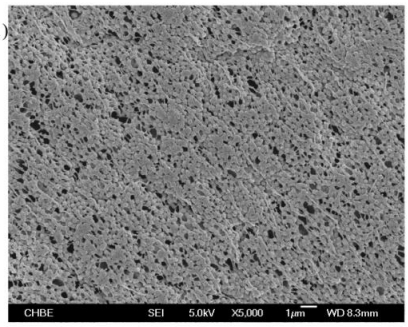

D(2)

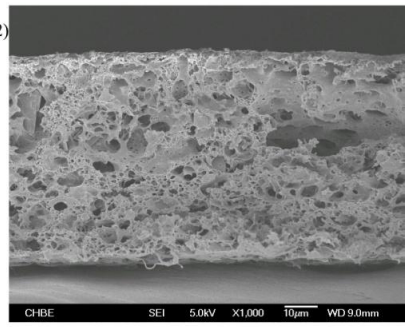

E(1)

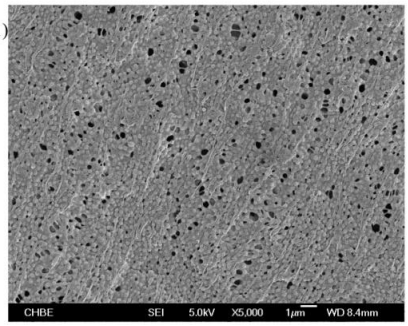

E(2)

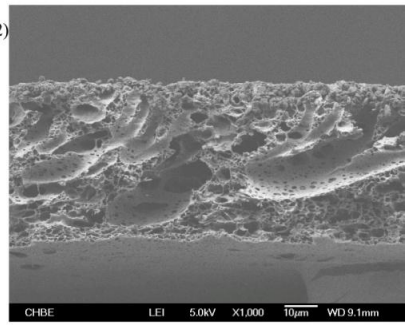

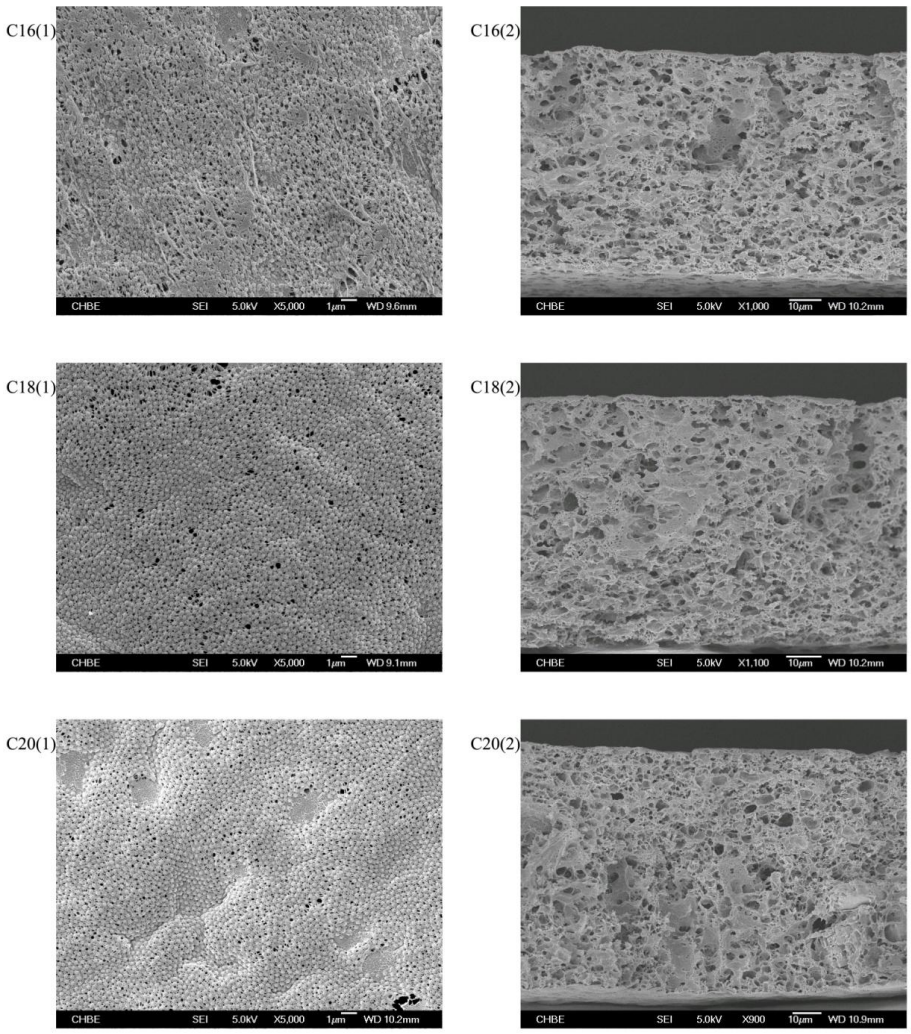

Figure 5.3 Surface (left) and cross section (right) SEM images of the prepared membranes.

Furthermore, the membranes were produced with the same blend ratio (3:7 of additive polymer: PVDF), but different casting solution concentrations. The produced membranes were found to produce denser and less porous surface, with the increase of the polymer concentration in the casting solution; see C15(1) to C20(1) in Figure 5.3. However, no obvious differences but the thicknesses were observed in the cross sections of those membranes; see C16(2) to C20(2) in Figure 5.3.

In summary, the prepared membranes all showed porous cross sections, but different surface morphologies or porosities, which could be varied through changing the ratio of the additive polymer to PVDF or the polymer concentration in the casting solution.

5.3.3 Membrane surface wetting properties and mechanical strengths

Table 5.2 Membrane wettabilities and mechanical properties

Membrane	Water contact angle (°)	Oil (hexadecane) contact angle (°)	Tensile stress (MPa)	Tensile strain (%)
B	21	78	3.8	5.42
C	26	75	4.52	7.9
D	29	64	6.92	8.55
E	40	42	7.30	19.70
C16	26	73	4.57	6.3
C18	26	72	5.79	6
C20	25	72	6.44	5.43

The membrane surface wetting properties were evaluated with water and oil contact angles. The synthesized additive polymer was grafted with FPEG containing a highly hydrophilic polyethylene glycol chain. The prepared membranes with the additive polymer were found to become very hydrophilic that the water droplet on the dry membrane surface would immediately seep into the membrane. Thus, the water contact angles of the prepared membranes were measured with the static captive bubble method rather than the static sessile drop method. It was found that with the increase of the additive polymer ration in the

membrane materials, the water contact angle became smaller, indicating higher hydrophilicity of the membrane surface; see Table 5.2. Moreover, the grafted FPEG surfactant also had a highly oleophobic perfluoroalkyl chain. As can be found in Table 5.2, a higher portion of the additive polymer in the casting solution also resulted in a higher oleophobicity or higher oil contact angle for the fabricated membrane. In addition, membranes prepared by casting solutions with the same additive polymer ratio but different total polymer concentrations showed similar surface wetting properties in terms of their hydrophilicity and oleophobicity; see Table 5.2. Hence, it is the additive polymer that gave the desired properties of the prepared membranes. The hydrophilic as well as oleophobic surface of the prepared membrane can be expected to provide improved antifouling performance.

Mechanical strength is also important for a membrane because it has to sustain the transmembrane pressure during the filtration operation. The mechanical properties including tensile stress and tensile strain of the fabricated membranes had been measured. The membrane with a greater ratio of the additive polymer was found to have a lower tensile stress; see Table 5.2. The existence of the additive polymer made the fabricated membrane more porous but weaker. On the other hand, increasing the casting solution polymer concentration was found to greatly increase the membrane's tensile stress; see Table 5.2. However, all the membranes in Table 5.2 had a tensile stress of 3.8 MPa or above, which is higher than that of a commercially used PVDF membrane at 3.5 MPa (Shi et al., 2007).

PVDF has a good ductility that usually can reach a more than 100 % tensile strain (Shi et al., 2007). In this study, the higher portion of PVDF or lower portion of the additive polymer also caused the fabricated membranes more ductile; see Table 5.2. The casting solution polymer concentration did not dramatically affect the tensile strain of the prepared membranes, but the increase of the additive polymer remarkably reduced the membrane's tensile strain; see Table 5.2.

5.3.4 Oil/water emulsion filtration and membrane antifouling performance

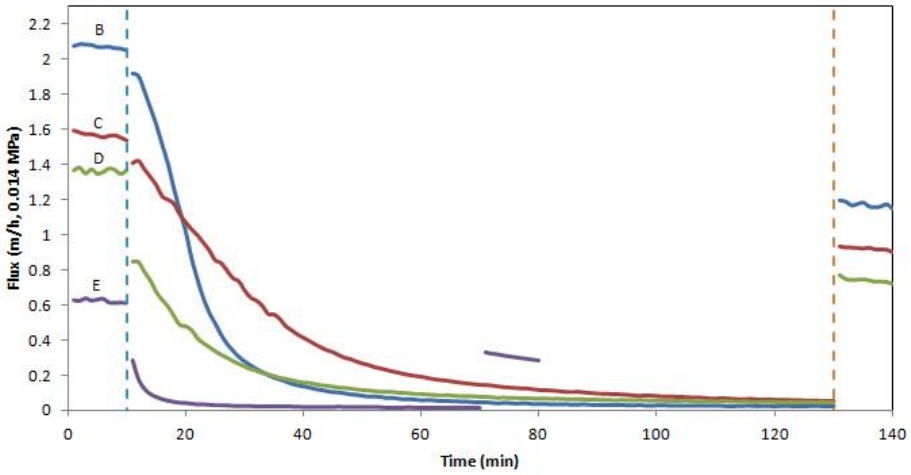

Figure 5.4 Permeate fluxes of the membranes prepared with the same casting solution concentration (12 wt%) but varied additive polymer to PVDF ratios in the filtration of pure water and oil/water emulsion.

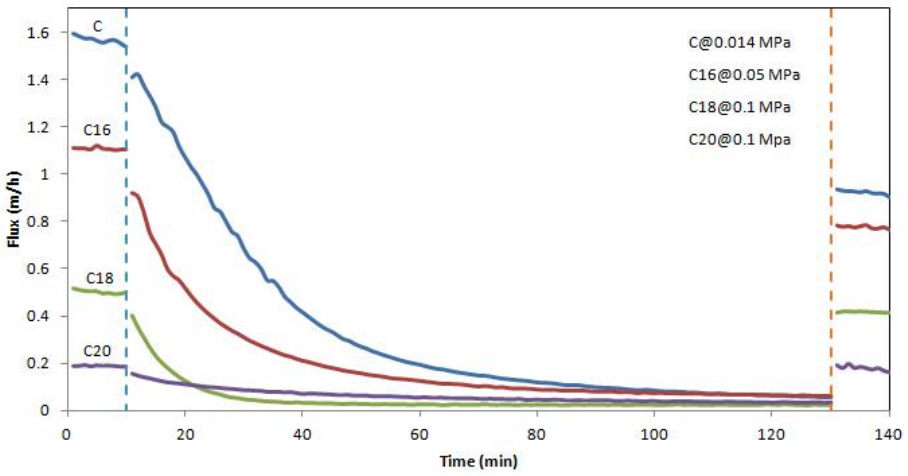

Figure 5.5 Permeate fluxes of the membranes prepared with different casting solution polymer concentrations but the same additive polymer to PVDF ratio (3:7) in the filtration of pure water and oil/water emulsion.

Table 5.3 Relative flux recoveries of the prepared membranes after oil/water emulsion filtration

Membrane	**J_{w0} ($m \cdot h^{-1}$)**	**J_{w1} ($m \cdot h^{-1}$)**	**RFR (%)**
B	2.07	1.17	57%
C	1.56	0.92	59%
D	1.38	0.74	54%
E	0.62	0.31	49%
C16	1.11	0.78	70%
C18	0.50	0.42	83%
C20	0.19	0.18	95%

The filtration experiments collected the data for the changes of the membrane permeate flux during the oil/water emulsion filtration. The membrane pure water

flux before (J_{w0}) and after (J_{w1}) the oil/water emulsion filtration were also measured, from which the relative flux recovery can be calculated, i.e., J_{w1}/ J_{w0}.

Figure 5.4 shows the flux changes of the membranes prepared with the same casting solution polymer concentration (12 wt%) but different additive polymer to PVDF ratios. It is found that the membrane with a higher portion of additive polymer had a higher pure water flux. This is consistence with analysis result in Figure 5.3 where the higher portion of additive polymer is shown to produce more porous membrane structure. However, during the oil/water emulsion filtration, the permeate flux of the B membrane (with 40 wt% of the additive polymer) dropped very quickly; see in Figure 5.4. The emulsified oil droplets usually with a diameter less than 20 μm (Cheryan and Rajagopalan, 1998). Some of these droplets might easily get into the pores of the B membrane (which was more porous) under pressure, and thus fouled the membrane more significantly. However, the B membrane still obtained a 57% RFR after the oil/water emulsion filtration. This should be contributed to the oleophobicity of the membrane so that oil was not strongly adsorbed by the membrane and thus can be partly removed by the water rinse cleaning. The permeate flux of C membrane with smaller pores than B on the surface [see Figure 5.3 C(1)] decreased more slowly than that of B, as shown in Figure 5.4. Moreover, the relative flux recovery of C was 59 %, similar to that of B (57 %) prepared with a higher portion of the additive polymer. The D membrane with even smaller pores than C on the surface [see Figure 5.3 D(1)] also showed a slower permeate flux drop than C; see Figure 5.4. However, the relative flux recovery of D was only 54 %. Since PVDF is very oleophilic and

oil droplets can be easily absorbed by PVDF, the membrane prepared with a higher portion of PVDF had more oil droplets absorbed, and was more difficult to be fully cleaned. Even though the E membrane had the smallest pores on surface, as compared to B, C and D [see Figure 5.3 E(1)], its permeate flux dropped quickly and almost decreased to 0 after 1 h oil/water emulsion filtration; see Figure 5.4. The E membrane also had the lowest relative flux recovery of 49 %. Both the quick permeate flux drop and the low relative flux recovery of the E membrane can be attributed to the low additive polymer ratio and thus more oil adsorption by PVDF. It seems that the C membrane had a better additive polymer to PVDF ratio that provided a compromise between surface pore size and surface oleophobicity for the filtration of the oil/water emulsion tested.

Surface morphology as a factor affecting oil fouling also can be adjusted by the polymer concentration in the casting solution. Membranes prepared with different casting solution polymer concentrations but at the same additive polymer to PVDF ratio (3:7) were also investigated. The SEM images in Figure 5.3 show that the pore size decreased with the increase of the casting solution polymer concentration. Hence, higher transmembrane pressures were applied to the membranes with smaller pores during the filtration of the oil/water emulsion. As shown in Figure 5.5, the initial pure water fluxes of the membranes with smaller pores decreased, even though higher pressures were used. This should be attributed to the membrane surface pore size decrease. However, the permeate flux of the membrane prepared with a higher casting solution concentration dropped more slowly, and a higher relative flux recovery was also achieved; see

Table 5.3. For example, the C20 membrane prepared with the highest casting solution concentration had the smallest flux drop and the highest relation flux recovery. Hence, the membranes prepared with the same additive polymer to PVDF ratio can be adjusted to have better antifouling performance by changing the casting solution polymer concentrations.

Oil concentrations of the permeates were monitored and the results showed oil content of less than 1 $mg \cdot L^{-1}$in all permeates, indicating at least 99.8 % of removal efficiencies.

5.4 Conclusion

In this chapter, a novel additive polymer was synthesized based on P(VDF-co-CTFE). tBMA was grafted onto P(VDF-co-CTFE) through ATRP. P(VDF-co-CTFE)-g-PtBMA was then hydrolyzed to produce carboxylic groups to react with hydroxyl groups of FPEG. The synthesis processes were verified from the ATR-FTIR and NMR spectra. The synthesized additive polymer was blend with PVDF in different ratios to prepare membranes. The SEM images of the prepared membranes indicated that the surface morphology or pore size could be adjusted through the ratio of the additive polymer to PVDF or the total polymer concentration of the casting solution. The membrane prepared with a higher portion of the additive polymer or a lower polymer concentration casting solution provided more porous surface. More importantly, it is confirmed that the more additive polymer was added the more hydrophilic and oleophobic membrane surface was obtained. Although higher additive polymer content lowered the tensile stress, the mechanical properties of the prepared membranes were still

good. The prepared membranes with the additive polymer were examined for oil/water separation and removal efficiencies reached at least 99.8%. However, the antifouling performances of the membranes were various, depending on both the membrane morphology and the additive polymer content. The membrane containing 30 wt% of the additive polymer was found to show the best anti oil fouling results in this study. Hence, the additive polymer provided great prospect to prepare or develop membranes that have both high hydrophilicity and oleophobicity to minimize membrane organic and biological fouling for various applications in water or wastewater treatment.

Chapter 6 **A novel membrane with two different wettabilities and its non-organic and non-biological fouling performance for potential water treatment applications**

Summary

Membrane organic and biological fouling has been one of the major problems for membrane technology applications in water and wastewater treatment. In this chapter, a novel membrane with two different wettabilities was prepared and was evaluated for its resistance against organic and biological fouling. The membranes in flat sheet configuration were produced from PVDF as the base matrix polymer incorporated with the hydrophilic and oleophobic additive polymer that was developed in Chapter 5. The prepared novel membranes showed high water affinity but low oil affinity. Experimental results confirmed that the developed membrane provided high water flux and showed non-organic fouling performance during the filtration of protein solution, humic acid solution and oil/water emulsion, displayed as slow flux decay and high flux recovery rate after membrane cleaning. The biofouling tests, including bacteria suspension immersion and filtration of the prepared membranes, showed that the developed membrane effectively prevented bacteria adhesion on the membrane and the flux decay during filtration can be fully recovered after a membrane cleaning with water. The study in this chapter demonstrated in much greater details that the developed novel membrane with two different wettabilities can provide good

antifouling performances for both organic and biological foulants, and thus, has a great potential for water treatment applications.

6.1 Introduction

Membrane separation is an emerging technology that offers great potential for applications in effective water treatment. However, one of the major obstacles in the application of membrane technology is the effect of membrane fouling. Various types of foulants including inorganic (clays, flocs and mineral particles), biological (bacteria, fungi) and organic (oils, polyelectrolytes, humics) components in the feed can cause membrane fouling (Baker, 2004). According to the interaction strength between foulants and the membrane surface, membrane fouling can be divided into reversible and irreversible fouling (Choi et al., 2005). Inorganic fouling is usually considered as reversible fouling because it can be removed by a simple physical cleaning method such as water backflushing. In contrast, biological and organic foulants usually result in irreversible fouling of membranes that cannot be effectively recovered by simple physical cleaning methods. Since irreversible membrane fouling will cause permanent loss of permeate flux, a lot of research efforts have been made to develop membranes that can prevent organic and biological fouling through membrane surface modification.

In general, it is commonly accepted that a hydrophilic membrane surface provides better performance against organic and biological fouling caused by proteins, natural organic matters (NOM) and bacteria in the nature (Rana and Matsuura, 2010). Various methods have therefore been developed to enhance the

hydrophilicity of membrane surface. For example, hydrophilic substances were immobilized onto base membranes *via* adsorption and surface coating (Akthakul et al., 2004; Combe et al., 1999; Nunes et al., 1995); surface chemical reactions induced by high energy substances (UV, plasma) or strong acids were applied to improve the hydrophilicity of membrane surfaces (Munoz et al., 2006; Yu et al., 2005); and surface grafting of functional monomers or polymers on membrane surfaces was used to modify the hydrophilicity (Howarter and Youngblood, 2009; Pieracci et al., 1999; Zhao et al., 2010). In addition, incorporation or blending of hydrophilic polymers in membrane base materials was also used as a method to enhance membranes' hydrophilicity (Asatekin et al., 2007; Zhao et al., 2007). The possible antifouling mechanism of a hydrophilic surface has been considered to be that a compact hydration layer which may reduce the possibility of foulants contacting or adhesion on the membrane surface will be produced on the highly hydrophilic surface during water filtration (Chen et al., 2011b).

However, membrane surfaces with only high hydrophilicity possess relatively high surface free energy, which is subject to adhesion of organic compounds such as oils that usually have low surface tensions. It has been proved that if the membrane's surface free energy is higher than the oils' surface tensions, the oils will spread on the membrane surface or exhibit very small contact angle (C.J, 1993; Stamm, 2008). This often leads to adhesion and fouling of the membrane by oils. To reduce the adhesion strength of organic foulants, low surface free energy membrane surfaces may be desired. In the literature, ultrafiltration membrane with low surface free energy had been tested for oil/water emulsion

separation to facilitate cleaning (Hamza et al., 1997). However, low surface free energy membrane surfaces exhibit poor affinity with water or are highly hydrophobic, resulting in low water permeability. In addition, a highly hydrophobic membrane surface is often observed to be easily fouled by foulants such as microorganisms (Pasmore et al., 2001; Zhu et al., 2010) and aquatic humic substances (Jucker and Clark, 1994).

Ideally, a membrane surface for water treatment should have two different wettabilities, e.g. both hydrophilic and oleophobic for high water permeability, low adhesion rate and low interaction strength between the membrane surface and foulants. In this line, only very limited research works have been reported in the literature. Surfactants containing perfluorinated end (oleophobic) and polyethylene glycol chain (hydrophilic) were covalently grafted onto glass membranes for oil/water emulsion separation (Howarter and Youngblood, 2009). Even though improved performance was observed, glass membranes are relative expensive and more difficult to be prepared in comparison with polymeric membranes. Another work constructed ternary amphiphilic block copolymers consisting hydrophilic block (polyethylene oxide), and hydrophobic fluorine-containing blocks (oleophobic) as additive to prepare modified PVDF antifouling membranes (Chen et al., 2011b). However, the modified PVDF membrane had water contact angle of above 80 °, indicating still a highly hydrophobic membrane surface. More important, a complete evaluation of a novel polymeric membrane with two different wettabilities (i.e., hydrophilic and oleophobic) for anti organic and biological fouling has not been reported so far.

In this chapter, the hydrophilic and oleophobic additive polymer developed in Chapter 5 was blended with PVDF to obtain membranes with two different wettabilities. The prepared membranes were characterized, and evaluated for their antifouling performances for organic and biological foulants in water.

6.2 Materials and methods

6.2.1 Materials

The additive polymer was synthesized in our group. The detail synthesis procedure of the additive polymer can be found in Chapter 5.

Polyvinylidene fluoride (PVDF, Mw ca. 534,000), bovine serum albumin (BSA, Mw ca. 66,000), humic acid (HA), hexadecane and polyethylene glycol (PEG, Mw ca. 600) were purchased from Sigma-Aldrich and used without further purification. N,N-dimethylformamide (DMF, Tedia, HPLC grade) was used as received without further purification. Deionized (DI) water (18 MΩ) purified with a Milli-Q system from Millipore was used to prepare all solutions as needed in the study.

6.2.2 Membrane preparation

The compositions of the casting solutions for the five different membranes examined are shown in Table 6.1. All membranes had the same casting solution polymer concentration at 20 wt%. M0 was the base PVDF membrane without any additive. M1 was the control PVDF membrane with the common commercial polymer of PEG 600 as the additive to improve the pore forming and enhance the hydrophilicity of the membrane. M2, M3 and M4 were the novel membranes

prepared with different ratio of the synthesized additive polymer to PVDF in this chapter.

The membrane preparation procedures were the same as those in Section 5.2.6.

6.2.3 Membrane characterization

Membrane characteristics including morphology, mechanical properties and surface wetting properties were evaluated in this chapter, and the measuring methods were the same as those described in Chapter 5.

6.2.4 Bacteria suspension immersion tests

Escherichia coli (*E. coli*) and *Staphylococcus aureus* (*S. aureus*) were used in the experiments for membrane biofouling tests. *E. coli* as a typical Gram-negative bacterium and *S. aureus* as a typical Gram-positive bacterium both are commonly found in water and wastewater. *E. coli* strain 15597 and *S. aureus* ATCC 6538 were obtained from the Environmental Molecular Biotechnology Laboratory at the National University of Singapore. *E. coli* and *S. aureus* were cultured in a Tryptone Soya Broth (TSB) solution (30 $g \cdot L^{-1}$), and then grew on Agar No.3 containing TSB (TSB and Agar No.3 were purchased from OXOID) (Feng et al., 2000; Yao et al., 2008).

Membrane samples were immersed in mixed suspension of stationary phase *E. coli* and *S. aureus* for a time up to 6 d, respectively. During the test period, the membranes were transferred to a newly prepared stationary phase bacteria suspension in every 48 h to maintain the viable bacteria concentration. A small piece of sample was taken from each of the immersed membranes after 2d and 6d immersion. The collected membrane samples with bacteria on the surfaces were

fixed in 3 vol. % glutaraldehyde phosphate buffered saline (PBS) solutions for 5 h at 4 °C. After the fixation, these membrane samples were rinsed with PBS to remove remaining glutaraldehyde and then dried at 60 °C for 24 h. The dried membrane samples were then scanned by SEM for bacteria adhesion information.

6.2.5 Organic and biological fouling tests through dead-end filtration experiments

The dead-end filtration experiments with the prepared membranes were conducted using a dead-end filtration system with details as described in Section 4.2.3.5. In this chapter, the transmembrane pressure was set at 0.1 MPa.

Organic foulants including protein (BSA), NOM (HA) and oil (hexadecane) were used in the dead-end filtration experiments to evaluate the prepared membranes' non-organic fouling performances. The feed concentration of BSA or HA solution was 1 $g \cdot L^{-1}$ by dissolving BSA or HA in DI water. The hexadecane (oil)/water emulsion was prepared by homogenizing 0.5 g of hexadecane in 1 L DI water at 14,000 rpm for 20 min to give a oil concentration of 500 $mg \cdot L^{-1}$.

The anti-biofouling performance of the prepared membrane was further evaluated by the filtration of bacteria suspensions. The feed bacteria suspensions were prepared by mixing and diluting the stationary phase *E. coli* and *S. aureus* to give a concentration of about ~10^5 $CFU \cdot L^{-1}$.

The dead-end filtration was conducted in 3 stages: firstly, pure water flux was recorded for 0.5 h and the stabilized flux was denoted as J_0; secondly, the membrane was filtered with BSA solution, HA solution, oil/water emulsion or mixed bacteria suspension for 2 h and the permeate flux change was recorded

versus filtration time and the final flux was denoted as J_P; finally, after the membrane was cleaned, pure water flux was recorded again for 0.5 h and the stabilized flux was denoted as J_1. The membrane cleaning procedure was simply by immersing the membrane in 50 mL DI water and being stirred at 200 rpm in a shaker for 30 min.

The relative flux decay (RFD) was calculated by RFD = $[(J_0-J_P)/J_0] \times 100\%$. The relative flux recovery (RFR), indicating the extent of the possible reversible fouling, was calculated by RFR = $(J_1/J_0) \times 100\%$.

The BSA, HA and mixed bacteria suspension concentrations of the feed and permeate solutions were measured with a UV-VIS spectrophotometer (Agilent - HP 8452A) at wavelengths of 278, 400 and 600 nm, respectively. The oil concentrations in the feed and in the filtrate were analyzed with a TOC analyzer (SHIMADZU, TOC-V). The retention percentage of a foulant was calculated by Retention= (1- the permeate solution's concentration / the feed solution's concentration) × 100%.

6.3 Results and discussion

6.3.1 Morphology of the prepared membranes

The surface and cross section morphologies of the prepared membranes were observed from the SEM images as shown in Figure 6.1. The average surface pore sizes of the prepared membranes, as analyzed with the software of Smile View with the SEM machine and included in Table 6.1, are all at around 0.1 μm, i.e., in the border of microfiltration and ultrafiltration membrane pore size range.

Table 6.1 Prepared membranes' compositions and properties

Membrane name	M0	M1	M2	M3	M4
Base polymer	PVDF	PVDF	PVDF	PVDF	PVDF
Additive	\	PEG 600	AP	AP	AP
PVDF: Additive ratio	\	8:2	9:1	8:2	7:3
Casting solution polymer concentration (wt%)	20 (PVDF)	20 (PVDF)	20 (PVDF + AP)	20 (PVDF + AP)	20 (PVDF + AP)
Membrane surface pore size (μm)	\	0.075±0.022	0.095±0.02	0.112±0.028	0.116±0.030
Tensile stress (MPa)	7.75	7.53	7.72	7.22	6.43
Tensile strain (%)	118.13	117.01	19.88	10.42	5.45
Water contact angle (°)	96	79	41	31	26
Oil (hexadecane) contact angle (°)	~15	~15	40	63	74

*AP stands for additive polymer.

The SEM images in the left column of Figure 6.1 show the surface morphologies of the prepared membranes. As shown in Figure 6.1(a), no noticeable pores were observed on the top surface of the M0 membrane. However, the addition of PEG (20 wt%) as commonly practiced as a pore-forming agent in PVDF resulted in the formation of pores with an average pore size at about 0.075 μm on the surface of M1; see Figure 6.1(b). On the other hand, due to the addition of 10 wt% of the additive polymer as indicated in Figure 6.1(c), it resulted in the formation of pores at about 0.095 μm on the top surface of M2. The average pore sizes of M3 and M4 became larger, at about 0.112 μm and 0.115 μm, respectively, with more percentages of the additive polymer being added in PVDF for the preparation of the membranes. In general, the pore sizes of the prepared membranes were not significantly altered, which is desired because the separating effect of the prepared membrane will not be obviously changed. It is expected that when the membrane became more porous with the increase of the additive

polymer content as shown in Figure 6.1 left column, improved permeate water flux can be obtained in the filtration operation.

The right column of Figure 6.1 shows the cross sections of the prepared membranes. As shown in Figure 6.1(a), the M0 membrane displayed elongated finger-like voids and these macrovoids spanned almost half of the membrane's cross section. In comparison, the M1 membrane showed similar finger-like voids and macrovoids distribution to those of the M0 membrane; see Figure 6.1 (b). It appears that the presence of the pore forming agent, PEG, did not noticeably change the cross section structure of the M1 membrane. However, the membranes with the additive polymer showed very different cross section structures. As shown in Figures 6.1(c) to (e), with the increase of the amount of the additive polymer, the formation of the finger-like macrovoids was greatly suppressed, and a more sponge-like cross section structure was obtained; especially see that of the M4 membrane. The sponge-like cross section structure is usually more desired because it provides more uniform flow distribution and physical supporting.

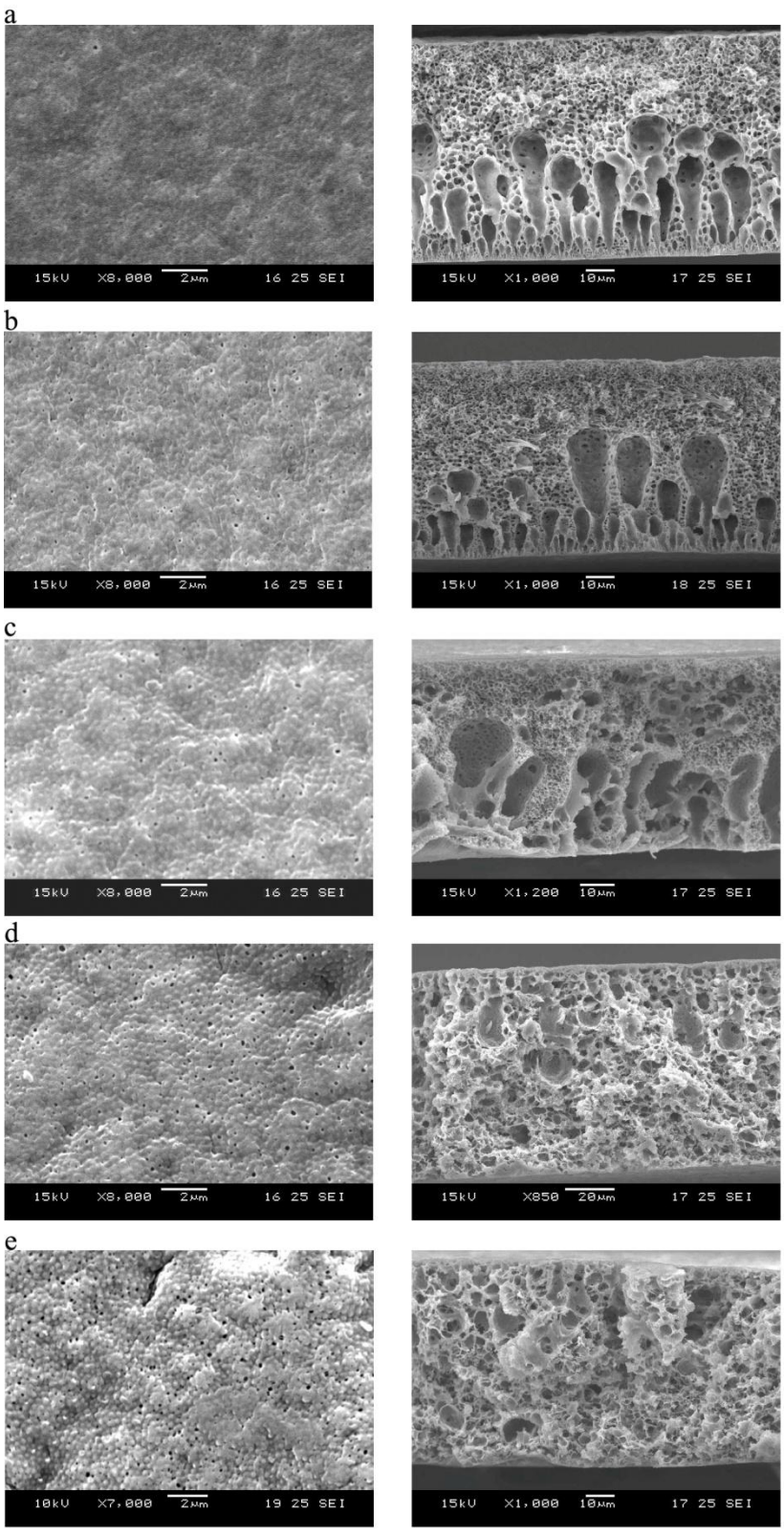

Figure 6.1 Top surface (left) and cross section (right) SEM images of membranes (a) M0, (b) M1, (c) M2, (d) M3 and (e) M4.

6.3.2 Membrane mechanical strength

Mechanical property is an important parameter for pressure-driven membranes because the membrane should be strong enough to stand the transmembrane pressure during filtration. In addition, a weaker membrane may be easily broken in the cleaning process such as backflushing. The mechanical properties in terms of the tensile stress and tensile strain of the prepared membranes are also given in Table 6.1.

The M0 membrane without any of the additive polymer had the highest tensile stress. The addition of a certain amount of PEG (20 wt%) or the additive polymer (10 – 20 wt%) only slightly decreased the membrane's tensile stress. However, if more additive polymer was added (30 wt%), the M4 membrane showed a moderate decrease in the tensile stress. Nevertheless, the lowest tensile stress of 6.43 MPa for the M4 membrane is still good enough, which is much higher than the operation transmembrane pressure of 0.1 MPa in this study and is greater than the tensile stress of a commercially used PVDF membrane reported at 3.5 MPa (Shi et al., 2007).

It is well known that PVDF membranes have high ductility that usually can reach a more than 100 % tensile strain (Shi et al., 2007). The tensile strains of the M0 and M1 membranes in this study were found to be over 110 %; see Table 6.1. However, the presence of the additive polymer in PVDF dramatically reduced the tensile strain of the prepared membranes to as low as 5% for the M4 membrane, for instance. In other words, a higher portion of the additive polymer in PVDF

made the fabricated membranes less ductile. The low ductility of the prepared membrane would make it more stable during filtration operation.

6.3.3 Membrane surface wetting properties

The surface wetting properties of the prepared membranes are of great importance in this study. The water and oil contact angles of the prepared membranes can indicate the membranes' hydrophilicity and oleophobicity, respectively.

As shown in Table 6.1, the M0 membrane was quite hydrophobic and had the highest water contact angle at 96°. The surface hydrophilicity of M1 was slightly improved and it had a water contact angle at around 79°. This can be attributed to the blending of PEG, a highly hydrophilic polymer, into PVDF in the preparation of the M1 membrane casting solution. However, the surface hydrophilicity of the developed novel membrane was significantly enhanced with the addition of the additive polymer. It is clear that with the increase of the additive polymer portion in the membrane, the developed novel membrane had a smaller water contact angle, for example, 26° for the M4 membrane which can be considered to be highly hydrophilic; see Table 6.1.

The oil contact angles of the prepared membranes are also included in Table 6.1. During the experiments, the oil droplet on the M0 or M1 membrane surface had a contact angle at around 15° and the oil droplet quickly disappeared due to the adsorption by the membrane. These findings suggest that the M0 and M1 membranes were not oleophobic. In contrast, a much higher oil contact angle of

40° was observed for the M2 membrane that had an addition of 10 wt% of the additive polymer in PVDF. As shown in Table 6.1, with the increase of the additive polymer, higher oil contact angles were observed for the M3 and M4 membranes at 63° and 74°, respectively. In other words, the M4 membrane became oleophobic. Hence, the additive polymer made the prepared membranes not only hydrophilic but also oleophobic, possessing two different wettabilities.

6.3.4 Membrane anti organic fouling performance

The anti organic fouling performances of the prepared membranes were evaluated with BSA, HA and oil. Although it is well known that the shear force of a cross-flow will greatly reduce or delay the membrane fouling effect, dead-end mode filtration was used in the tests in order to examine the possible more severe fouling scenario in this study.

Figure 6.2 shows the permeate fluxes of the prepared membranes during the filtration of BSA solution, HA solution and oil/water emulsion. Correspondingly, the typical process performance data of the prepared membranes are summarized in Tables 6.2 – 6.4.

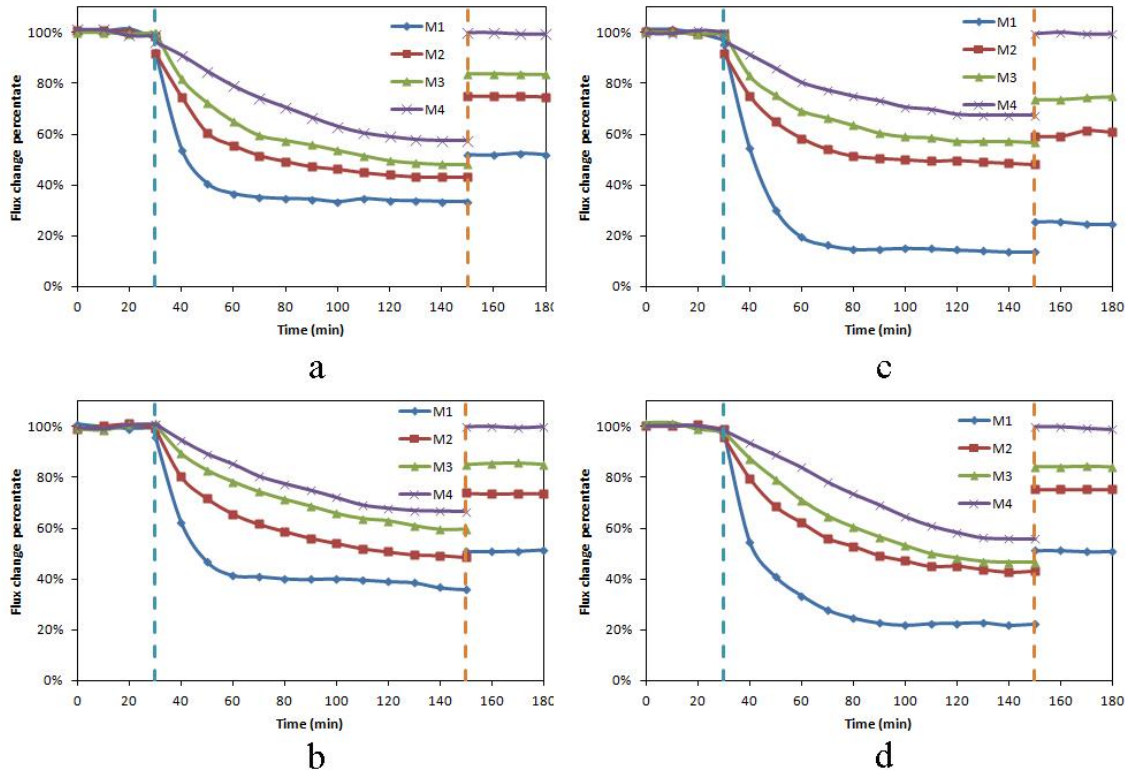

Figure 6.2 Permeate fluxes of the M1, M2, M3 and M4 membranes in the filtration of (a) BSA solution, (b) HA solution, (c) oil/water emulsion and (d) mixed bacteria suspension.

Table 6.2 Relative flux decay (RFD) and relative flux recovery (RFR) of the membranes in BSA solution filtration experiments

Membrane	J_0 ($L \cdot m^{-2} \cdot h^{-1}$)	J_P ($L \cdot m^{-2} \cdot h^{-1}$)	J_1 ($L \cdot m^{-2} \cdot h^{-1}$)	RFD	RFR	Retention
M1	2.71	0.91	1.41	67%	52%	75%
M2	3.61	1.56	2.7	57%	75%	74%
M3	47.81	22.98	40.02	52%	84%	72%
M4	177.72	102.01	177.31	43%	100%	71%

Table 6.3 Relative flux decay (RFD) and relative flux recovery (RFR) of the membranes in HA solution filtration experiments

Membrane	J_0 ($L \cdot m^{-2} \cdot h^{-1}$)	J_P ($L \cdot m^{-2} \cdot h^{-1}$)	J_1 ($L \cdot m^{-2} \cdot h^{-1}$)	RFD	RFR	Retention
M1	2.73	0.98	1.39	64%	51%	65%
M2	3.58	1.74	2.64	51%	74%	63%
M3	47.27	28.17	40.37	40%	85%	62%
M4	174.68	116.27	174.33	33%	100%	60%

Table 6.4 Relative flux decay (RFD) and relative flux recovery (RFR) of the membranes in oil/water emulsion filtration experiments

Membrane	J_0 ($L \cdot m^{-2} \cdot h^{-1}$)	J_P ($L \cdot m^{-2} \cdot h^{-1}$)	J_1 ($L \cdot m^{-2} \cdot h^{-1}$)	RFD	RFR	Retention
M1	2.52	0.35	0.63	86%	25%	99%
M2	3.56	1.71	2.14	52%	60%	99%
M3	47.72	27.08	35.41	43%	74%	99%
M4	172.52	116.39	171.72	33%	100%	99%

6.3.4.1 Filtration of BSA solution

As shown in Figure 6.2 (a) and Table 6.2, the M1, M2, M3 and M4 membranes' initial pure water fluxes (J_0) were 2.71, 3.61, 47.81 and 177.72 $L \cdot m^{-2} \cdot h^{-1}$, respectively. The control membrane (M1) had the lowest initial pure water flux. The initial pure water flux of the prepared membrane increased dramatically with the addition of the additive polymer, consistently with the increased hydrophilicity.

During the two hours of filtration of the BSA solution, the permeate flux of the M1 membrane decreased rapidly from the beginning of the filtration. A relatively steady but very low flux was quickly reached. However, the membranes with the additive polymer exhibited much slower flux declines in the filtration process; as shown in Figure 6.2 (a). With the increase of the additive polymer, the rate of flux decline became more gradual for the prepared membrane. The final permeate flux (J_p) of the membranes, i.e., M1, M2, M3 and M4 at the end of two hours filtration (t=150 min), were 0.91, 1.56, 22.98, and 102.01 $L \cdot m^{-2} \cdot h^{-1}$, respectively. In other words, the RFD for M1 reached 67% but those for M2, M3 and M4 were only 57%, 52% and 43%, respectively. After the BSA solution filtration, the membrane was simply cleaned and the pure water flux (J_1) was measured again. As shown in Figure 6.2(a) and Table 6.2, the flux was recovered back to 1.41, 2.70, 40.02 or 177.31 $L \cdot m^{-2} \cdot h^{-1}$, respectively, for M1, M2, M3 or M4, which gave a recovery rate of 52%, 75%, 84% and 100% for the M1, M2, M3 and M4 membranes, respectively. In other words, when the additive polymer content reached a certain level, the developed membrane exhibited a flux decline complete recovery in BSA filtration.

The presence of the additive polymer improved the prepared membranes' initial pure water flux. This could be attributed to the enhanced hydrophilicity. It has been reported that the membrane surface with improved hydrophilicity would effectively increase the membrane's water flux (Wang et al., 2005a; Yang et al., 2005). More important, the prepared membranes with the additive polymer exhibited much better antifouling performance than the control membrane,

including lower flux decline rate and higher flux recovery rate. These results can be attributed to the two different wettabilities of the synthesized additive polymer and therefore the prepared membranes. During the filtration, the hydrophilic domains of the prepared membranes would cause the generation of a compact hydration layer that could provide a non-specific repulsion to foulants approaching to the membrane surface, in addition to facilitate high water permeation. On the other hand, the non-polar oleophobic segments with very low surface free energy may weaken the interactions between the foulants and the membrane surface (Chen et al., 2011b).

6.3.4.2 Filtration of HA solution

The prepared membranes' antifouling performances were further evaluated through filtration of HA solution, simulating the organic fouling that may be caused by NOM in water treatment. As shown in Figure 6.2 (b) and Table 6.3, the experimental results of HA solution filtration tests showed similar behaviors to those of BSA filtration. The control membrane (M1) had a flux drop of 64% after the 2 h filtration and a flux recovery of 51% after membrane cleaning. Hence, the control membrane (M1) was highly subject to organic fouling caused by NOM. However, the developed membranes with the additive polymer had much lower flux decays at 51%, 40% and 33% and higher flux recovery rates at 74%, 85% and 100% for the M2, M3 and M4 membranes, respectively. These results indicate that the prepared novel membrane can effectively resist organic fouling caused by NOM such as in the case of M4 membrane.

It was found that the BSA and HA removal efficiency of the four types of membranes were not significantly different, all at about 70% for BSA and 60% for HA (see Table 6.2 and 6.3), respectively. This was attributed to the sizes of BSA and HA molecules. BSA has a molecular weight at about 66 kDa which may be converted to a molecule with a nominal diameter at around 0.06 μm. The sizes of HA macromolecules were reported usually not greater than 0.06 μm (von Wandruszka et al., 1999). Therefore, the sizes of those organic components appeared to be smaller than the surface pore sizes of the membranes at about 0.1 μm. If greater removal is needed, the membranes may be prepared into a denser structure in the ultrafiltration or nanofiltration range by increasing, for example, the dope concentration, which will be further investigated in future work.

6.3.4.3 Filtration of oil/water emulsion

Oils are another common group of organic foulants that can affect membrane filtration performance significantly. Due to the low surface tension of oils, hydrophilicity modification of membrane usually did not reduce the membrane adhesion strength by oily foulants. However, the oleophobicity of the prepared membrane provided the possibility to resist oil adhesion and thus inhibit oil fouling.

As shown in Figure 6.2 (c) and Table 6.4, the control membrane (M1) was seriously fouled by oil and reached an 86% flux drop after 2h filtration of the oil/water emulsion. Furthermore, only 25% flux was recovered after the membrane cleaning, indicating serious and irreversible fouling of the control PVDF membrane by oil. On the contrary, the novel membranes with the additive

polymer (M2, M3 and M4) had lower flux decays at 52%, 43% and 33% but much higher flux recovery rates at 60%, 74% and 100%, respectively. Compared to the irreversible adsorption of oil on the control membrane (M1), most of the oil droplets on the surface of the novel membranes with the additive polymer were easily removed by a physical cleaning method, especially in the case of M4 membrane. This can be attributed to the oleophobic property of the additive polymer and the developed membranes, which could effectively prevent the adsorption or adhesion of oils. As given in Table 6.4, the average oil retention percentages for all the four types of prepared membranes were at about 99% in the oil/water emulsion filtration experiments.

Overall, the developed novel membranes with the additive polymer were not only highly hydrophilic but also oleophobic, which were capable of incurring high water flux and resisting various organic foulants including protein, NOM and oil.

6.3.5 Membrane anti biofouling performance

Attachment is the first step of microbes to form biofilm on a membrane surface. The reduction, delay or inhibition of the initial adhesion of bacteria on the membrane surface is an important strategy to prevent membrane biofouling. In this study, two types of typical bacteria including *E.coli* (Gram-negative) and *S. aureus* (Gram-positive) were used in the biofouling tests. These two bacteria are commonly found in water and wastewater and widely used as probes for antifouling tests. Two experiments including bacteria suspension immersion and filtration tests were conducted to evaluate the developed novel membranes' resistances for biofouling in static and dynamic systems, respectively.

The fouling conditions of the membranes immersed in bacteria suspension for 2d and 6d were observed with SEM, as shown in Figure 6.3. After 2d immersion, as indicated in Figure 6.3(a1), widespread bacteria adhesion was evident on the M0 membrane. A lower coverage but not a small amount of bacteria were also found on the surface of M1 membrane after 2d immersion; see Figure 6.3(b1). However, only very limited or even no bacteria were on the surface of the novel membranes of M2, M3 and M4, respectively, after 2d immersion; see Figures 6.3(c1) – 6.3(e1). When the immersion time was extended to 6d, more bacteria clusters were observed on the M0 and M1 membrane surfaces. Thick and uniform bacteria clusters were found completely covering the M0 membrane surface; see Figure 6.3 (a2). The M1 membrane surface was also almost completely covered with uniform bacteria clusters after the 6 d immersion; as shown in Figure 6.3 (b2). In contrast, the surfaces of the novel membranes with the additive polymer did not exhibit obvious differences between 2d and 6d immersion. Their surfaces were relatively clean and free of bacteria during the 6d experiments. It is clear that the M0 and M1 membranes were prone to bacteria adhesion and biofouling. However, the membranes with the additive polymer can effectively prevent the adhesion of bacteria, thus exhibited excellent non-biofouling performance during the bacteria suspension immersion experiments.

Dead-end filtration of the prepared membranes for the mixed *S. aureus* and *E. coli* suspensions exhibited similar flux changing trends to those of the organic foulant filtration experiments; as shown in Figure 6.2(d). The flux for the M1 membrane decreased rapidly to a steady-state value after a short period of

filtration. This could be attributed to the rapid bacterial adhesion and accumulation on the M1 surface. In another words, the M1 membrane was strongly subjected to biofouling by the tested bacteria. However, with the addition of the additive polymer, the novel membranes exhibited a slower rate of flux decline during the filtration of the mixed bacteria suspension. The slower flux decrease indicated a surface more difficult to be fouled or a better biofouling resistance of the membrane. From Table 6.5, after 2h filtration of the mixed bacteria suspension, the control membrane (M1) is found to have the highest flux decay at 78% and the lowest flux recovery rate only at 51%. In contrast, the RFD of M2, M3 and M4 were 57%, 53% and 44%, respectively, and more importantly, the RFR of M2, M3 and M4 reached 75%, 84% and 100%, respectively. It is clear that the presence of the additive polymer in the developed novel membranes effectively reduced the flux decay and increased the flux recovery rate. These results indicated that the control membrane (M1) was highly subject to irreversible biofouling. However, the bacteria retained on the novel membranes with the additive polymer could be easily removed by a simple physical cleaning. Compared to the control PVDF membrane, the novel membranes with the additive polymer effectively inhibited membrane biofouling *via* changing the irreversible biofouling to reversible biofouling. As given in Table 6.5, the average bacteria retention percentages for all the four prepared membranes were above 95% in the mixed bacteria suspension filtration experiments.

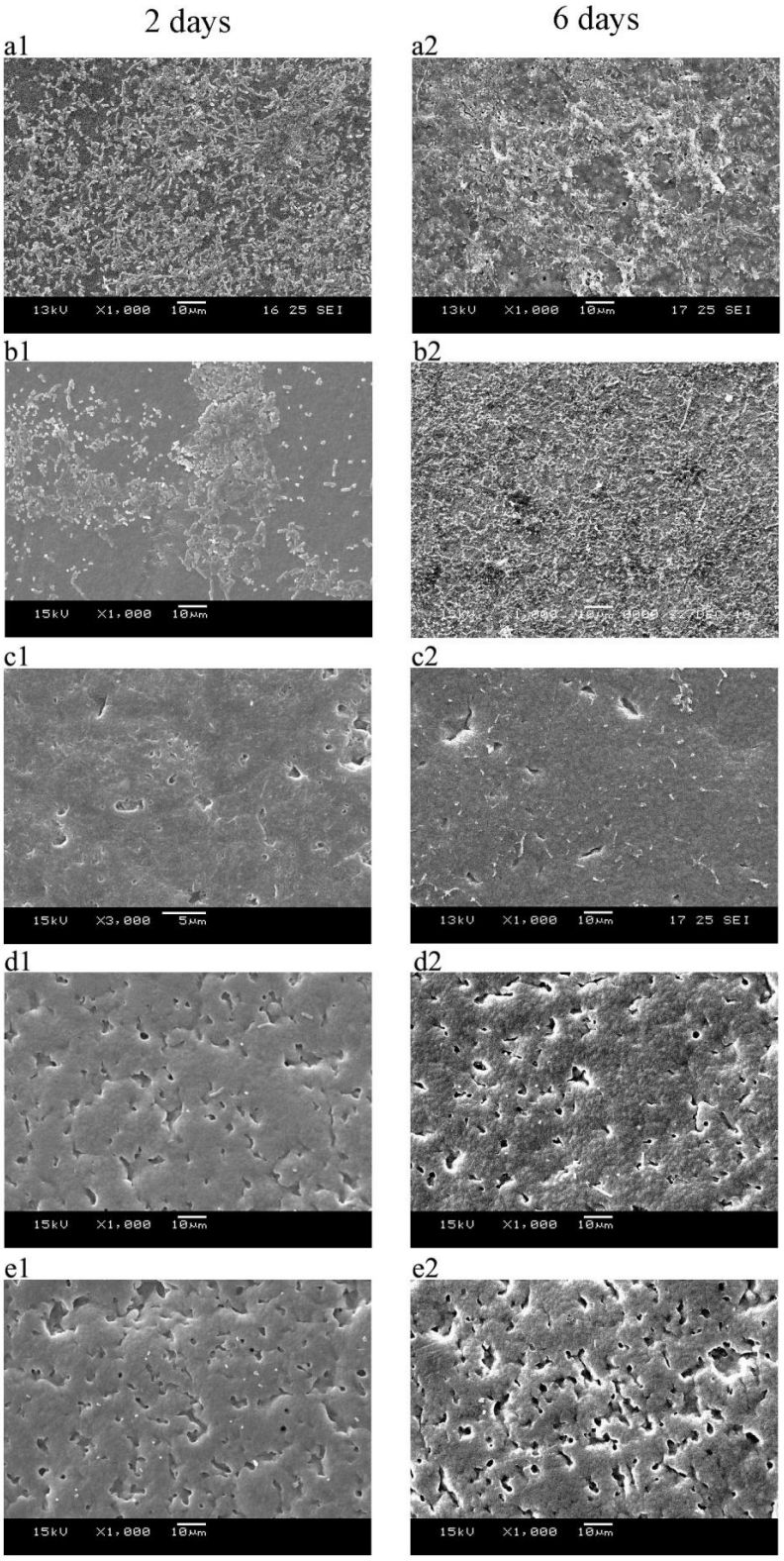

Figure 6.3 SEM images of bacteria on (a) M0, (b) M1, (c) M2, (d) M3 and (e) M4 after (1) 2d and (2) 6d immersion in bacteria suspension.

Table 6.5 Relative flux decay (RFD) and relative flux recovery (RFR) of the membranes in mixed bacteria suspension filtration experiments

Membrane	J_0 ($L \cdot m^{-2} \cdot h^{-1}$)	J_P ($L \cdot m^{-2} \cdot h^{-1}$)	J_1 ($L \cdot m^{-2} \cdot h^{-1}$)	RFD	RFR	Retention
M1	2.55	0.57	1.3	78%	51%	98%
M2	3.59	1.55	2.7	57%	75%	97%
M3	46.27	21.54	38.92	53%	84%	97%
M4	176.79	98.65	176.2	44%	100%	95%

6.4 Conclusion

In this chapter, a novel membrane with two different wettabilities was developed to resist various organic and biological fouling for potential water treatment applications. The presence of the additive polymer in the developed novel membrane not only improved the membrane's surface porosity but also suppressed undesired macrovoid formation in the cross section. A higher portion of the additive polymer in PVDF made the fabricated membranes much less ductile, but their tensile stresses were only slightly declined. The novel membrane with the additive polymer was highly hydrophilic and oleophobic. The novel membrane provided high pure water flux and excellent organic fouling resistances exhibited as slow flux decay and high flux recovery after membrane cleaning in the filtration of BSA solution, HA solution and oil/water emulsion. Moreover, the novel membrane effectively prevented the adhesion of bacteria and thus biofouling in the bacteria suspension immersion and filtration tests. Especially, when the additive polymer amount in PVDF reached 30 wt%, the developed novel membrane exhibited almost non-fouling performance. Hence, the developed

membrane had outstanding fouling resistances, which has a great potential to be used in water treatment applications.

Chapter 7 **Effective and low fouling oil/water separation by a novel hollow fiber membrane with both hydrophilic and oleophobic surface properties**

Summary

Membrane filtration for oil/water separation has the potential to provide a simple system with high separation efficiency for oily wastewater treatment. However, conventional membranes are usually subject to severe oil fouling, which has greatly limited the application of membrane technology in oily wastewater treatment so far. In this chapter, a novel hollow fiber membrane with both hydrophilic and oleophobic surface properties was prepared and tested for its oil/water separation performance. The hollow fiber membrane was prepared from PVDF as the base material and the additive polymer developed in Chapter 5 (denoted as AP). It was found that the developed hollow fiber membrane not only showed good mechanical strength, but also had a surface that exhibited both high hydrophilicity as well as oleophobicity simultaneously. The hollow fiber membrane was packed into membrane modules that can be operated under either the dead-end or cross-flow filtration mode and tested for the treatment of artificial oily wastewater samples prepared from hexadecane or crude oil and real oily wastewater samples collected from a palm oil mill in Malaysia. The experimental results indicated that, as compared to the control PVDF membrane, the developed novel hollow fiber membrane exhibited excellent separation and antifouling performances, including much higher pure water flux, less flux decay during oily

wastewater filtration, significantly higher or almost complete flux recovery by a simple physical cleaning method (i.e., DI water flushing or backwashing) after a filtration run, similar or usually higher oil removal efficiency. Since the hollow fiber membrane can be easily scaled up to the full module for practical use, there is a great prospect for the developed novel hollow fiber membrane to be used for oily wastewater treatment.

7.1 Introduction

Everyday large quantities of oily wastewater are generated from various oil-related industries, such as the oil and gas industry, oil refinery industry, petrochemical industry and food or plant oil industry, as well as many other sources including domestic homes, hotels, machinery or car washing, etc. For example, on average of a global spectrum, it is estimated that for every barrel of crude oil produced, three or much more barrels of oily wastewater are generated (Khatib and Verbeek, 2003; Mondal and Wickramasinghe, 2008). Because of the low surface tension, oil in oily wastewater can easily attach and thus contaminate almost any surfaces in contact with it in the natural environment or other engineered systems. In addition, oil in oily wastewater if discharged can cause serious problems to the aquatic environment and lives due to the increase of oxygen demand or the development of septic conditions in the receiving water bodies. Hence, effective removal of oil from oily wastewater before its discharge is one of the very important issues for pollution control in the world. Also, effective removal of oil from oily wastewater provides a great prospect for water

reclamation and reuse due to the large quantities of oily wastewater and the global scarcity of fresh water resources.

Oil in oily wastewater may be broadly classified, according to the sizes of the oil droplets, into three groups: free oil (> 150 μm), dispersed oil (20 μm - 150 μm), and emulsified and dissolved oil (< 20 μm) (Cheryan and Rajagopalan, 1998). Traditionally, gravity separation, flotation and centrifugal separation have been used to remove oil from oily wastewater. Those processes may effectively remove free and dispersed oil but not the emulsified or, especially, the dissolved oil because their separation mechanisms are relied on both the oil droplet sizes and the density differences between water and the oil. The conventional separation systems usually occupy large space (due to long process time), are expensive (due to the need for gas and chemical input) and often cannot meet the stringent treatment requirement for discharge or reuse (Cheryan and Rajagopalan, 1998; Elmaleh and Ghaffor, 1996a). There has been a great interest to use membrane processes for oily wastewater treatment, attributed to the potential advantages of simpler systems, short process time, small footprint, and high separation efficiency. Virtually, any components with sizes larger than the water molecules may be separated by various membranes. In the literature, many studies using various inorganic and polymeric membranes for oil/water separation have been reported (Benito et al., 2001; Chakrabarty et al., 2008; Chen et al., 2009a; Chen et al., 2009b; Ju et al., 2008; Karakulski et al., 1995; Li et al., 2006b; Wandera et al.). However, one of the common problems has been the severe membrane fouling by oil. The oil droplets in the feed water attached on or

adsorbed by the membranes, narrowing or blocking the membrane pores, which resulted in rapid decline of the permeate flux with the operation time. This is inevitable because oil has low surface tension and can easily wet the surface of various conventional membrane materials. As a consequence, the application of membrane separation technology in the field of oily wastewater treatment has been rather limited so far.

One of the solutions to the oil fouling problem has been to develop antifouling or low fouling membranes that can resist oil attachment and thus reduce permeate flux decay as well as provide longer membrane life span. It has been well known that membrane surface properties play very important roles in membrane antifouling performance (Xu et al., 1999). Because most commercially available membranes have hydrophobic surfaces, the common practices in research and development have focused on the improvement of the membrane surface hydrophilicity. Due to the high affinity with water, the high hydrophilic membrane surface would generate a compact hydration layer which might reduce the possibility of foulants to directly contact the membrane surface (Chen et al., 2011b). Membranes of improved hydrophilicity were prepared by various methods, such as blending hydrophilic components with hydrophobic matrix materials,(Asatekin and Mayes, 2009; Li et al., 2006b; Xu et al., 1999) coating hydrophobic membrane surface with hydrophilic materials,(Chang et al., 2010; Wang et al., 2005a; Wang et al., 2006a) or grafting hydrophilic components on to hydrophobic membrane surfaces,(Howarter and Youngblood, 2009; Pieracci et al., 1999; Zhao et al., 2010) etc.

Although membrane hydrophilicity modification may reduce the possibility of oil droplets to contact the membrane surface, membrane with only hydrophilicity cannot completely prevent oily fouling. Membrane surface with only high hydrophilicity has relatively high surface free energy. In contrast, oils are usually with low surface tensions (Lange and Dean, 1992). If the membrane's surface free energy is higher than the oils' surface tensions, the total free energy would be minimized by maximizing the area of liquid/vapour interface, and the oil droplets would spread on the membrane surface or exhibit very small contact angle (C.J, 1993; Stamm, 2008). The contact angle is not limited to a liquid/vapour interface; it is equally applicable to the interface of two liquids. As a result, the hydrophilic membrane surfaces are also subject to adhesion of oils once in contact, which will lead to oil fouling of the membrane. In other words, a hydrophilic membrane surface does not equal to a membrane surface with the oleophobic property and an oleophobic surface should usually have a lower surface free energy than the surface tension of oil to be separated (Stamm, 2008).

There has been one report that purposely prepared oleophobic ultrafiltration membrane with low surface free energy for oil/water separation at very high cross-flow rates (Hamza et al., 1997). Because of the lower attachment strength between the membrane surface and oil, oil fouling of the membrane surface was effectively prevented by the high shearing force from the high cross-flow fluid. However, the membrane with low surface free energy is also highly hydrophobic, as expected, providing very low water flux due to the poor affinity of the membrane to water. In addition, if the shearing force is not high enough, a highly

hydrophobic membrane is known to be easily fouled by various foulants, including microorganisms (Pasmore et al., 2001; Zhu et al., 2010) and aquatic humic substances (Jucker and Clark, 1994).

It appears clear that an effective membrane for oil/water separation should be not only highly hydrophilic but also oleophobic. In this direction, there was only very limited research work reported in the literature. In one team, glass fiber membranes were covalently grafted with surfactants that have perfluorinated end (oleophobic) and polyethylene glycol chain (hydrophilic) for oil/water separation (Howarter and Youngblood, 2009). Another team also constructed ternary amphiphilic block copolymers consisting of hydrophilic block (polyethylene oxide) and nonpolar hydrophobic fluorine-containing blocks (oleophobic) as additive to prepare modified PVDF antifouling membranes (Chen et al., 2011b). Both studies demonstrated the improved performance of the developed membranes in water flux and oil fouling resistance. However, these studies were still largely limited on a small piece of flat sheet membrane for laboratory tests and there might be a gap in the scale-up of the membrane preparation for practical applications.

In this chapter, we report a novel hollow fiber membrane with both hydrophilic and oleophobic surface properties. The hollow fiber membrane was packed in membrane modules and tested for oil/water separation performance. The fouling behaviors of the membrane was compared with the control membrane through filtration of oil-in-water samples prepared from hexadecane and crude oil emulsions and real oily wastewater sample taken from a palm oil mill in Malaysia.

7.2 Materials and methods

7.2.1 Hollow fiber membrane preparation

A popular membrane material (PVDF), was used as the base or matrix material for the hollow fiber membrane in this chapter and was supplied by Solvay Solexis (PVDF, 6010, Mw ca. 322,000 g·mol^{-1}).

Table 7.1 Prepared hollow fiber membranes' compositions and properties

Membrane name	PVDF	M1	M2	M3
Base polymer	PVDF	PVDF	PVDF	PVDF
Additive	\	PEG 600	AP	AP
PVDF: Additive ratio	\	8:2	7:3	7:3
Dope solution polymer concentration (wt%)	18 (PVDF)	18 (PVDF)	18 (PVDF + AP)	20 (PVDF + AP)
Membrane surface pore size (μm)	\	0.097±0.03	0.136±0.04	0.116±0.03
Tensile stress (MPa)	\	6.22±0.06	6.28±0.03	6.75±0.05
Tensile strain (%)	\	117.38±3.64	2.83±0.58	2.53±0.94
Water contact angle (°)	96	79	26	29
Oil (hexadecane) contact angle (°)	~15	~15	75	74
Oil (hexadecane) adsorption amount (mg·g^{-1})	39	37.7	26.6	27.1

A copolymer, P(VDF-co-CTFE)-g-PMAA-g-fPEG, was synthesized and used as the additive with the PVDF to spin the desired hollow fiber membrane. The detailed methods to prepare the additive polymer can be found in Chapter 5. The additive polymer P(VDF-co-CTFE)-g-PMAA-g-fPEG which will be denoted as 'AP' hereafter in this chapter.

PVDF and AP were blended in different ratios and dissolved in N,N-dimethylformamide (DMF, Tedia, HPLC grade) as the solvent to prepare the

dope solutions for spinning the hollow fiber membranes. Table 7.1 shows the three typical types of hollow fiber membranes examined, including PVDF control membrane [PVDF with polyethylene glycol (PEG, Mw ca. 600 $g \cdot mol^{-1}$from Sigma-Aldrich) as the pore forming agent], and the new membranes with PVDF and AP in the weight ratio of 7:3 at different dope concentrations. Polymers dissolved in DMF were mechanically stirred at 350 rpm and 80 °C for 6 h to obtain a homogeneous and viscous dope solution. Before the spinning, the dope solution in an air-tight stainless steel tank was forced, under compressed nitrogen gas, through a 15 μm stainless steel filter to remove any insoluble or undissolved particles that may be present in the solution. The filtered blend dope solution was subsequently transferred into a syringe pump (ISCO 100D), and then degassed by a vacuum pump at 0.2 mbar vacuum for 5 h to remove any air bubbles that may be entrapped in the dope solution.

The fabrication of hollow fiber membrane was done by the common dry-wet spin phase inversion method.(Liu and Bai, 2006) The dope solution was extruded through a spinneret (with outer and inner diameters at 1.5 and 0.5 mm respectively) into an external coagulation bath (with an air gap of 0.5 cm). A core or bore coagulation liquid was also supplied simultaneously on the luman side of the hollow fiber. Both liquids in the coagulation bath and in the bore were deionized (DI) water at 60 °C. After stayed 6 h in the coagulant bath, the hollow fiber membrane was moved out and dried in air at 25 □C for 24 h. Then, the hollow fiber membrane was ready for characterization analysis or for packing into a module for filtration tests.

7.2.2 Characterization of hollow fiber membranes

The surface and the cross section of a hollow fiber membrane sample were observed with SEM (JEOL JSM-5600LV). The membrane sample was dried at 60 °C for 24 h and then coated with platinum with a vacuum electric sputter coater (JEOL JFC-1300) following the standard operation before scanning for the SEM images. Surface pore sizes of the prepared membranes were measured from the surface SEM images by the software named Smile View (JEOL) supplied with the microscope.

The mechanical property of the prepared hollow fiber membranes was also measured with an advanced mechanical testing system, INSTRON 5542. A dry hollow fiber membrane sample was cut into a 6 cm length piece and vertically attached to the two clamps of the machine to give an initial gauge length of 5 cm. The dragging rate of the grip was set at 1 $cm \cdot min^{-1}$. At least five tests for each type of the hollow fiber membrane were made and the average was reported in this paper.

The surface wetting properties of the prepared hollow fiber membranes were evaluated through water and oil surface contact angle measurements, water adsorption and oil adsorption tests. To estimate the surface contact angles, the same blend dope solutions were cast onto glass plates to form membrane films which were coagulated and dried in the same conditions as for the hollow fiber membranes. A contact angle goniometer (250-F1, from Ramé-Hart Instrument Co.) was used for the surface contact angle measurements. A membrane sample, first dried at 60 °C for 6 h and then cooled to the ambient temperature (25 ^{o}C),

was placed on the horizontal platform of the instrument. A 10 μL droplet of DI water or hexadecane was dropped onto the membrane surface. The droplet image was analyzed by the instrument to obtain the water or oil contact angle value of the tested membrane. Each sample was measured for 10 times at different locations and the reported result was the average value of these measurements.

Water or oil adsorption to the prepared hollow fiber membranes was evaluated through adsorption tests. A 100 mg amount of each type of the prepared hollow fiber membranes were cut into ~2 mm length pieces and added into 20 mL of DI water or an oil/water emulsion [200 $mg \cdot L^{-1}$, prepared by mixing 0.2 g hexadecane in 1 L DI water with a homogenizer (Cole-Parmer, Labgen 700) at 14,000 rpm for 20 min] in a 30 mL vial. The mixture was stirred in a shaker at 200 rpm for 24 h. For water adsorption, the buoyancy of the fiber pieces was observed. For oil adsorption, the initial and final total organic carbon (TOC) values of the emulsion were measured with a TOC analyzer (SHIMADZU, TOC-V), and the oil adsorption amount on the hollow fiber pieces was calculated through a calibration formula.

7.2.3 Oil/water separation experiments

Oil/water separation experiments were conducted with a membrane filtration system that can be operated on either the cross-flow or the dead-end filtration mode (see Figure 7.1). The system included a feed tank, a feed pump (Micro pump, ISMATEC IP65), a membrane module and a permeate tank. Before the membrane module, a flow meter and a pressure gauge were installed and, after the membrane module, another pressure gauge and a back pressure regulator were

installed in the system. The permeate weights were recorded with a digital balance (M.R.C., ββ-1550) connected to a computer at desired time intervals.

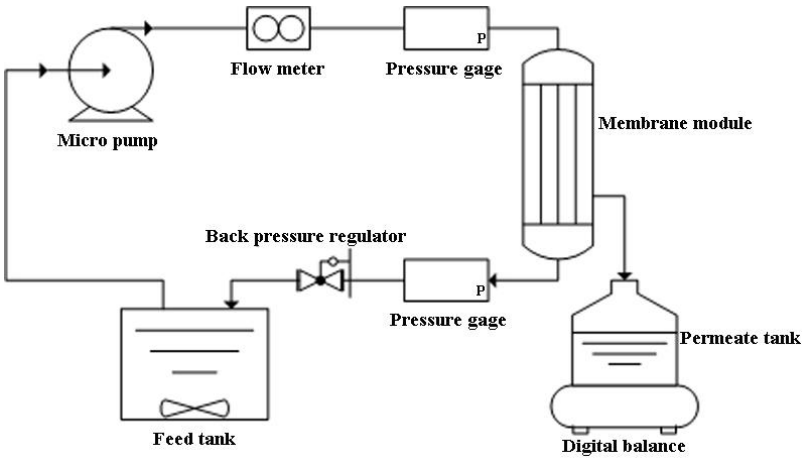

Figure 7.1 Schematic diagram of cross-flow and dead-end switchable filtration system.

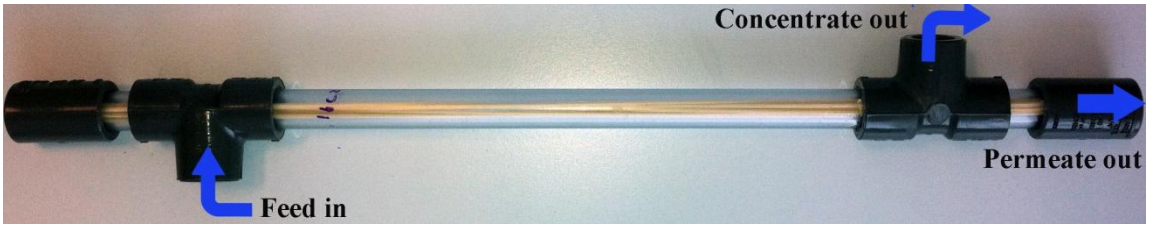

Figure 7.2 The hollow fiber module.

The hollow fiber membrane module consisted of a clear PVC tube (ID = 6.35 mm) with an effective length of 0.3 m. Within the tube six hollow fibers of the same length as the tube were installed in parallel (see Figure 7.2). Similar membrane modules were prepared for each type of the hollow fiber membranes tested. The filtration direction was from outside to inside of the hollow fibers and the total filtration area in a membrane module was 0.0085 m^2.

Three types of oily wastewater samples were tested. The first type was prepared with hexadecane supplied by Sigma-Aldrich. A 500 $mg \cdot L^{-1}$ emulsion was obtained by mixing 0.5 g of hexadecane in 1 L DI water with a homogenizer

(Cole-Parmer, Labgen 700) at 14,000 rpm for 20 min. This type of sample is denoted as ‘H-oil’ in the study. The second type of sample was similarly prepared but with crude oil supplied by an oil-refinery company in Singapore. It is expected that the oil properties would be more complicated in the second type of sample than that in the first type. The second type of sample is denoted as ‘C-oil’ in this chapter. The third type of sample was real oily wastewater collected from a palm oil mill in Malaysia. Its oil concentration was at around 91 $mg \cdot L^{-1}$. The third type of sample is denoted as ‘P-oil’ in this chapter.

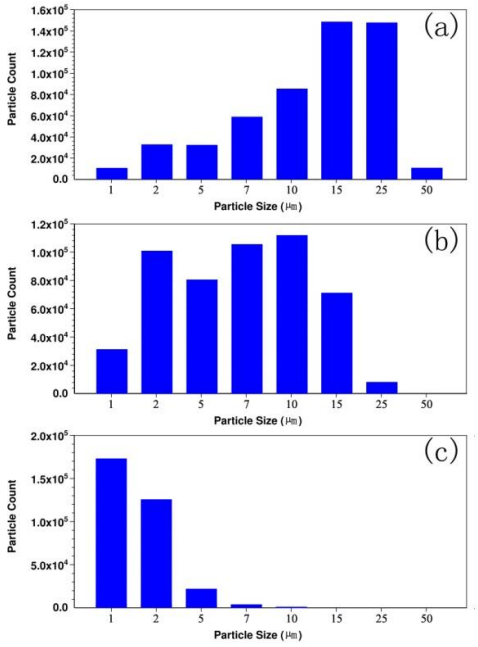

Figure 7.3 Average oil droplet sizes distribution of (a) hexadecane water emulsion, (b) crude oil water emulsion and (c) palm oil mill wastewater.

The oil droplet size distributions in the three types of samples were estimated with a particle counter (LIGHTHOUSE, LS-20) which can provide size readings in eight different size channels of 1.0, 2.0, 5.0, 7.0, 10.0, 15.0, 25.0 and 50.0 μm. It was found that the oil droplet sizes in ‘H-oil’ covered all channels from 1 to 50 μm and the distribution was negatively skewed with the majority at a size around

15-25 μm. For 'C-oil', the oil droplet sizes also covered all channels from 1 to 50 μm but the majority was more normally distributed at the size around 7 μm. The oil droplet size in the 'P-oil' sample was much smaller (in 1-5 μm range) and the majority was positively skewed to the lower end of the size distribution at around 1 μm. (The details on the oil droplet size distribution in the three samples can be found in Figure 7.3. Note: the particle counter was unable to give readings for those with size smaller than 1 μm.)

For a typical filtration experimental run, the hollow fiber membrane module was first filtered with DI water for 1 h. Then the stable DI water flux was recorded for 30 min and denoted as J_0. After that, the feed was switched to the oily wastewater sample and the filtration was continued for 2 h. The changes of the permeate flux was determined at every 10 min intervals and the final permeate flux at the end of 2 h filtration was denoted as J_P. After the oily wastewater sample filtration, the hollow fiber module was flushed with DI water at a cross-flow velocity of 0.5 $m \cdot s^{-1}$ for 10 min. Then, the DI water filtration was resumed for the hollow fiber membrane module and the constant DI water flux (during 30 min run) was recorded and denoted as J_1. The relative flux decay (RFD) for each run was calculated by $RFD = [(J_0-J_P)/J_0] \times 100\%$ and the relative flux recovery (RFR) indicating the extent of the possible reversible fouling was calculated by $RFR = (J_1/J_0) \times 100\%$. For the 'C-oil' filtration which appeared to be more challenging than the other two types of samples, the membrane module was also backwashed for 30 min under the same operation pressure as the filtration with DI water after the DI water flushing and the filtration run was repeated for a second

cycle. This was to examine whether the permeate flux can be completely recovered using backwashing as in normal membrane system operation and whether the fouling behavior of the membrane module would change significantly in repeated usage. In all the filtration runs, the transmembrane pressure was set and controlled at 0.34 MPa. For 'H-oil' filtration, both cross-flow and dead-end filtration runs were conducted and the cross-flow velocities of 0.05, 0.1 and 0.2 $m \cdot s^{-1}$ were tested. For the more difficult samples of 'C-oil' and 'P-oil', only dead-end filtration was conducted. This was to evaluate the worst case scenario in possible oil fouling of the membranes. The TOC values of oils in the feed and in the permeate were analyzed with a TOC analyzer (SHIMADZU, TOC-V) to determine the retention percentages or removal efficiencies.

7.3 Results and discussion

7.3.1 Properties of prepared hollow fiber membranes

The results on the properties of the prepared hollow fiber membranes from various analytical characterizations are also summarized in Table 7.1. The average surface pore sizes of the prepared membranes, as analyzed with the software of Smile View with the SEM machine, were at around 0.1 μm. It is known that PVDF without pore forming agent will usually form nonporous membrane. (Liu et al., 2011) In this chapter, the control membrane (M1) of PVDF with PEG as pore former had a pore size of about 0.097 μm. At the same total polymer concentration of 18 wt% in the dope, the M2 membrane had a larger pore size of 0.136 μm than that of M1, indicating that the additive polymer of AP also enhanced pore formation in the developed novel hollow fiber membranes. With

the increase of the total polymer concentration in the dope, the surface pores became smaller, with 0.116 μm for M3 (20 wt%) as compare to 0.136 μm for M2 (18 wt%). Hence, polymer concentration of the dope can be used as one of the factors to adjust the pore size of the hollow fiber membranes to be prepared.

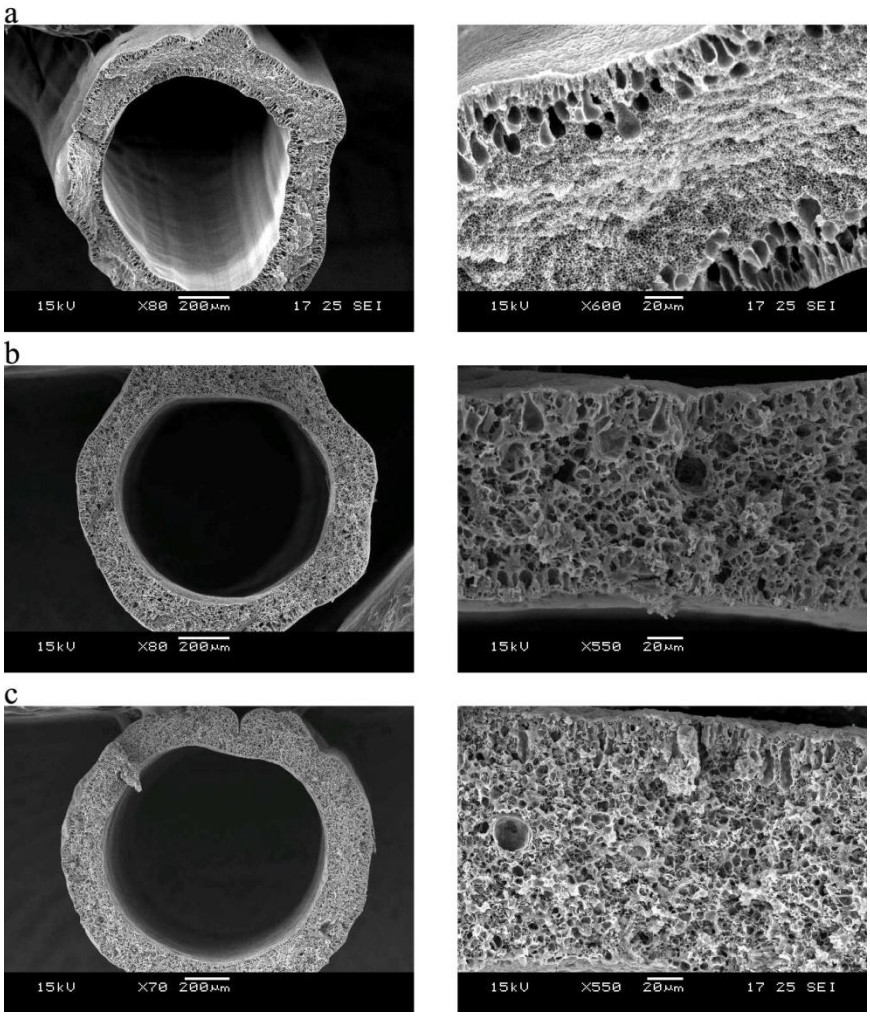

Figure 7.4 Overview (left) and partial view (right) of the cross section SEM images of the hollow fiber membranes of (a) M1, (b) M2 and (c) M3.

The cross section morphologies of the prepared hollow fiber membranes from the SEM analysis are shown in Figure 7.4. The control hollow fiber membrane (M1) did not retain a good cylindrical structure and the cross section had obvious finger-like macrovoids; see Figure 7.4(a). The formation of finger-like

macrovoids was often observed in many types of hollow fiber membranes fabricated *via* the phase inversion method due to the instantaneous liquid–liquid demixing during the coagulation process. (Smolders et al., 1992) In contrast, the developed hollow fiber membranes of M2 and M3 typically had the sponge-like substructure in their cross section. The sponge-like structure is often known to be formed due to delayed liquid–liquid demixing in the coagulation process, attributed to a lower phase inversion rate of the spinning dope solution. (Smolders et al., 1992) Hence, the blending of AP with PVDF appeared to change the phase inversion properties of the membrane materials. The sponge-like structure is usually more desired because it provides more uniform flow and structural properties. The results also indicate that the synthesized AP was highly compatible with PVDF and they formed homogeneous spinning dope solution and thus uniform membrane structure. It was also observed in the experiments that the spinning dope solution with AP was more viscous than that without AP even though they were at the same total polymer concentration, suggesting the existence of a strong interaction between the base polymer of PVDF and the additive polymer of AP. Comparing M3 with M2, it is also observed that with the increase of total polymer concentration in the dope, the hollow fiber membrane became denser with smaller pores in the cross section.

The mechanical property of a hollow fiber membrane is important as the transmembrane pressure acting on the hollow fiber membrane may cause deformations of the membrane structure. As shown in Table 7.1, the tensile stresses of the three types of hollow fiber membranes were compatible at around 6

MPa, with no obvious differences of for the developed hollow fiber membranes as compared to the control PVDF hollow fiber membrane, indicating that the blending of the additive polymer of AP with the base polymer of PVDF did not bring significant changes to the tensile stresses. These tensile stresses in fact appeared to be higher than that of a commercially used PVDF membrane at 3.5 MPa (Shi et al., 2007). For the transmembrane pressure used in this study is 0.34 MPa, all the hollow fiber membranes tested in this chapter were actually strong enough for practical use. As expected, the tensile stress could be increased by increasing the polymer concentration of the dope solution (see tensile stress values of M2 and M3 in Table 7.1). On the other hand, the tensile strain of the prepared hollow fiber membrane was affected by the blending of AP in PVDF. It is well known that PVDF has a high ductility that usually can reach a more than 100 % tensile strain (Shi et al., 2007). Similarly, the control membrane (M1) which had a tensile strain of 117.38 % in this chapter; see Table 7.1. The tensile strain of M2 or M3 was significantly reduced to around 2.5-3 %. The existence of AP in M2 or M3 made the hollow fiber membrane much less ductile. This probably also explains the better cylindrical structure of the M2 or M3 hollow fiber membrane in comparison with that of M1 shown in Figure 7.4.

The wetting properties of the prepared hollow fiber membranes by water and oil are of the most concern in this chapter. The synthesized AP contained both hydrophilic segment of PEG and oleophobic segment of perfluorinated hydrocarbon end. During the coagulation process, the segregation of AP in PVDF was promoted on the membrane surface, which created both hydrophilic and

oleophobic surface properties for the developed novel hollow fiber membranes. It was reported that the level of surface segregation achieved during coagulation would depend on the temperature of the coagulation bath. (Hester et al., 1999; Hester et al., 2002; Hester and Mayes, 2002) Thus, a 60 °C coagulation bath was used in the experiment to enhance the surface segregation effect. The hydrophilic and oleophobic surface properties of the developed hollow fiber membranes were verified with the contact angle measurements and adsorption tests. As given in Table 7.1, the M1 control membrane had a water contact angle of 79°, lower than 96° for the pure PVDF film, indicating that the pore former of PEG used in the control membrane (M1) slightly improved the hydrophilicity of the membrane. It was found that the surface hydrophilicity of the developed hollow fiber membrane was significantly increased, with a water contact angle of 26 or 29° for M2 or M3, respectively.

On the other hand, the oleophobicity of the novel membrane was also remarkably improved. The control membrane (M1) had an oil contact angle of about 15° or lower, indicating a high oleophilicity rather than oleophobicity; see Table 7.1. In contrast, the developed hollow fiber membrane of M2 or M3 had an oil contact angle of about 75°, much higher than that of M1. Hence, the additive polymer of AP had made the developed hollow fiber membranes much more oleophobic. The enrichment of both the hydrophilic and oleophobic segments of AP on the membrane surface can be considered as the mechanism that contributed to the membrane surface with the desired hydrophilicity as well as the oleophobicity in this chapter.

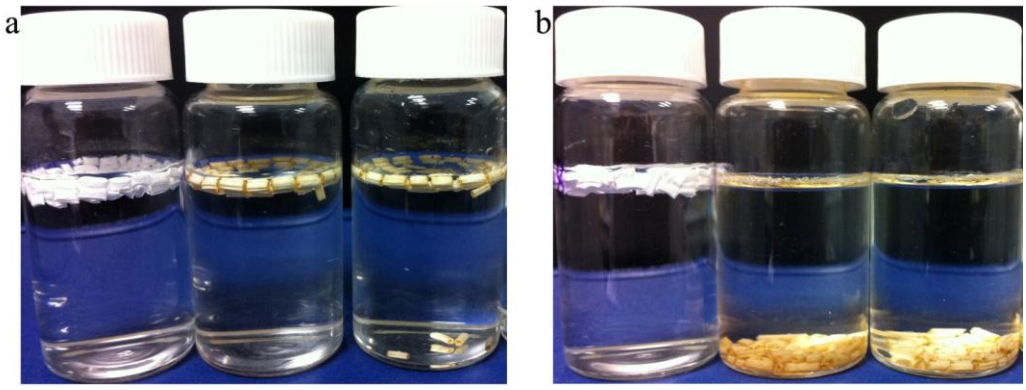

Figure 7.5 Image of hollow fibers (M1, M2 and M3 from left to right) (a) before and (b) after water adsorption.

The affinity of water and oil to the hollow fiber membranes was also indirectly assessed through water adsorption and oil adsorption testes. The hollow fiber membrane pieces were placed in water and stirred for 24 h. Those from M1 remained floating on the water surface but those from M2 or M3 were observed to all settle down in water after less than 1 h, suggesting that the developed hollow fiber membranes were indeed highly hydrophilic but the control one (M1) was not (see Figure 7.5). Similar adsorption experiments were done for oil adsorption. As expected, the control hollow fiber membrane (M1) had a much higher oil adsorption amount than those of the developed hollow fiber membranes of M2 and M3 (see Table 7.1), confirming that the developed hollow fiber membrane was much more oleophobic (considering that only 30 wt% of AP in the developed membranes).

7.3.2 Filtration of H-Oil sample

The prepared membranes were first evaluated for filtration of 500 $mg \cdot L^{-1}$ hexadecane in DI water emulsion. This gave a relatively simple composition as only hexadecane was the foulant. The filtration run was operated from dead-end

to cross-flow mode with the cross-flow velocity (average flow velocity on the membrane outer surface) was controlled at 0 $m \cdot s^{-1}$ (dead-end), 0.05, 0.1 and 0.2 $m \cdot s^{-1}$(cross-flow), respectively. The permeate volume was recorded and the corresponding permeate flux decay was determined throughout the filtration run.

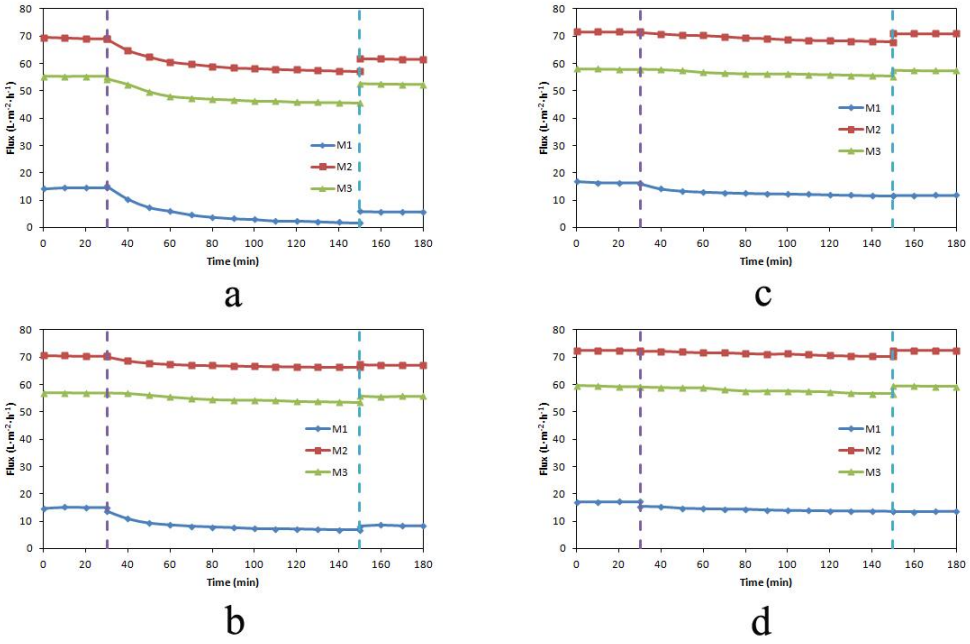

Figure 7.6 Permeate fluxes of M1, M2 and M3 at cross-flow velocities of (a) 0 $m \cdot s^{-1}$, (b) 0.05 $m \cdot s^{-1}$, (c) 0.1 $m \cdot s^{-1}$and (d) 0.2 $m \cdot s^{-1}$ in the filtration of DI water and H-oil sample (ΔP=0.34 MPa, 25°C).

Figure 7.6 shows the experimental results of permeate changes with the filtration time for the three types of hollow fiber membranes (M1, M2 and M3) under dead-end or cross-flow filtration mode with different cross-flow velocities. For the dead-end filtration case shown in Figure 7.6(a), the initial pure water fluxes (during the first 30 min) of M1, M2 and M3 were found to be 14.49, 69.22 and 55.20 $L \cdot m^{-2} \cdot h^{-1}$, respectively. The developed hollow fiber membranes (M2 and M3) had significantly higher pure water flux than the control membrane (M1). This should be attributed to the much higher hydrophilicity as well as the more

porous structure of the novel membrane (M2 or M3) than the control membrane (M1). It is well know that hydrophilic modification will improve the membrane's pure water flux (Liu et al., 2011).

During the next two hours of filtration of the H-oil sample (i.e., from 30 to 150 min), the permeate fluxes through all the three types of hollow fiber membranes were observed to decline with the filtration time but to a significantly different extent. The final permeate flux of M1, M2 or M3 at 150 min was 1.73, 57.10 or 45.58 $L \cdot m^{-2} \cdot h^{-1}$, respectively. In other words, the flux decay for M1 reached about 88% but those for M2 and M3 were at around 17%. After the H-oil sample filtration, the membrane was simply flashed and the pure water flux was measured again. As shown in the filtration time of 150 to 180 min in Figure 7.6(a), the flux was recovered back to 5.83, 61.63 or 52.41 $L \cdot m^{-2} \cdot h^{-1}$, respectively, for M1, M2 or M3, which gave a recovery rate of 40%, 89% and 95% for M1, M2 and M3, respectively. It is clear that the developed hollow fiber membranes showed much lower oil fouling effect and much higher flux recovery rate, in comparison with that of the control membrane, M1. This can be attributed to the double wetting properties of the developed novel hollow fiber membranes. The high hydrophilicity of the novel hollow fiber membrane can reduce the possibility of the oil droplets contacting the membrane surface. More important, the oleophobicity of the novel membrane will prevent the adhesion or adsorption of the oil droplets on the membrane surface.

In the literature, it is often recognized that a membrane operated at a much higher permeate flux would have a more severe membrane fouling.(Chen et al.,

1997; Li et al., 1998) This is due to the greater convective flow force directed to and the more foulants brought to the membrane surface. In this chapter, although the developed hollow fiber membrane of M2 or M3 had a much higher permeate flux than the control membrane of M1, the M2 or M3 hollow fiber membrane in fact exhibited lower oil fouling and better flux recovery, demonstrating the advantage of the developed novel hollow fiber membrane for oil/water separation application.

Table 7.2 Relative flux decay (RFD) and relative flux recovery (RFR) of the prepared hollow fiber membranes in H-oil filtration experiments at different cross-flow velocities

Membrane type	**Oil removal efficiency**	**Cross-flow velocity ($m \cdot s^{-1}$)**	**J_0 ($L \cdot m^{-2} \cdot h^{-1}$)**	**J_P ($L \cdot m^{-2} \cdot h^{-1}$)**	**J_1 ($L \cdot m^{-2} \cdot h^{-1}$)**	**RFD**	**RFR**
M1	98%	0	14.49	1.73	5.83	88%	40%
		0.05	15.00	6.78	8.29	55%	55%
		0.1	16.47	11.61	11.81	30%	72%
		0.2	17.09	13.55	13.45	21%	79%
M2	99%	0	69.22	57.10	61.63	18%	89%
		0.05	70.54	66.27	67.12	6%	95%
		0.1	71.62	67.85	70.91	5%	99%
		0.2	72.49	70.32	72.43	3%	100%
M3	99%	0	55.20	45.58	52.41	17%	95%
		0.05	56.93	53.46	55.68	6%	98%
		0.1	58.00	55.30	57.42	5%	99%
		0.2	59.32	56.56	59.35	5%	100%

When a cross-flow was applied, as shown in Figures 7.6(b), (c) and (d), some reduction in permeate flux decay and improvement in flux recovery rate were

observed and the effects increased with the increase of the cross-flow velocity. For cross-flow velocity from 0.05 to 0.2 $m.s^{-1}$, M1 still had a flux decay from 55% to 21% but only a flux recovery rate from 55% to 79% after the water flashing. Correspondingly, however, M2 had only a flux decay in the range from 6% to 3% but a flux recovery from 95% to 100%, similar to those results of M3, suggesting that the developed hollow fiber membranes achieved a feature of possibly no fouling and full flux recovery in the H-oil sample filtration, even at a reasonably low cross-flow velocity such as 0.2 $m{\cdot}s^{-1}$. The results indicate that oil fouling to the developed hollow fiber membranes, even existed, was weak and it can be easily removed by a simple water flush to the membrane surface. For all the three types of membranes, the oil removal efficiency was high, above 98% (with M2 and M3 achieved slightly better than M1). The typical data from all the relevant experiments are summarized in Table 7.2.

7.3.3 Filtration of C-Oil sample

The prepared hollow fiber membranes were also further tested to separate crude oil emulsion in a dead-end filtration mode. Although the study in the previous section demonstrated the effect of cross-flow on reducing oil fouling, the study in this section intended to examine the possible more severe oil fouling scenario. Crude oil is a complex mixture containing various hydrocarbon oils such as mostly alkanes, cycloalkanes and various aromatic hydrocarbons, the other organic compounds with nitrogen, oxygen and sulfur elements, and also possibly trace amounts of metals such as iron, nickel, copper and vanadium. (Speight and NetLibrary Inc., 1999) The organic compounds in crude oil can also cover a wide

range of surface tension. (Speight, 2001) It is expected that some hydrocarbons with very long carbon chains such as asphalt or coke may be easier to stick on the membrane surface and cause fouling. The filtration experiment was conducted for two consecutive cycles and a water backwashing was also used at the end of the two filtration cycles to clean the used membranes.

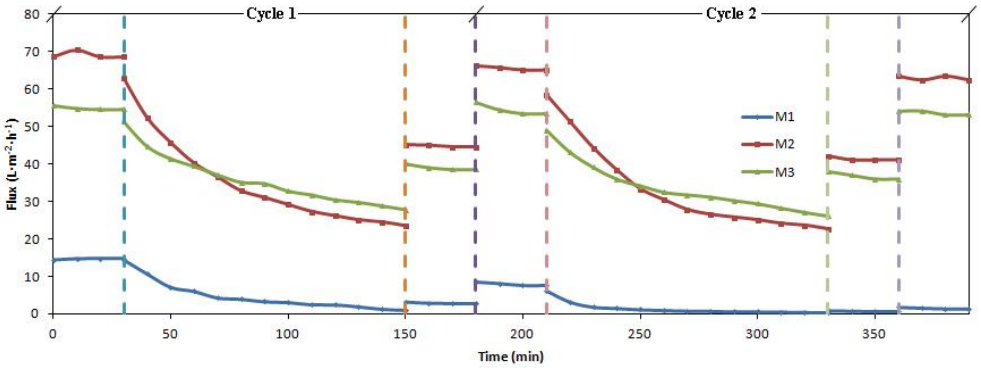

Figure 7.7 Permeate fluxes of the prepared membranes in the filtration of DI water and C-oil emulsion.

Table 7.3 Relative flux decay (RFD) and relative flux recovery (RFR) of the membranes in C-oil emulsion filtration experiments

		Cycle 1				Cycle 2			
Membrane type	**Oil removal efficiency**	**J_0 ($L \cdot m^{-2} \cdot h^{-1}$)**	**RFD**	**RFR**	**RFR_B**	**J_{0_1} ($L \cdot m^{-2} \cdot h^{-1}$)**	**RFD_1**	**RFR_1**	**RFR_B1**
M1	99%	14.67	93%	20%	54%	7.97	95%	10%	20%
M2	99%	69.03	66%	65%	95%	65.52	66%	63%	96%
M3	99%	54.93	49%	71%	99%	54.49	52%	68%	99%

The experimental results in the permeate flux change with the filtration time for the three types of hollow fiber membranes (M1, M2 and M3) are shown in Figure 7.7 and some typical data are summarized in Table 7.3. For the control

hollow fiber membrane (M1), a flux decay of 93% after 2 h filtration in the first cycle was recorded. By the simple membrane surface flushing, a 20% flux recovery rate was achieved. After the backwashing, the control membrane (M1) obtained a 54% flux recovery rate. In comparison, the M2 hollow fiber membrane had a permeate flux decay of 66% after the 2h filtration in the first cycle. The flux recovery rate was up to 65% after the simply membrane surface flushing, and reached 95% by the membrane backwashing. Similarly, the M3 hollow fiber membrane showed a 49% flux decay in the end of the first cycle filtration and a 71% flux recovery rate after the surface flushing, with a almost complete flux recovery (up to 99%) by the membrane backwashing. These results indicate that the developed hollow fiber membranes (M2 and M3) again showed much better antifouling performances than the control membrane (M1) in the filtration of crude oil emulsion.

In the second filtration cycle, the permeate flux of M1 dropped quickly and most of the flux decay was irreversible. In contrast, the M2 and M3 hollow fiber membranes showed very similar filtration performance in the second cycle to that of the first cycle. More important, most of their flux decays could be recovered by the backwashing. Bear in mind that the backwashing pressure in this chapter was the same as the filtration operation pressure. However, the backwashing pressures used in actual membrane microfiltration or ultrafiltration applications were usually much higher than their operation pressures. (Hillis et al., 1998; Kennedy et al., 1998)

As given in Table 7.3, the average oil removal efficiency for all the three types of hollow fiber membranes were at 99% and above in C-oil filtration separation.

7.3.4 Filtration of P-Oil sample

Finally, a real oily wastewater sample from a palm oil mill in Malaysia was also tested with the prepared hollow fiber membranes in the dead-end filtration mode.

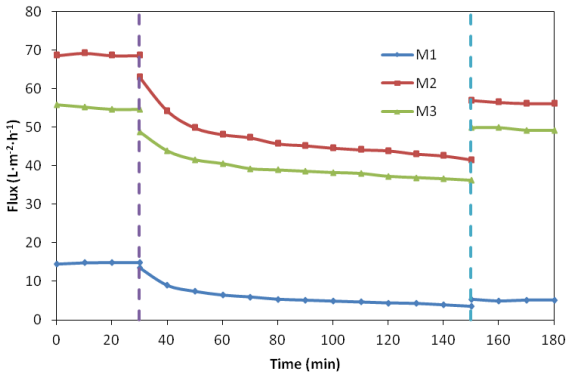

Figure 7.8 Permeate fluxes of the prepared membranes in the filtration of DI water and P-oil mill wastewater.

Table 7.4 Relative flux decay (RFD) and relative flux recovery (RFR) of the membranes in P-oil emulsion filtration experiments

Membrane type	Oil removal efficiency	J_0 ($L \cdot m^{-2} \cdot h^{-1}$)	J_P ($L \cdot m^{-2} \cdot h^{-1}$)	J_1 ($L \cdot m^{-2} \cdot h^{-1}$)	RFD	RFR
M1	69%	14.73	3.46	5.08	77%	35%
M2	68%	68.73	41.53	56.43	40%	82%
M3	70%	55.05	36.15	49.51	34%	90%

As shown in Figure 7.8 and summarized in Table 7.4, the M1 membrane was found to have a flux drop of 77% after the 2 h filtration and a flux recovery rate of 35% was achieved after the membrane surface flushing. Hence, the control membrane (M1) was highly subject to the oil fouling in the palm oil wastewater filtration. For the developed hollow fiber membrane of M2 or M3, the flux decay was 40% or 34%, and the flux recovery rate was 82% or 90%, respectively. These results indicate that the novel hollow fiber membranes had significantly improved antifouling performances.

It was found that the oil removal efficiency of the three types of membranes were all at about 70% (see Table 7.4) in palm oil wastewater filtration. This was attributed to the oil droplet sizes in the palm oil wastewater were much smaller than those in H-oil and C-oil samples. It has been shown that most of the palm oil droplets had a diameter at around 1 μm (see Figure 7.8). Particularly, the palm oil wastewater may contain dissolved oil that cannot be effectively removed by the membranes prepared in this chapter. If more complete removal is needed, the developed novel hollow fiber membrane may be prepared into ultrafiltration or nanofiltration type by increasing, for example, the dope concentration, which may be further investigated in future work.

7.4 Conclusion

In summary, this chapter demonstrated a novel hollow fiber membrane for effective and low fouling oil/water separation applications. The hollow fiber membrane was fabricated from PVDF and a modified PVDF copolymer as the additive and possessed the surface properties to be both highly hydrophilic as well

as oleophobic. The hollow fiber membrane was placed in membrane modules and tested for artificial and real oily wastewater samples. The developed hollow fiber membrane exhibited high pure water flux, low oil fouling behavior and the fouling, if existed, can be easily removed by a simple membrane surface flushing or backwashing method. Since the hollow fiber membrane can be readily scaled up for industrial applications, there is a great prospect for the developed hollow fiber membrane to be used in oily wastewater treatment.

Chapter 8 **Conclusions and future work**

8.1 Conclusions

This study aims at providing effective methods to reduce or eliminate the membrane fouling caused by the biological and organic foulants.

In the first part of the study, membrane surfaces immobilized with ionic or reduced silver were successfully prepared and showed effective antibacterial and anti-biofouling performance. XPS spectra verified the valence states of the immobilized silvers on membrane surfaces and their coordination with the amino groups of the chitosan membrane. The leaching test showed that the metallic silver was more stably immobilized than the ionic silver on the membrane surface. From the disk diffusion experiment, both metallic and ionic silver exhibited excellent antibacterial properties for *E. coli* and *pseudomonas sp.* In the longer time anti-biofouling experiments, only discrete bacteria, most of them being dead cells, were observed on the membranes immobilized with silver. But the membrane with the metallic silver seemed to be more stable and showed slightly better overall anti-biofouling performance than the membrane with the ionic silver. The results indicate that the immobilization of silver on a membrane surface as a biocide is an effective method to control membrane biofouling.

In the second part of the study, the stability of the immobilized silver and the use of inert commercial membranes were of the major interest. A method was developed to graft thiol groups to PP membrane surface that does not have any functional groups and silver ions were immobilized onto the modified PP membrane through coordinating with the thiol groups. The grafted thiol groups on

the PP membrane were verified with the ATR-FTIR analysis, and the coordination between the thiol groups and silver ions were confirmed from the XPS spectra. The immobilized silver was found to be stable in the leaching test, and only about 1.1 % of the immobilized silver was subject to leaching. From the disk diffusion experiment, both *E. coli* and *S. aureus* were found unable to grow on the PPS-Ag membrane, suggesting that the prepared PPS-Ag membrane may have a broad-spectrum antibacterial performance. In the mixed bacteria suspension immersion test, only discrete bacteria, most of them being unviable cells, were observed on the PPS-Ag membrane. Furthermore, in the mixed bacteria suspension filtration experiments, the PPS-Ag membrane showed higher permeate fluxes, slower flux decay and, particularly, greater relative flux recovery (RFR) than the control PP membrane, indicating that the fouling on the PPS-Ag membrane, if any, mostly were reversible, and the flux can be recovered by simple physical cleaning. The silver immobilized PP membrane exhibited long term stable anti-biofouling performance. The results suggest that the method of immobilizing silver for control biofouling can probably be extended to many types of membranes, including the common commercial ones.

In the third part of the study, a novel additive polymer was synthesized to prepare membrane that may have greater affinity to water and enhanced resistance to the adhesion and hence fouling of both organic and biological origins. The additive was prepared on the basis of P(VDF-co-CTFE). tBMA was grafted onto P(VDF-co-CTFE) through ATRP. P(VDF-co-CTFE)-g-PtBMA was then hydrolyzed to produce carboxylic groups to react with the hydroxyl groups of

FPEG. The synthesis processes and reactions were verified through the ATR-FTIR and NMR spectra of the polymers. The synthesized additive polymer was blend with PVDF in different ratios to prepare membranes. The prepared membranes were found to show the properties of the additive polymer, i.e., being both hydrophilic and oleophobic. The surface morphology of the prepared membranes can be adjusted through different ratios of the additive polymer to PVDF or different polymer concentrations of the casting solutions in various concentrations. The membranes prepared with higher portions of the additive polymer or lower casting solution polymer concentrations showed more porous surfaces. The more additive polymer was added, the more hydrophilic and oleophobic membrane surface was produced. The prepared membranes with the additive polymer all showed good oil/water separation performances, with the oil removal efficiencies being at least 99.8 % for the samples tested. However, the antifouling performances of the membranes were dependant on both the additive polymer content and the surface morphology. The membrane containing 30 wt% of the additive polymer was found to most effectively prevent the oil adsorption or oil fouling in this study. The results indicate that blending additive polymer with the base membrane polymer can be an effective method to prepare functional surface with two distinctively different wettabilities, i.e., both hydrophilic and oleophobic, which was of the potential for enhanced antifouling performance, including for oils.

In the fourth part of the study, antifouling performances of the membranes prepared from blending the additive polymer with PVDF at certain ratios were

further evaluated with various organic and biological foulants. The novel membrane's hydrophilicity and oleophobicity were significantly improved by the additive polymer. During the organic fouling tests, the developed novel membrane showed enhanced pure water flux and good organic fouling resistances, exhibited as slow flux decay and high flux recovery rate. The developed novel membrane also effectively prevented the adhesion of bacteria and thus provided excellent anti-biofouling performance. Especially, when the additive polymer amount in PVDF reached 30 wt%, the developed novel membrane exhibited almost non-fouling performance. Hence, the developed novel membrane with both hydrophilic and oleophobic surface properties had outstanding antifouling performance, which has a great potential to be used in water treatment applications.

In the last part of the study, the developed novel membrane was fabricated in the hollow fiber configuration and especially examined for antifouling performance in oil/water separation. The hollow fiber membrane was packed in membrane modules and tested by artificial and real oily wastewater samples. The developed hollow fiber membrane exhibited high pure water flux, low oil fouling behavior and, the fouling, if existed, can be easily removed by a simple membrane surface flushing or backwashing method with water. Since the hollow fiber membrane can be readily scaled up for industrial applications, there is hence a great prospect for the developed hollow fiber membrane to be used in oily wastewater treatment.

8.2 Future work

Although the solutions were proved to be effective in inhibiting membrane fouling especially by organic and biological origins, more experiments could be performed for extended and more detailed application studies.

The prepared membranes could be further investigated for their potential performances in real membrane filtration environments. In addition, membrane characteristics should be further determined. Some other modification strategies can also be attempted to achieve the enhanced performance.

In this study, the membrane filtration tests were performed with feed solutions containing only one or two types of foulants. However, in a real membrane operation environment, the membrane is usually fed with a more complex wastewater containing a mixture of various biological and organic foulants. Filtration in a MBR is a close simulation of the actual operating conditions of a wastewater treatment system. In order to evaluate the performances of the membranes in an actual environment, the prepared membranes can be applied in a MBR under certain operating conditions to further substantiate their antifouling performances.

Pore size and porosity are very important factors of a membrane for filtration. In this study, the membrane surface morphology was only observed with SEM. Quantitative determination of membrane pore size and porosity should be done in the future. There are various available evaluation methods. For example, membrane pore size distribution could be determined, using the fractional rejection of nonionic and charged macromolecules (Lee et al., 2002).

PVDF is a good candidate for membrane fabrication because of its special property such as chemical stability. However, PVDF is highly oleophilic, which made it to be more easily subject to membrane oil fouling. Some other polymers such as cellulose acetate are much less oleophilic. Modifications based on these polymers should achieve better inhibition efficiency for oily foulants.

In Chapter 5, an additive polymer was synthesized based on PVDF-co-CTFE. However, the functional hydrophilic and oleophobic chains are with the surfactant which was grafted onto the modified PVDF-co-CTFE. The future work could be conducted based on the modification of the surfactant. It can be expected that the modified surfactant can be directly reacted to a desire matrix polymer and endow the polymer surface with both hydrophilicity and oleophobicity.

Reference

Akthakul, A., R. F. Salinaro and A. M. Mayes. Antifouling polymer membranes with subnanometer size selectivity, Macromolecules, *37*, 20, pp. 7663-7668. 2004.

Al-Ahmad, M., F. A. A. Aleem, A. Mutiri and A. Ubaisy. Biofuoling in RO membrane systems Part 1: Fundamentals and control, Desalination, *132*, 1-3, pp. 173-179. 2000.

Al-Tahhan, R. A., T. R. Sandrin, A. A. Bodour and R. M. Maier. Rhamnolipid-induced removal of lipopolysaccharide from Pseudomonas aeruginosa: Effect on cell surface properties and interaction with hydrophobic substrates, Applied and Environmental Microbiology, *66*, 8, pp. 3262-3268. 2000.

Asatekin, A., S. Kang, M. Elimelech and A. M. Mayes. Anti-fouling ultrafiltration membranes containing polyacrylonitrile-graft-poly (ethylene oxide) comb copolymer additives, Journal of Membrane Science, *298*, 1-2, pp. 136-146. 2007.

Asatekin, A. and A. M. Mayes. Oil industry wastewater treatment with fouling resistant membranes containing amphiphilic comb copolymers, Environmental Science & Technology, *43*, 12, pp. 4487-4492. 2009.

Baker, J. S. and L. Y. Dudley. Biofouling in membrane systems - A review. Conference on Membranes in Drinking and Industrial Water Production, Amsterdam, Netherlands. 1998. pp. 81-89

Baker, R. W. Membrane technology and applications. pp. Chichester ; New York: J. Wiley. 2004.

Benito, J. M., S. Ebel, B. Gutierrez, C. Pazos and J. Coca. Ultrafiltration of a waste emulsified cutting oil using organic membranes, Water Air and Soil Pollution, *128*, 1-2, pp. 181-195. 2001.

Bilstad, T. and E. Espedal. Membrane separation of produced water, Water Science and Technology, *34*, 9, pp. 239-246. 1996.

Bohner, H. F. and R. L. Bradley Jr. Effective Cleaning and Sanitizing of Polysulfone Ultrafiltration Membrane Systems, Journal of Dairy Science, *75*, 3, pp. 718-724. 1992.

Bos, R., H. C. Van Der Mei and H. J. Busscher. Physico-chemistry of initial microbial adhesive interactions - Its mechanisms and methods for study, FEMS Microbiology Reviews, *23*, 2, pp. 179-229. 1999.

Brinck, J., A. S. Jönsson, B. Jönsson and J. Lindau. Influence of pH on the adsorptive fouling of ultrafiltration membranes by fatty acid, Journal of Membrane Science, *164*, 1-2, pp. 187-194. 2000.

Brink, L. E. S. and D. J. Romijn. Reducing the protein fouling of polysulfone surfaces and polysulfone ultrafiltration membranes: Optimization of the type of presorbed layer, Desalination, *78*, 2, pp. 209-233. 1990.

C.A.M, S., A. J. Burggraaf and L. Cot. Chapter 13 Applications of ceramic membranes in liquid filtration. Membrane Science and Technology, Elsevier. *4***:** 619-639. 1996.

C.J, v. O. Acid-base interfacial interactions in aqueous media, Colloids and Surfaces A: Physicochemical and Engineering Aspects, *78*, 0, pp. 1-49. 1993.

Castner, D. G., K. Hinds and D. W. Grainger. X-ray photoelectron spectroscopy sulfur 2p study of organic thiol and disulfide binding interactions with gold surfaces, Langmuir, *12*, 21, pp. 5083-5086. 1996.

Chakrabarty, B., A. K. Ghoshal and M. K. Purkait. Ultrafiltration of stable oil-in-water emulsion by polysulfone membrane, Journal of Membrane Science, *325*, 1, pp. 427-437. 2008.

Chang, Q. B., J. E. Zhou, Y. Q. Wang, J. M. Wang and G. Y. Meng. Hydrophilic modification of Al2O3 microfiltration membrane with nano-sized gamma-Al2O3 coating, Desalination, *262*, 1-3, pp. 110-114. 2010.

Chang, Y., T. Y. Cheng, Y. J. Shih, K. R. Lee and J. Y. Lai. Biofouling-resistance expanded poly(tetrafluoroethylene) membrane with a hydrogel-like layer of surface-immobilized poly(ethylene glycol) methacrylate for human plasma protein repulsions, Journal of Membrane Science, *323*, 1, pp. 77-84. 2008a.

Chang, Y., Y. J. Shih, R. C. Ruaan, A. Higuchi, W. Y. Chen and J. Y. Lai. Preparation of poly(vinylidene fluoride) microfiltration membrane with uniform surface-copolymerized poly(ethylene glycol) methacrylate and improvement of blood compatibility, Journal of Membrane Science, *309*, 1-2, pp. 165-174. 2008b.

Chen, S., G. Wu and H. Zeng. Preparation of high antimicrobial activity thiourea chitosan-Ag+ complex, Carbohydrate Polymers, *60*, 1, pp. 33-38. 2005.

Chen, V., A. G. Fane, S. Madaeni and I. G. Wenten. Particle deposition during membrane filtration of colloids: transition between concentration polarization and cake formation, Journal of Membrane Science, *125*, 1, pp. 109-122. 1997.

Chen, W., Y. Su, J. Peng, Y. Dong, X. Zhao and Z. Jiang. Engineering a robust, versatile amphiphilic membrane surface through forced surface segregation for ultralow flux-decline, Advanced Functional Materials, *21*, 1, pp. 191-198. 2011a.

Chen, W. J., J. M. Peng, Y. L. Su, L. L. Zheng, L. J. Wang and Z. Y. Jiang. Separation of oil/water emulsion using Pluronic F127 modified polyethersulfone ultrafiltration membranes, Separation and Purification Technology, *66*, 3, pp. 591-597. 2009a.

Chen, W. J., Y. L. Su, J. M. Peng, X. T. Zhao, Z. Y. Jiang, Y. A. Dong, Y. Zhang, Y. G. Liang and J. Z. Liu. Efficient wastewater treatment by membranes through constructing tunable antifouling membrane surfaces, Environmental Science & Technology, *45*, 15, pp. 6545-6552. 2011b.

Chen, W. J., Y. L. Su, L. L. Zheng, L. J. Wang and Z. Y. Jiang. The improved oil/water separation performance of cellulose acetate-graft-polyacrylonitrile membranes, Journal of Membrane Science, *337*, 1-2, pp. 98-105. 2009b.

Cheng, G., H. Xite, Z. Zhang, S. F. Chen and S. Y. Jiang. A switchable biocompatible polymer surface with self-sterilizing and nonfouling capabilities, Angewandte Chemie-International Edition, *47*, 46, pp. 8831-8834. 2008.

Cheryan, M. and NetLibrary Inc. Ultrafiltration and microfiltration handbook. pp. Lancaster, Pa: Technomic Pub. Co. 1998.

Cheryan, M. and N. Rajagopalan. Membrane processing of oily streams. Wastewater treatment and waste reduction, Journal of Membrane Science, *151*, 1, pp. 13-28. 1998.

Childress, A. E. and M. Elimelech. Relating nanofiltration membrane performance to membrane charge (electrokinetic) characteristics, Environmental Science & Technology, *34*, 17, pp. 3710-3716. 2000.

Choi, H., K. Zhang, D. D. Dionysiou, D. B. Oerther and G. A. Sorial. Effect of permeate flux and tangential flow on membrane fouling for wastewater treatment, Separation and Purification Technology, *45*, 1, pp. 68-78. 2005.

Combe, C., E. Molis, P. Lucas, R. Riley and M. M. Clark. The effect of CA membrane properties on adsorptive fouling by humic acid, Journal of Membrane Science, *154*, 1, pp. 73-87. 1999.

Daufin, G., U. Merin, J. P. Labbé, A. Quémerais and F. L. Kerhervé. Cleaning of inorganic membranes after whey and milk ultrafiltration, Biotechnology and Bioengineering, *38*, 1, pp. 82-89. 1991.

Dror-Ehre, A., A. Adin, G. Markovich and H. Mamane. Control of biofilm formation in water using molecularly capped silver nanoparticles, Water Research, *44*, 8, pp. 2601-2609. 2010.

Elmaleh, S. and N. Ghaffor. Cross-flow ultrafiltration of hydrocarbon and biological solid mixed suspensions, Journal of Membrane Science, *118*, 1, pp. 111-120. 1996a.

Elmaleh, S. and N. Ghaffor. Upgrading oil refinery effluents by cross-flow ultrafiltration, Water Science and Technology, *34*, 9, pp. 231-238. 1996b.

Fan, F.-R. F. and A. J. Bard. Chemical, Electrochemical, Gravimetric, and Microscopic Studies on Antimicrobial Silver Films, The Journal of Physical Chemistry B, *106*, 2, pp. 279-287. 2001.

Fane, A. G., C. J. D. Fell and K. J. Kim. The effect of surfactant pretreatment on the ultrafiltration of proteins, Desalination, *53*, 1-3, pp. 37-55. 1985.

Feng, Q. L., J. Wu, G. Q. Chen, F. Z. Cui, T. N. Kim and J. O. Kim. A mechanistic study of the antibacterial effect of silver ions on Escherichia coli and Staphylococcus aureus, Journal of Biomedical Materials Research, *52*, 4, pp. 662-668. 2000.

Feng, X. J. and L. Jiang. Design and creation of superwetting/antiwetting surfaces, Advanced Materials, *18*, 23, pp. 3063-3078. 2006.

Flemming, H. C., G. Schaule, T. Griebe, J. Schmitt and A. Tamachkiarowa. Biofouling - the Achilles heel of membrane processes. Workshop on Membranes in Drinking Water Production - Technical Innovations and Health Aspects, Laquila, Italy, Elsevier Science Bv. 1997. pp. 215-225

Fu, J. H., J. Ji, D. Z. Fan and J. C. Shen. Construction of antibacterial multilayer films containing nanosilver via layer-by-layer assembly of heparin and chitosan-silver ions complex, Journal of Biomedical Materials Research Part A, *79A*, 3, pp. 665-674. 2006.

Gan, D., W. Cao and Z. Wang. Synthesis and surface properties of a fluorinated polyether, Journal of Fluorine Chemistry, *116*, 1, pp. 59-63. 2002.

Gancarz, I., G. Poźniak and M. Bryjak. Modification of polysulfone membranes 1. CO2 plasma treatment, European Polymer Journal, *35*, 8, pp. 1419-1428. 1999.

Gancarz, I., G. Poźniak and M. Bryjak. Modification of polysulfone membranes: 3. Effect of nitrogen plasma, European Polymer Journal, *36*, 8, pp. 1563-1569. 2000.

Geesey, G. G., R. J. Gillis, R. Avci, D. Daly, M. Hamilton, P. Shope and G. Harkin. The influence of surface features on bacterial colonization and subsequent substratum chemical changes of 316L stainless steel, Corrosion Science, *38*, 1, pp. 73-95. 1996.

Gerhart, D. J., D. Rittschof, I. R. Hooper, K. Eisenman, A. E. Meyer, R. E. Baier and C. Young. Rapid and inexpensive quantification of the combined polar components of surface wettability: Application to biofouling, Biofouling, *5*, 4, pp. 251 - 259. 1992.

Ghandour, W., J. A. Hubbard, J. Deistung, M. N. Hughes and R. K. Poole. The uptake of silver ions by Escherichia coli K12: toxic effects and interaction with copper ions, Applied Microbiology and Biotechnology, *28*, 6, pp. 559-565. 1988.

Giangiordano, R. A. and D. A. Klein. Silver ion effects on Hyphomicrobium species growth initiation and apparent minimum growth temperatures, Letters in Applied Microbiology, *18*, 4, pp. 181-183. 1994.

Golomb, G. and A. Shpigelman. Prevention of bacterial colonization on polyurethane in vitro by incorporated antibacterial agent, Journal of Biomedical Materials Research, *25*, 8, pp. 937-952. 1991.

Gottenbos, B., D. W. Grijpma, H. C. van der Mei, J. Feijen and H. J. Busscher. Antimicrobial effects of positively charged surfaces on adhering Gram-positive and Gram-negative bacteria, Journal of Antimicrobial Chemotherapy, *48*, 1, pp. 7-13. 2001.

Grundke, K., M. Stamm, H.-J. Adler, A. Roosjen, W. Norde, H. van der Mei and H. Busscher. The use of positively charged or low surface free energy coatings versus polymer brushes in controlling biofilm formation. Characterization of Polymer Surfaces and Thin Films, Springer Berlin / Heidelberg. *132***:** 138-144. 2006.

Gupta, M. and K. K. Gleason. Surface modification of high aspect ratio structures with fluoropolymer coatings using chemical vapor deposition, Thin Solid Films, *517*, 12, pp. 3547-3550. 2009.

Gutkin, V., J. Gun and O. Lev. Electrochemical deposition-stripping analysis of molecules and proteins by online electrochemical flow cell/mass spectrometry, Analytical Chemistry, *81*, 20, pp. 8396-8404. 2009.

Gwon, E. M., M. J. Yu, H. K. Oh and Y. H. Ylee. Fouling characteristics of NF and RO operated for removal of dissolved matter from groundwater, Water Research, *37*, 12, pp. 2989-2997. 2003.

Hamza, A., V. A. Pham, T. Matsuura and J. P. Santerre. Development of membranes with low surface energy to reduce the fouling in ultrafiltration applications, Journal of Membrane Science, *131*, 1-2, pp. 217-227. 1997.

Hester, J. F., P. Banerjee and A. M. Mayes. Preparation of protein-resistant surfaces on poly(vinylidene fluoride) membranes via surface segregation, Macromolecules, *32*, 5, pp. 1643-1650. 1999.

Hester, J. F., P. Banerjee, Y. Y. Won, A. Akthakul, M. H. Acar and A. M. Mayes. ATRP of amphiphilic graft copolymers based on PVDF and their use as membrane additives, Macromolecules, *35*, 20, pp. 7652-7661. 2002.

Hester, J. F. and A. M. Mayes. Design and performance of foul-resistant poly(vinylidene fluoride) membranes prepared in a single-step by surface segregation, Journal of Membrane Science, *202*, 1-2, pp. 119-135. 2002.

Hillis, P., M. B. Padley, N. I. Powell and P. M. Gallagher. Effects of backwash conditions on out-to-in membrane microfiltration, Desalination, *118*, 1-3, pp. 197-204. 1998.

Hong, S. K. and M. Elimelech. Chemical and physical aspects of natural organic matter (NOM) fouling of nanofiltration membranes, Journal of Membrane Science, *132*, 2, pp. 159-181. 1997.

Howarter, J. A., K. L. Genson and J. P. Youngblood. Wetting behavior of oleophobic polymer coatings synthesized from fluorosurfactant-macromers, ACS Applied Materials & Interfaces, *3*, 6, pp. 2022-2030. 2011.

Howarter, J. A. and J. P. Youngblood. Amphiphile grafted membranes for the separation of oil-in-water dispersions, Journal of Colloid and Interface Science, *329*, 1, pp. 127-132. 2009.

Huisman, I. H., P. Prádanos and A. Hernández. The effect of protein-protein and protein-membrane interactions on membrane fouling in ultrafiltration, Journal of Membrane Science, *179*, 1-2, pp. 79-90. 2000.

Hyun, J., H. Jang, K. Kim, K. Na and T. Tak. Restriction of biofouling in membrane filtration using a brush-like polymer containing oligoethylene glycol side chains, Journal of Membrane Science, *282*, 1-2, pp. 52-59. 2006.

Jin, L. and R. B. Bai. Mechanisms of lead adsorption on chitosan/PVA hydrogel beads, Langmuir, *18*, 25, pp. 9765-9770. 2002.

Ju, H., B. D. McCloskey, A. C. Sagle, Y. H. Wu, V. A. Kusuma and B. D. Freeman. Crosslinked poly(ethylene oxide) fouling resistant coating materials for oil/water separation, Journal of Membrane Science, *307*, 2, pp. 260-267. 2008.

Jucker, C. and M. M. Clark. Adsorption of aquatic humic substances on hydrophobic ultrafiltration membranes, Journal of Membrane Science, *97*, pp. 37-52. 1994.

Judd, S., C. Judd, J. Simon and J. Claire. Fundamentals. The MBR Book. Oxford, Elsevier Science**:** 21-121. 2006.

Kaiya, Y., Y. Itoh, K. Fujita and S. Takizawa. Study on fouling materials in the membrane treatment process for potable water, Perth, Australia. 1994. pp. 71-77

Kang, S., A. Asatekin, A. M. Mayes and M. Elimelech. Protein antifouling mechanisms of PAN UF membranes incorporating PAN-g-PEO additive, Journal of Membrane Science, *296*, 1-2, pp. 42-50. 2007.

Karakulski, K., A. Kozlowski and A. W. Morawski. Purification of oily wastewater by ultrafiltration, Separations Technology, *5*, 4, pp. 197-205. 1995.

Kasemura, T., Y. Oshibe, H. Uozumi, S. Kawai, Y. Yamada, H. Ohmura and T. Yamamoto. Surface modification of epoxy resin with fluorine-containing methacrylic ester copolymers, Journal of Applied Polymer Science, *47*, 12, pp. 2207-2216. 1993.

Katz, I. and C. G. Dosoretz. Desalination of domestic wastewater effluents: phosphate removal as pretreatment, Desalination, *222*, 1-3, pp. 230-242. 2008.

Kennedy, M., S.-M. Kim, I. Mutenyo, L. Broens and J. Schippers. Intermittent crossflushing of hollow fiber ultrafiltration systems, Desalination, *118*, 1-3, pp. 175-187. 1998.

Khatib, Z. and P. Verbeek. Water to value - Produced water management for sustainable field development of mature and green fields, Journal of Petroleum Technology, *55*, 1, pp. 26-28. 2003.

Kilduff, J. E., S. Mattaraj, J. P. Pieracci and G. Belfort. Photochemical modification of poly(ether sulfone) and sulfonated poly(sulfone) nanofiltration membranes for control of fouling by natural organic matter, Desalination, *132*, 1-3, pp. 133-142. 2000.

Kim, D., S. Jung, J. Sohn, H. Kim and S. Lee. Biocide application for controlling biofouling of SWRO membranes - an overview, Desalination, *238*, 1-3, pp. 43-52. 2009.

Kim, J. Y., C. Lee, M. Cho and J. Yoon. Enhanced inactivation of E. coli and MS-2 phage by silver ions combined with UV-A and visible light irradiation, Water Research, *42*, 1-2, pp. 356-362. 2008.

Kim, K. J., A. G. Fane and C. J. D. Fell. The performance of ultrafiltration membranes pretreated by polymers, Desalination, *70*, 1-3, pp. 229-249. 1988.

Kim, K. S., K. H. Lee, K. Cho and C. E. Park. Surface modification of polysulfone ultrafiltration membrane by oxygen plasma treatment, Journal of Membrane Science, *199*, 1-2, pp. 135-145. 2002.

Kim, S. S. and D. R. Lloyd. Microporous membrane formation via thermally-induced phase separation. III. Effect of thermodynamic interactions on the structure of isotactic polypropylene membranes, Journal of Membrane Science, *64*, 1-2, pp. 13-29. 1991.

Knoell, T., J. Safarik, T. Cormack, R. Riley, S. W. Lin and H. Ridgway. Biofouling potentials of microporous polysulfone membranes containing a sulfonated polyether-ethersulfone/polyethersulfone block copolymer: correlation of membrane surface properties with bacterial attachment, Journal of Membrane Science, *157*, 1, pp. 117-138. 1999.

Kochkodan, V., S. Tsarenko, N. Potapchenko, V. Kosinova and V. Goncharuk. Adhesion of microorganisms to polymer membranes: a photobactericidal effect of surface treatment with TiO2, Desalination, *220*, 1-3, pp. 380-385. 2008.

Kou, R. Q., Z. K. Xu, H. T. Deng, Z. M. Liu, P. Seta and Y. Y. Xu. Surface modification of microporous polypropylene membranes by plasma-induced graft polymerization of alpha-allyl glucoside, Langmuir, *19*, 17, pp. 6869-6875. 2003.

Krishnan, S., R. Ayothi, A. Hexemer, J. A. Finlay, K. E. Sohn, R. Perry, C. K. Ober, E. J. Kramer, M. E. Callow, J. A. Callow and D. A. Fischer. Anti-biofouling properties of comblike block copolymers with amphiphilic side chains, Langmuir, *22*, 11, pp. 5075-5086. 2006.

Krishnan, S., C. J. Weinman and C. K. Ober. Advances in polymers for anti-biofouling surfaces, Journal of Materials Chemistry, *18*, 29, pp. 3405-3413. 2008.

Kwon, B., S. Lee, J. Cho, H. Ahn, D. Lee and H. S. Shin. Biodegradability, DBP formation, and membrane fouling potential of natural organic matter: Characterization and controllability, Environmental Science & Technology, *39*, 3, pp. 732-739. 2005.

Lange, N. A. and J. A. Dean. Lange's handbook of chemistry. pp. New York: McGraw-Hill. 1992.

Lebleu, N., C. Roques, P. Aimar and C. Causserand. Role of the cell-wall structure in the retention of bacteria by microfiltration membranes, Journal of Membrane Science, *326*, 1, pp. 178-185. 2009.

Lee, S., K. Lee, W. M. Wan and Y. S. Choi. Comparison of membrane permeability and a fouling mechanism by pre-ozonation followed by membrane filtration and residual ozone in membrane cells, Desalination, *178*, 1-3, pp. 287-294. 2005.

Lee, S., G. Park, G. Amy, S.-K. Hong, S.-H. Moon, D.-H. Lee and J. Cho. Determination of membrane pore size distribution using the fractional rejection of nonionic and charged macromolecules, Journal of Membrane Science, *201*, 1-2, pp. 191-201. 2002.

Lee, S. Y., H. J. Kim, R. Patel, S. J. Im, J. H. Kim and B. R. Min. Silver nanoparticles immobilized on thin film composite polyamide membrane:

characterization, nanofiltration, antifouling properties, Polymers for Advanced Technologies, *18*, 7, pp. 562-568. 2007.

Lei, J. and X. Liao. Surface graft copolymerization of 2-hydroxyethyl methacrylate onto low-density polyethylene film through corona discharge in air, Journal of Applied Polymer Science, *81*, 12, pp. 2881-2887. 2001.

Li, C. H., J. C. Zhu, Z. D. Qi, H. N. Hou, Y. J. Hu and Y. Liu. Antibacterial properties of a kind of schiff base and its neodymium(III) and Zn(II) complex (ZnNdL) on Escherichia coli, Chinese Journal of Chemistry, *27*, 9, pp. 1657-1662. 2009.

Li, H.-J., Y.-M. Cao, J.-J. Qin, X.-M. Jie, T.-H. Wang, J.-H. Liu and Q. Yuan. Development and characterization of anti-fouling cellulose hollow fiber UF membranes for oil-water separation, Journal of Membrane Science, *279*, 1-2, pp. 328-335. 2006a.

Li, H., A. G. Fane, H. G. L. Coster and S. Vigneswaran. Direct observation of particle deposition on the membrane surface during crossflow microfiltration, Journal of Membrane Science, *149*, 1, pp. 83-97. 1998.

Li, H. H., Y. M. Cao, H. J. Qin, X. M. Jie, T. H. Wang, J. H. Liu and Q. Yuan. Development and characterization of anti-fouling cellulose hollow fiber UF membranes for oil-water separation, Journal of Membrane Science, *279*, 1-2, pp. 328-335. 2006b.

Li, J.-B., J.-W. Zhu and M.-S. Zheng. Morphologies and properties of poly(phthalazinone ether sulfone ketone) matrix ultrafiltration membranes with entrapped TiO2 nanoparticles, Journal of Applied Polymer Science, *103*, 6, pp. 3623-3629. 2007.

Li, N. and R. B. Bai. Copper adsorption on chitosan-cellulose hydrogel beads: behaviors and mechanisms, Separation and Purification Technology, *42*, 3, pp. 237-247. 2005.

Li, Q. and M. Elimelech. Organic fouling and chemical cleaning of nanofiltration membranes: measurements and mechanisms, Environmental Science & Technology, *38*, 17, pp. 4683-4693. 2004.

Liau, S. Y., D. C. Read, W. J. Pugh, J. R. Furr and A. D. Russell. Interaction of silver nitrate with readily identifiable groups: relationship to the antibacterial action of silver ions, Letters in Applied Microbiology, *25*, 4, pp. 279-283. 1997.

Lin, N. H., M.-m. Kim, G. T. Lewis and Y. Cohen. Polymer surface nano-structuring of reverse osmosis membranes for fouling resistance and improved flux performance, Journal of Materials Chemistry, *20*, 22, pp. 4642-4652. 2010.

Liu, C. X. and R. B. Bai. Preparation of chitosan/cellulose acetate blend hollow fibers for adsorptive performance, Journal of Membrane Science, *267*, 1-2, pp. 68-77. 2005.

Liu, C. X. and R. B. Bai. Adsorptive removal of copper ions with highly porous chitosan/cellulose acetate blend hollow fiber membranes, Journal of Membrane Science, *284*, 1-2, pp. 313-322. 2006.

Liu, C. X., D. R. Zhang, Y. He, X. S. Zhao and R. B. Bai. Modification of membrane surface for anti-biofouling performance: Effect of anti-adhesion and anti-bacteria approaches, Journal of Membrane Science, *346*, 1, pp. 121-130. 2010.

Liu, F., N. A. Hashim, Y. Liu, M. R. M. Abed and K. Li. Progress in the production and modification of PVDF membranes, Journal of Membrane Science, *375*, 1-2, pp. 1-27. 2011.

Liu, Y., L. He, A. Mustapha, H. Li, Z. Q. Hu and M. Lin. Antibacterial activities of zinc oxide nanoparticles against Escherichia coli O157:H7, Journal of Applied Microbiology, *107*, 4, pp. 1193-1201. 2009.

Lohokare, H. R., S. C. Kumbharkar, Y. S. Bhole and U. K. Kharul. Surface modification of polyacrylonitrile based ultrafiltration membrane, Journal of Applied Polymer Science, *101*, 6, pp. 4378-4385. 2006.

Lok, C. N., C. M. Ho, R. Chen, Q. Y. He, W. Y. Yu, H. Z. Sun, P. K. H. Tam, J. F. Chiu and C. M. Che. Proteomic analysis of the mode of antibacterial action of silver nanoparticles, Journal of Proteome Research, *5*, 4, pp. 916-924. 2006.

Luo, M.-L., J.-Q. Zhao, W. Tang and C.-S. Pu. Hydrophilic modification of poly(ether sulfone) ultrafiltration membrane surface by self-assembly of TiO2 nanoparticles, Applied Surface Science, *249*, 1-4, pp. 76-84. 2005.

Ma, H. M., C. N. Bowman and R. H. Davis. Membrane fouling reduction by backpulsing and surface modification, Journal of Membrane Science, *173*, 2, pp. 191-200. 2000.

Ma, X., Q. Sun, Y. Su, Y. Wang and Z. Jiang. Antifouling property improvement of poly(vinyl butyral) ultrafiltration membranes through acid treatment, Separation and Purification Technology, *54*, 2, pp. 220-226. 2007.

Ma, Y., T. Zhou and C. Zhao. Preparation of chitosan-nylon-6 blended membranes containing silver ions as antibacterial materials, Carbohydrate Research, *343*, 2, pp. 230-237. 2008.

Malaisamy, R., D. Berry, D. Holder, L. Raskin, L. Lepak and K. L. Jones. Development of reactive thin film polymer brush membranes to prevent biofouling, Journal of Membrane Science, *350*, 1-2, pp. 361-370. 2010.

Matsumura, Y., K. Yoshikata, S. Kunisaki and T. Tsuchido. Mode of bactericidal action of silver zeolite and its comparison with that of silver nitrate, Applied and Environmental Microbiology, *69*, 7, pp. 4278-4281. 2003.

McMurry, J. Organic chemistry. pp. Belmont, CA: Thomson-Brooks/Cole. 2004.

Miura, Y., Y. Watanbe and S. Okabe. Membrane biofouling in pilot-scale membrane bioreactors (MBRs) treating municipal wastewater: Impact of biofilm formation, Environmental Science & Technology, *41*, 2, pp. 632-638. 2007.

Mondal, S. and S. R. Wickramasinghe. Produced water treatment by nanofiltration and reverse osmosis membranes, Journal of Membrane Science, *322*, 1, pp. 162-170. 2008.

Morra, M. and C. Cassinelli. Bacterial adhesion to polymer surfaces: A critical review of surface thermodynamic approaches, Journal of Biomaterials Science, Polymer Edition, *9*, 1, pp. 55-74. 1997.

Moulder, J. F. and J. Chastain. Handbook of X-ray photoelectron spectroscopy : a reference book of standard spectra for identification and interp retation of XPS data. pp. Eden Prairie, Minn.: Perkin-Elmer Corporation. 1992.

Munoz, M. P. G., R. Navarro, I. Saucedo, M. Avila, P. Pradanos, L. Palacio, F. Martinez, A. Martin and A. Hernandez. Hydrofluoric acid treatment for improved performance of a nanofiltration membrane, Desalination, *191*, 1-3, pp. 273-278. 2006.

Myint, A. A., W. Lee, S. Mun, C. H. Ahn, S. Lee and J. Yoon. Influence of membrane surface properties on the behavior of initial bacterial adhesion and biofilm development onto nanofiltration membranes, Biofouling: The Journal of Bioadhesion and Biofilm Research, *26*, 3, pp. 313 - 321. 2010.

Ngah, W. S. W., C. S. Endud and R. Mayanar. Removal of copper(II) ions from aqueous solution onto chitosan and cross-linked chitosan beads, Reactive & Functional Polymers, *50*, 2, pp. 181-190. 2002.

Nilson, J. A. and F. A. DiGiano. Influence of NOM composition on nanofiltration, Journal American Water Works Association, *88*, 5, pp. 53-66. 1996.

Norberg, D., S. Hong, J. Taylor and Y. Zhao. Surface characterization and performance evaluation of commercial fouling resistant low-pressure RO membranes, Desalination, *202*, 1-3, pp. 45-52. 2007.

Nunes, S. P., M. L. Sforça and K.-V. Peinemann. Dense hydrophilic composite membranes for ultrafiltration, Journal of Membrane Science, *106*, 1-2, pp. 49-56. 1995.

Pang, C. M., P. Y. Hong, H. L. Guo and W. T. Liu. Biofilm formation characteristics of bacterial isolates retrieved from a reverse osmosis membrane, Environmental Science & Technology, *39*, 19, pp. 7541-7550. 2005.

Park, N., B. Kwon, I. S. Kim and J. W. Cho. Biofouling potential of various NF membranes with respect to bacteria and their soluble microbial products (SMP): Characterizations, flux decline, and transport parameters, Journal of Membrane Science, *258*, 1-2, pp. 43-54. 2005.

Pasmore, M., P. Todd, S. Smith, D. Baker, J. Silverstein, D. Coons and C. N. Bowman. Effects of ultrafiltration membrane surface properties on Pseudomonas aeruginosa biofilm initiation for the purpose of reducing biofouling, Journal of Membrane Science, *194*, 1, pp. 15-32. 2001.

Perrier, S., S. G. Jackson, D. M. Haddleton, B. Ameduri and B. Boutevin. Preparation of fluorinated copolymers by copper-mediated living radical polymerization, Macromolecules, *36*, 24, pp. 9042-9049. 2003.

Pieracci, J., J. V. Crivello and G. Belfort. Photochemical modification of 10 kDa polyethersulfone ultrafiltration membranes for reduction of biofouling, Journal of Membrane Science, *156*, 2, pp. 223-240. 1999.

Podgorsek, A., S. Stavber, M. Zupan and J. Iskra. Free radical bromination by the H2O2-HBr system on water, Tetrahedron Letters, *47*, 40, pp. 7245-7247. 2006.

Pretsch, E., P. Bühlmann and M. Badertscher. Structure determination of organic compounds tables of spectral data. pp. Berlin: Springer. 2009.

Rana, D., Y. Kim, T. Matsuura and H. A. Arafat. Development of antifouling thin-film-composite membranes for seawater desalination, Journal of Membrane Science, *367*, 1-2, pp. 110-118. 2011.

Rana, D. and T. Matsuura. Surface modifications for antifouling membranes, Chemical Reviews, *110*, 4, pp. 2448-2471. 2010.

Russell, A. D., W. B. Hugo, G. P. Ellis and D. K. Luscombe. 7 Antimicrobial activity and action of silver. Progress in Medicinal Chemistry, Elsevier. *Volume 31***:** 351-370. 1994.

Sanpui, P., A. Murugadoss, P. V. D. Prasad, S. S. Ghosh and A. Chattopadhyay. The antibacterial properties of a novel chitosan-Ag-nanoparticle composite, International Journal of Food Microbiology, *124*, 2, pp. 142-146. 2008.

Santos, S. M. and M. R. Wiesner. Ultrafiltration of water generated in oil and gas production, Water Environment Research, *69*, 6, pp. 1120-1127. 1997.

Sarkar, A., P. I. Carver, T. Zhang, A. Merrington, K. J. Bruza, J. L. Rousseau, S. E. Keinath and P. R. Dvornic. Dendrimer-based coatings for surface modification of polyamide reverse osmosis membranes, Journal of Membrane Science, *349*, 1-2, pp. 421-428. 2010.

Shaw, H., H. D. Perlmutter, C. Gu, S. D. Arco and T. O. Quibuyen. Free-radical bromination of selected organic compounds in water, The Journal of Organic Chemistry, *62*, 2, pp. 236-237. 1997.

Shea, D. and W. A. Maccrehan. Determination of hydrophilic thiols in sediment porewater using ion-pair liquid chromatography coupled to electrochemical detection, Analytical Chemistry, *60*, 14, pp. 1449-1454. 1988.

Shi, L., R. Wang, Y. Cao, C. Feng, D. T. Liang and J. H. Tay. Fabrication of poly(vinylidene fluoride-co-hexafluropropylene) (PVDF-HFP) asymmetric microporous hollow fiber membranes, Journal of Membrane Science, *305*, 1-2, pp. 215-225. 2007.

Smolders, C. A., A. J. Reuvers, R. M. Boom and I. M. Wienk. Microstructures in phase-inversion membranes 1. formation of macrovoids, Journal of Membrane Science, *73*, 2-3, pp. 259-275. 1992.

Speight, J. G. Handbook of petroleum analysis. pp. New York: Wiley. 2001.

Speight, J. G. and N. A. Lange. Lange's handbook of chemistry. pp. New York: McGraw-Hill. 2005.

Speight, J. G. and NetLibrary Inc. The chemistry and technology of petroleum. pp. New York: Marcel Dekker. 1999.

Speth, T. F., R. S. Summers and A. M. Gusses. Nanofiltration foulants from a treated surface water, Environmental Science & Technology, *32*, 22, pp. 3612-3617. 1998.

Stamm, M. Polymer surfaces and interfaces : characterization, modification and applications. pp. Berlin ; Heidelberg: Springer. 2008.

Stuart, B. Infrared spectroscopy : fundamentals and applications. pp. Chichester, England ; Hoboken, NJ: J. Wiley. 2004.

Tang, C. Y., Y.-N. Kwon and J. O. Leckie. Effect of membrane chemistry and coating layer on physiochemical properties of thin film composite polyamide RO and NF membranes: I. FTIR and XPS characterization of polyamide and coating layer chemistry, Desalination, *242*, 1-3, pp. 149-167. 2009.

Teodosiu, C. C., M. D. Kennedy, H. A. van Straten and J. C. Schippers. Evaluation of secondary refinery effluent treatment using ultrafiltration membranes, Water Research, *33*, 9, pp. 2172-2180. 1999.

Tragardh, G. Membrane cleaning, Desalination, *71*, 3, pp. 325-335. 1989.

United States. Environmental Protection Agency. National secondary drinking water regulations. pp. Washington, D.C.: The Agency. 1984.

Uyanik, M., E. Arpaç, H. Schmidt, M. Akarsu, F. Sayilkan and H. Sayilkan. Heat-resistant hydrophobic–oleophobic coatings, Journal of Applied Polymer Science, *100*, 3, pp. 2386-2392. 2006.

Van der Hoek, J. P., J. Hofman, P. A. C. Bonne, M. M. Nederlof and H. S. Vrouwenvelder. RO treatment: selection of a pretreatment scheme based on fouling characteristics and operating conditions based on environmental impact, Desalination, *127*, 1, pp. 89-101. 2000.

Vanloosdrecht, M. C. M., J. Lyklema, W. Norde, G. Schraa and A. J. B. Zehnder. The role of bacterial cell-wall hydrophobicity in adhesion, Applied and Environmental Microbiology, *53*, 8, pp. 1893-1897. 1987.

Vincent, T. and E. Guibal. Cr(VI) extraction using Aliquat 336 in a hollow fiber module made of chitosan, Industrial & Engineering Chemistry Research, *40*, 5, pp. 1406-1411. 2001.

von Wandruszka, R., M. Schimpf, M. Hill and R. Engebretson. Characterization of humic acid size fractions by SEC and MALS, Organic Geochemistry, *30*, 4, pp. 229-235. 1999.

Vrouwenvelder, J. S. and D. van der Kooij. Diagnosis, prediction and prevention of biofouling of NF and RO membranes. European Conference on Desalination and the Environment Water Shortage, Lemesos, Cyprus, Elsevier Science Bv. 2001. pp. 65-71

Wandera, D., S. R. Wickramasinghe and S. M. Husson. Modification and characterization of ultrafiltration membranes for treatment of produced water, Journal of Membrane Science, *373*, 1-2, pp. 178-188. 2011.

Wang, X. F., X. M. Chen, K. Yoon, D. F. Fang, B. S. Hsiao and B. Chu. High flux filtration medium based on nanofibrous substrate with hydrophilic nanocomposite coating, Environmental Science & Technology, *39*, 19, pp. 7684-7691. 2005a.

Wang, X. F., D. F. Fang, K. Yoon, B. S. Hsiao and B. Chu. High performance ultrafiltration composite membranes based on poly(vinyl alcohol) hydrogel coating on crosslinked nanofibrous poly(vinyl alcohol) scaffold, Journal of Membrane Science, *278*, 1-2, pp. 261-268. 2006a.

Wang, Y.-Q., Y.-L. Su, Q. Sun, X.-L. Ma and Z.-Y. Jiang. Generation of anti-biofouling ultrafiltration membrane surface by blending novel branched amphiphilic polymers with polyethersulfone, Journal of Membrane Science, *286*, 1-2, pp. 228-236. 2006b.

Wang, Y.-q., T. Wang, Y.-l. Su, F.-b. Peng, H. Wu and Z.-y. Jiang. Remarkable reduction of irreversible fouling and improvement of the permeation properties of poly(ether sulfone) ultrafiltration membranes by blending with Pluronic F127, Langmuir, *21*, 25, pp. 11856-11862. 2005b.

Wang, Y., Y. Su, Q. Sun, X. Ma, X. Ma and Z. Jiang. Improved permeation performance of Pluronic F127-polyethersulfone blend ultrafiltration membranes, Journal of Membrane Science, *282*, 1-2, pp. 44-51. 2006c.

Weis, A., M. R. Bird and M. Nyström. The chemical cleaning of polymeric UF membranes fouled with spent sulphite liquor over multiple operational cycles, Journal of Membrane Science, *216*, 1-2, pp. 67-79. 2003.

Wend, C. F., P. S. Stewart, W. Jones and A. K. Camper. Pretreatment for membrane water treatment systems: a laboratory study, Water Research, *37*, 14, pp. 3367-3378. 2003.

Xu, Z.-L., T.-S. Chung and Y. Huang. Effect of polyvinylpyrrolidone molecular weights on morphology, oil/water separation, mechanical and thermal properties of polyetherimide/polyvinylpyrrolidone hollow fiber membranes, Journal of Applied Polymer Science, *74*, 9, pp. 2220-2233. 1999.

Yang, H. L., J. C. T. Lin and C. Huang. Application of nanosilver surface modification to RO membrane and spacer for mitigating biofouling in seawater desalination, Water Research, *43*, 15, pp. 3777-3786. 2009.

Yang, Q., Z. K. Xu, Z. W. Dai, J. L. Wang and M. Ulbricht. Surface modification of polypropylene microporous membranes with a novel glycopolymer, Chemistry of Materials, *17*, 11, pp. 3050-3058. 2005.

Yao, F., G. D. Fu, J. P. Zhao, E. T. Kang and K. G. Neoh. Antibacterial effect of surface-functionalized polypropylene hollow fiber membrane from surface-initiated atom transfer radical polymerization, Journal of Membrane Science, *319*, 1-2, pp. 149-157. 2008.

Yimin Qin, C. Z., Jie Chen, Jinhuan Zhong,. Preparation and characterization of silver containing chitosan fibers, Journal of Applied Polymer Science, *104*, 6, pp. 3622-3627. 2007.

Yu, H.-Y., Y.-J. Xie, M.-X. Hu, J.-L. Wang, S.-Y. Wang and Z.-K. Xu. Surface modification of polypropylene microporous membrane to improve its antifouling property in MBR: CO2 plasma treatment, Journal of Membrane Science, *254*, 1-2, pp. 219-227. 2005.

Yu, H. Y., L. Q. Liu, Z. Q. Tang, M. G. Yan, J. S. Gu and X. W. Wei. Surface modification of polypropylene microporous membrane to improve its antifouling characteristics in an SMBR: Air plasma treatment, Journal of Membrane Science, *311*, 1-2, pp. 216-224. 2008.

Yuan, S. J. and S. O. Pehkonen. Microbiologically influenced corrosion of 304 stainless steel by aerobic Pseudomonas NCIMB 2021 bacteria: AFM and XPS study, Colloids and Surfaces B-Biointerfaces, *59*, 1, pp. 87-99. 2007.

Zhao, Y. H., X. Y. Zhu, K. H. Wee and R. B. Bai. Achieving highly effective non-biofouling performance for polypropylene membranes modified by UV-induced surface graft polymerization of two oppositely charged monomers, Journal of Physical Chemistry B, *114*, 7, pp. 2422-2429. 2010.

Zhao, Y. Y., M. T. Carvajal, Y. Y. Won and M. T. Harris. Preparation of calcium alginate microgel beads in an electrodispersion reactor using an internal source of calcium carbonate nanoparticles, Langmuir, *23*, 25, pp. 12489-12496. 2007.

Zhu, X. Y., R. B. Bai, K. H. Wee, C. K. Liu and S. L. Tang. Membrane surfaces immobilized with ionic or reduced silver and their anti-biofouling performances, Journal of Membrane Science, *363*, 1-2, pp. 278-286. 2010.

Zodrow, K., L. Brunet, S. Mahendra, D. Li, A. Zhang, Q. L. Li and P. J. J. Alvarez. Polysulfone ultrafiltration membranes impregnated with silver nanoparticles show improved biofouling resistance and virus removal, Water Research, *43*, 3, pp. 715-723. 2009.

List of publications

Zhu, X. Y., R. B. Bai, K. H. Wee, C. K. Liu and S. L. Tang. Membrane surfaces immobilized with ionic or reduced silver and their anti-biofouling performances, Journal of Membrane Science, 363, 1-2, pp. 278-286. 2010.

Zhu, X. Y., L. Tang, K. H. Wee, Y. H. Zhao and R. B. Bai. Immobilization of silver in polypropylene membrane for anti-biofouling performance, Biofouling, 27, 7, pp. 773-786. 2011.

Zhu, X. Y., Y. H. Zhao, K. H. Wee, and R. B. Bai. Development of both hydrophilic and olephobic membrane surface for antifouling performance. Manuscript in preparation.

Zhu, X. Y., H. E. Loo, K. H. Wee, and R. B. Bai. A novel membrane with two different wettabilities and its non-organic and non-biological fouling performance for potential water treatment applications. Manuscript in preparation.

Zhu, X. Y., K. H. Wee, W. T. Tu and R. B. Bai. Effective and low fouling oil/water separation by a novel hollow fiber membrane with both hydrophilic and oleophobic surface properties. Manuscript in preparation.

Zhao, Y. H., X. Y. Zhu, K. H. Wee and R. B. Bai. Achieving highly effective non-biofouling performance for polypropylene membranes modified by UV-induced surface graft polymerization of two oppositely charged monomers, Journal of Physical Chemistry B, 114, 7, pp. 2422-2429. 2010.